Mixture Models for Dense Fluids And Polymers

by

Hassan Hammawa

A Thesis Presented to the

FACULTY OF THE COLLEGE OF GRADUATE STUDIES

KING FAHD UNIVERSITY OF PETROLEUM & MINERALS

DHAHRAN, SAUDI ARABIA

In Partial Fulfillment of the
Requirements for the Degree of

MASTER OF SCIENCE

In

CHEMICAL ENGINEERING

March, 1996

INFORMATION TO USERS

MIXTURE MODELS FOR DENSE FLUIDS AND POLYMERS

BY

HASSAN HAMMAWA

A Thesis Presented to the

FACULTY OF THE COLLEGE OF GRADUATE STUDIES

KING FAHD UNIVERSITY OF PETROLEUM & MINERALS

DHAHRAN, SAUDI ARABIA

In Partial Fulfillment of the
Requirements for the Degree of

MASTER OF SCIENCE

In

CHEMICAL ENGINEERING

March, 1996

KING FAHD UNIVERSITY OF PETROLEUM AND MINERALS

DHAHRAN 31261, SAUDI ARABIA
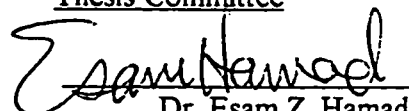
COLLEGE OF GRADUATE STUDIES
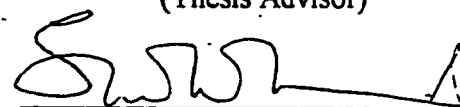
This thesis, written by
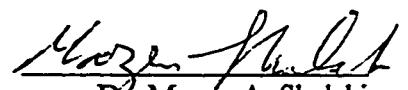
HASSAN HAMMAWA
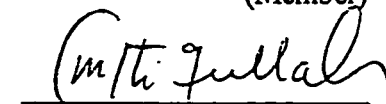
under the direction of his Thesis Advisor and approved by his Thesis Committee, has been presented to and accepted by the Dean of the College of Graduate Studies, in partial fulfillment of the requirements for the degree of **MASTER OF SCIENCE IN CHEMICAL ENGINEERING.**

Thesis Committee

Dr. Esam Z. Hamad
(Thesis Advisor)

Dr. Halim S. Hamid
(Member)

Dr. Mazen A. Shalabi
(Member)

Dr. Muhammad Atiqullah
(Member)

Department Chairman

Dean, College of Graduate Studies

18·5·96

Date

To Maisarah

ACKNOWLEDGMENT

!

TABLE OF CONTENTS

!

LIST OF TABLES

!

LIST OF FIGURES

!

THESIS ABSTRACT

FULL NAME OF STUDENT	HASSAN HAMMAWA
TITLE OF STUDY	MIXTURE MODELS FOR DENSE FLUIDS AND POLYMERS
MAJOR FIELD	CHEMICAL ENGINEERING
DATE OF DEGREE	MARCH, 1996

New consistent mixture models for simple molecules were developed from the pair correlation functions and the virial coefficients for hard core molecules. These models use equations of state of pure fluids to predict properties of their mixtures. The developed models were tested for mixtures of additive hard spheres, non-additive hard spheres, Lennard-Jones and simple real fluids. The molecular parameter ranges used were (1) Hard sphere size ratio of 1 to 3 and packing fraction of 0.23 to 0.55, (2) Non-additive hard spheres with non-additivity parameter Δ between - 0.5 to 1.0 and reduced density between 0 to 1.3, (3) Lennard-Jones molecules with size and energy ratio from 1 to 2.0 and from 1 to 4.5 respectively. Binary mixtures of simple real molecules, argon - krypton, neon - argon, methane - carbon tetrafluoride and carbondioxide - ethane were also tested. Comparison of the predictions of the new models with simulation and experimental data shows a satisfactory agreement. Among all the new models, the one based on the expansion of pair correlation function is the most accurate. This model predicted compressibility factor for binary mixtures with errors of less than 1% for hard spheres, about 2% for Lennard-Jones and about 5% for the simple real molecules.

A consistent mixture model was also developed for chain molecules. This was based on the consistency equations of the pair correlation function of Hamad (1994). The Tait equation of state for pure polymers was also extended to mixture of chain molecules. The extended Tait equation and the mixture model for chain molecules were used to predict the density of a binary mixture of poly(4-hydroxystyrene) and poly(vinylacetate). The mixture densities were predicted to within 1% of the experimental values. The mixture model for chain molecules is, in principle, also applicable to polymer solvent systems but cannot be used to predict phase separation.

خلاصة الرساله

اسم الطالـب : حسّان حمّاوه

عنوان الرساله : نماذج خليط الموائع عالية الكثافه والبوليمرات

التخصــــص : هندسه كيميائيه

تاريخ الرساله : مارس ١٩٩٦م

لقد طوّرت نماذج جديده منسجمه للذرات البسيطه من الدوال الزوجيه ذات العلاقه المتبادله ومن معاملات الفيريال لذرات الجوف الصلب . هذه النماذج تستخدم معادلات الحاله للموائع النقيه لإشتقاق خواص الخليط من تلك الموائع . لقد أختبرت هذه النماذج المشتقه لمخاليط الكرات الصلبه المضافه وللكرات الصلبه غير المضافه ولينارد – جونز وللموائع الحقيقيه البسيطه . صفات الذرات المستخدم كان (١) الكره الصلبه نسبة القطر من ١ إلى ٣ والكثافه النسبيه من ٢٢ر. إلى ٥٥ر. و (٢) الكرات الصلبه غير المضافه بمعامل غير الإضافه مـن – ٥ر. إلى ٠ر١ والكثافه النسبيه من : إلى ٣ر١ و (٣) ذرات ليمنارد – جونز بقطر ونسبه طاقه من ١ إلى ٢ ومن ١ إلى ٥ر٤ على التوالي .

أختبرت المخاليط الثنائيه للذرات الحقيقيه البسيطه وكذلك مخاليط الارجون – الكريبتون والنيون – الارجون والميثان – الكربون تيترا فلورايد وأكسيد الكربون الاحادي – الإيثان . أظهرت المقارنه لنتائج النماذج الجديده مع المحاكاه والنتائج المخبريه توافق مرضي . ومن كل النماذج الجديده كان الأكثر دقه النموذج الذي بني على التمدد لداله العلاقه الزوجيه . لقد حسب النموذج معامل الضغط للمخاليط الثنائيه بأخطاء أقل ١٪ للكرات الصلبه و ٢٪ لليمنارت جونز وتقريباً ٥٪ للذرات الحقيقيه البسيطه .

ولقد طوّر كذلك نموذج منسجم للذرات المسلسله . هذا النموذج أسس على إنسجام المعادلات لدوال العلاقه الزوجيه لحمد (١٩٩٤) ، لقد طورت معادلة تايت للحاله للبوليمرات النقيه لخليط الذرات المسلسله . استخدمت معادلة تايت المطوره ونموذج الخليط للذرات المسلسله لحساب الكثافه للمخاليط الثنائيه للبولي (٤ – هيدروكسي ستايرين) والبولي (فينايل أستيت) . لقد حصل على كثافه الخليط بفرق ١٪ من النتائج المخبريه من الممكن استخدام نموذج الخليط لمحاليل البوليمرات ولكن لايمكن استخدامه للحصول على معلومات عن انفصال الاطوار .

!

CHAPTER 1

INTRODUCTION

1.1   MOTIVATION

Successful design and operation of industrial chemical processes require considerable amount of thermophysical data of the substances involved. Traditionally, these data are derived from physical sciences (mainly physics and chemistry). Recently, however, other fields such as biology, medicine, ecology and materials science are significantly contributing to these data bases (Zeck and Wolf, 1993). In the past, most of these data were acquired exclusively experimentally. This is usually achieved either by direct experimental measurement at the desired condition, or from empirical model obtained by macroscopic treatment of the experimental data. These empirical methods are limited to the experimental range covered; as such they are of limited predictive value. In addition, experimental measurements are tedious and expensive to use for diverse substances and conditions that prevail in the industry.

On the other hand, appropriate concepts of molecular science can be used to develop physical models that estimate real properties from abstract thermodynamic functions (Prausnitz et al., 1986). This method provides insight into the relationship between molecular structure, intermolecular forces and the resulting thermophysical properties. Therefore, modern practice has shifted to molecular approach to develop completely theoretical relationships. The ultimate goal of this molecular approach is to

calculate bulk properties of substances from the first principle, namely: quantum theory and statistical mechanics. Achievement of this will considerably reduce the needed experiments.

In modeling the behavior of real fluid mixtures, equations of state and activity coefficient models are widely used. The activity coefficients can be derived from several bases such as:

i.   Composition power series expansion of Gibbs energy, for example,

       Margules and van Laar equations;

ii.   Local composition distribution expansion, such as the Wilson and the non-

       random two liquid NRTL models (Prausnitz et. al., 1986); and

iii.   Direct approximations from statistical mechanics (Abrams and Prausnitz, 1975).

These equations commonly require only two parameters to describe binary mixtures.

Most of the fluids dealt with in the industry are mixtures. A rich pure-fluid experimental data base already exists for most of the components of these mixtures. To exploit this resource, development of mixture models based on pure fluid properties is highly desirable. Statistical mechanics has proved to be an effective tool toward achieving this objective.

1.2   OBJECTIVES

Due to the above importance, several theoretical mixture models have been developed (for real and model fluids) using statistical mechanics approach. Of course, there are some inaccuracies in these theoretical models. One of the reasons for such

inaccuracies is inconsistency in approximations used to develop the models. In fact, even popular models such as the UNIFAC have some inconsistencies (Hamad, 1996).

The overall objective of this work, therefore, is to develop consistent mixture models (in terms of exact limiting conditions) that can predict thermodynamic properties of dense fluids and polymers. To be useful, the model should also be simple and accurate. Therefore, the specific objectives of the present study are as follows:

(i)   Develop simple models for dense fluids that satisfy the recently derived limiting

        condition results; which include identical components limit, infinite size ratio

        limit and independent components limit (for non-additive hard spheres);

(ii)   Compare the results of the developed model with those of molecular simulation,

        selected common existing models and available experimental data; and

(iii)   Extend the above models to highly asymmetric dense fluids and polymer systems.

1.3   ORGANIZATION OF THE THESIS

The basic concepts of statistical mechanics and other literature relevant to the development of mixture models considered in the present study are reviewed in Chapter 2. Chapter 3 details the procedures employed in developing these mixture models. This chapter also gives results of the derived binary mixture models. Satisfactory binary models from Chapter 3 are generalized to multicomponents in Chapter 4. Further, these generalized models are validated and tested for hard spheres (additive and non-additive), Lennard-Jones and real (simple) fluid mixtures. Chapter 5 describes the extension of pure polymer equation of state to mixture and parameterization and test of this extended

equation. Finally, the conclusions and recommendations for future work are given in

Chapter 6.

CHAPTER 2

REVIEW OF THE LITERATURE

2.1 Statistical Mechanics and Fluid Thermodynamics

Solution of mathematical equations of quantum mechanics provides permissible microscopic (quantum energy) states attainable by a particular system at any time. Statistical mechanics, on the other hand, allows averaging over those microstates to arrive at the macroscopic (bulk) properties of the system, such as pressure, heat capacity and viscosity. The time averaging process was conceptually avoided first by Gibbs through the introduction of statistical ensembles (Whalen, 1991).

2.1.1   Basic Postulates and Ensembles

An ensemble is a large collection of systems of particles in which the macroscopic properties of each of these systems is in the same thermodynamic state as that of a real system of interest. Although all the individual systems are of the same macroscopic properties, their quantum states may, however, differ. According to the fundamental postulate of statistical mechanics, therefore, the time averaged dynamic property (for example, pressure) of a real system is equal to the ensemble average of that property (Hill, 1960).

This simply allows replacement of the time-average value of a single system property by instantaneous average property value taken over a large number of systems of identical

macroscopic state as the real system. The second postulate was devised to facilitate calculations of the ensemble averages. It states that in a closed system of fixed energy, all the possible distinguishable quantum states are equally probable (Hill, 1960).

Thus, the probability of any system of the ensemble being in quantum state i is

$$P_i = {n_i}/{N} \qquad (2.1)$$

where n_i is the number of systems in state i and N is the total number of systems $\sum_i n_i$.

2.1.2 The Partition Function

All the individual systems of an ensemble are macroscopically identical. These identities are specified by appropriate set of thermodynamic (macroscopic) constraints on the ensemble. The overall statistical behavior of molecules in a system is described by its partition function which is a mathematical expression representing the probability of a system being in various molecular states. The partition function of each ensemble type is related to some basic thermodynamic properties. The most commonly encountered ensembles and their thermodynamic constraints are specified in Table 2.1. Once the basic thermodynamic expressions are obtained, other properties are easily derivable using the classical thermodynamic relations.

TABLE 2.1   Summary of Ensembles (Lee, 1988).

Ensemble		Partition	Thermodynamic
Type	Constraint	Function	Relation
Microcanonical	(N,V,U) Fixed	$\Omega = \sum_i 1$	$-TS = -kT\ln\Omega$
Canonical	(N,V,T) Fixed	$Q = \sum_i exp(-\beta\varepsilon_i)$	$A = -kT\ln Q$
Grand canonical	(μ,V,T) Fixed	$\Xi = \sum_i exp(\beta N\mu - \beta\varepsilon_i)$	$-PV = -kT\ln\Xi$
Isothermal-isobaric	(N,P,T) Fixed	$Y = \sum_{i,V} exp(-\beta PV - \beta\varepsilon_i)$	$G = -kT\ln Y$

For most real systems, at temperatures above about ~50 K, their translational energy is much larger than the energy gaps between consecutive quantum mechanical energy levels. In the classical limit, therefore, except for the quantum gases (hydrogen and helium), the discrete summations in the equations in Table 2.1 can be replaced by integrations over the phase space without introducing appreciable error (Reed and Gubbins, 1973). This results to semi-classical partition function. A similar approach is not valid for the internal (vibrational and rotational) motion energies of the molecules. Partition functions are, therefore, separated into configurational and internal parts to facilitate its use in calculating thermodynamic properties. The configurational partition function accounts for the motion of centers of mass of particles in their potential field, while the internal partition function represents the contribution from internal motion of the molecules.

The canonical partition function, therefore, takes the following form (Reed and Gubbins, 1973):

$$Q = \frac{1}{N!} Q_{int} \Lambda^{-3N} Z_N \qquad (2.2)$$

where Q_{int} is the internal partition function, $\Lambda = h/(2\pi m_i kT)^{1/2}$ is the de Broglie wave length of component i, h is Planck's constant, m_i is the mass of molecule i, k is Boltzmann constant, T is the absolute temperature, N is number of molecules. Z_N is the configurational integral given by

$$Z_N = \int_V \cdots \int_V \exp\left(-\phi/kT\right) d\mathbf{r}_1 \ldots d\mathbf{r}_N \qquad (2.3)$$

where $\mathbf{r}_i$ is the position vector of molecule i (x_i, y_i, z_i in Cartesian coordinates), ϕ is the intermolecular potential function, and V is the system volume.

2.2 Thermodynamic Properties from First Principles

2.2.1 Intermolecular Potential Energy

As seen from the partition function and their thermodynamic relationships, calculation of macroscopic properties of substances from the first principles involve two steps: specification of intermolecular potential energy function, and application of the laws of statistical mechanics to evaluate these properties at the desired state.

The intermolecular potential energy results from interaction among particles. The extent of these interactions depends on separation between the particles. The commonly encountered potential functions $\phi(r)$ are:

(i)   For ideal gas potential,

$$\phi(r) = 0 \qquad (2.4)$$

(ii)   For hard spheres potential,

$$\begin{aligned} \phi(r) &= +\infty & r \leq \sigma \\ \phi(r) &= 0 & r > \sigma \end{aligned} \qquad (2.5)$$

where σ is the hard sphere diameter.

(iii)   For square-well potential,

$$\phi(r) = +\infty \qquad\qquad r \leq \sigma$$
$$\phi(r) = -\varepsilon \qquad\qquad \sigma < r < \lambda\sigma \qquad\qquad (2.6)$$
$$\phi(r) = 0 \qquad\qquad r \geq \lambda\sigma$$

where σ is the repulsive diameter, λ is the attractive diameter, and ε is the potential well depth.

(iv)   For inverse-12 Soft-sphere (SS12) potential,

$$\phi(r) = 4\varepsilon \left(\frac{\sigma}{r}\right)^{12} \qquad\qquad (2.7)$$

where σ is the collision diameter of the molecules, and ε is the potential well depth.

(v)   For Lennard-Jones (LJ 12,6) potential,

$$\phi(r) = 4\varepsilon \left[\left(\frac{\sigma}{r}\right)^{12} - \left(\frac{\sigma}{r}\right)^{6} \right] \qquad\qquad (2.8)$$

(vi)   For Kihara KH potential,

$$\phi(r) = +\infty \qquad\qquad\qquad\qquad\qquad r \leq d$$
$$\phi(r) = 4\varepsilon \left[\left(\frac{\sigma - d}{r - d}\right)^{12} - \left(\frac{\sigma - d}{r - d}\right)^{6} \right] \qquad r > d \qquad (2.9)$$

2.2.2 Molecular Simulation

For a system of N molecules, the partition function Equation 2.2 involves N-body integrals over the total intermolecular potential energy function. Exact solution of these equations are only possible for some idealistic cases, for instance, independent molecules (ideal gas) or adsorption of a gas at low pressure (Gubbins, 1989). To solve the N-body integral equations, two methods are generally employed, molecular simulation and theoretical approximations using molecular theories.

Molecular simulation provides a reliable means (within a few percentage error) of evaluating macroscopic thermodynamic properties of hypothetical fluids based on assumed interaction potentials. Here, sufficient computer time is used to numerically estimate ratios of the full N-body integrals using the Monte Carlo (MC) method. Molecular dynamics (MD) techniques are used to determine equilibrium and non-equilibrium properties. Allen and Tildesley (1987) have given a good description of the two methods. A brief background of these methods is, however, given in what follows.

2.2.2.1 Monte Carlo Method

In MC method, system constraints are first fixed, then molecules of the system being simulated are randomly moved using a random number generator (hence the name Monte Carlo). The generated moves are either accepted or rejected based on compliance with statistical mechanics distribution laws. Several thousands of the acceptable moves are then averaged to obtain equilibrium properties of the system (Barker, 1963). Several algorithms have been developed for this purpose (Metropolis et al., 1953; Hansen and

Varlet, 1969). Using this technique, many investigators have simulated systems using different potential functions under widely varying conditions (Wood and Parker, 1957; Nicolas et al., 1979; Panagiotopoulus, 1987; Miyano, 1991; Miyano, 1993; Metropolis et al., 1953; Adams, 1976; Adams, 1979; Nixon and Silbert, 1984; Lotfi et al., 1992; Johnson et al., 1993; Guo et al., 1994).

2.2.2.2 Molecular Dynamics Method

In MD method, initial configuration and momenta are first assigned to all the particles/molecules of the system. The molecules are then allowed to move under the influence of their intermolecular forces. Newton's laws of motion are used to calculate the instantaneous spatial configuration and velocity distributions of the system at any time. Configurations of about 2×10^3 - 20×10^4 time steps are then averaged for equilibrium properties of the system (Lee, 1988). Molecular systems have been fairly simulated using MC method (Borgelt et al., 1990; Verlet, 1967; Levesque and Verlet, 1969; Adachi et al., 1988; Saager and Fischer, 1990; Johnson et al., 1993). The basic steps of both MC and MD techniques have been summarized by Gubbins (1989).

It should be noted that if sufficient run lengths (in terms of configurations or random moves for MC and in time steps for MD) are taken, both methods converge to the same results. Johnson et al. (1993) have summarized the system description, and temperature and density ranges for most of the published work of molecular simulation. The major limitations of molecular simulation methods are:

(i)   The CPU time increases exponentially with number of molecules which limits N
        to between hundreds to a few thousands;

(ii)   Both methods require the intermolecular potential used; and

(iii)   Their accuracy in predicting the properties of real substances is limited by the
        accuracy of the provided potentials.

Thermodynamic properties prediction by molecular simulations are exact for the
fluid potential used. These results, therefore, serve as a reference for testing other models
based on molecular approximations.

2.3   Distribution Functions and Thermodynamic Properties

The "structure" of matter (spatial distribution of its molecules) varies from completely
random as in ideal gas to completely ordered as in perfect crystal. Substances, whether in
pure or mixed form, exist somewhere between these two extremes. Dilute gases and
solids are easier to describe because of their closeness to completely random and
perfectly ordered arrangements of the molecules, respectively. The situation with dense
fluids (liquids and supercritical gases) is, however, different. For these systems,
distribution functions play a fundamental role in describing their structure, hence
macroscopic properties.

2.3.1 Distribution Functions

In a system of N particles enclosed in a volume V, the probability $P^{(N)}$ of finding molecule 1 in volume dr_1 at location r_1, molecule 2 in volume element dr_2 at r_2 and molecule N at volume element dr_N at r_N is given by (Reed and Gubbins, 1973):

$$P^{(N)}dr_1...dr_N = \frac{1}{Z(T,V,N)}exp(-\beta\phi)dr_1...dr_N \qquad (2.10)$$

where $Z(T,V,N)$ is the configurational integral, (see Equation 2.3), and β is the Boltzmann factor $1/kT$.

If each of the above probabilities is considered for each of n molecules irrespective of the configuration of the remaining (N-n) molecules, then by integrating over the position of the remaining ($n+1$, $n+2$,..., N) molecules, we have (Reed and Gubbins, 1973):

$$P^{(n)}(r_1,r_2,....r_n) = \frac{1}{Z(T,V,N)}\int...\int exp(-\beta\phi)dr_1...dr_N \qquad (2.11)$$

Therefore, if we consider the probability density of finding any molecule in dr_1 at r_1, any molecule in dr_2 at r_2 and any molecule in dr_n at r_n, irrespective of the configuration of the remaining ones, we have:

$$\rho^{(n)}(r_1,r_2,...r_n) = \frac{N!}{(N-n)!}P^{(n)}(r_1,r_2,...,r_n) \qquad (2.12)$$

This is the general distribution function of the system, which plays a major role in evaluation of the system's properties.

2.3.2 Pair Correlation Function (pcf)

In evaluating the configurational properties of substances, the relative pair position of molecules is of much importance. In an ensemble of particles, the pair correlation function is an expression that gives the probability of finding a molecule of type i in volume element dr_1 at position r_1 and a molecule of type j in volume element dr_2 at position r_2. From statistical mechanics, in the N-T-V (canonical) ensemble, this pair distribution function is given by (Hill, 1956):

$$\rho_{ij}^{(2)}(r_1, r_2) = N_i \left(N_j - \delta_{ij} \right) \int \cdots \int e^{-\Phi/kT} dr_3 \dots dr_N \Big/ Z(T, V, N) \tag{2.13}$$

where k is Boltzmann constant, T is the absolute temperature, V is the system volume, N is the set N_1, N_2, ...N_c molecules of type 1, 2, . . . , c. δ_{ij} is the Kronecker delta and Z(T, V, N) is the configurational integral given by Equation 2.3.

It is clear from Equations 2.13 and 2.3 that the pair distribution function depends on the temperature, density and composition of the system. The general pair distribution function in Equation 2.13 can reduce to a number of special cases for various limiting conditions. One of these cases is described below.

In the ideal gas limit ($\Phi/kT \rightarrow 0$)

$$\rho_{ij}^{(2)}(r_1,r_2) = N_i(N_j - \delta_{ij})/V^2 \qquad (2.14)$$

Equation 2.14 can be used to normalize Equation 2.13 to obtain a pair radial distribution

function (rdf), defined as:

$$g_{ij}(r) = \rho_{ij}^{(2)}(r)V^2/(N_i N_j) \qquad (2.15)$$

which is equivalent to:

$$g_{ij}(r) = V^2(1 - \delta_{ij}/N_j) \int \dots \int e^{-\Phi/kT} dr_3 \dots dr_N / Z(T,V,N) \qquad (2.16)$$

Equation 2.16 is only for the canonical ensemble. Expressions for other ensembles have

also been derived (Hill, 1962; Lee, 1988).

From the pair rdf, other thermodynamic properties of pure fluids and fluid

mixtures follow by definition. For an m-components mixture, the residual internal energy

U_r and the compressibility factor Z are, respectively, given by (Hill, 1962):

$$U_r = U - U^{ig} = \frac{N\rho}{2} \sum_{i=1}^{m} \sum_{j=1}^{m} x_i x_j \int_0^\infty \phi_{ij}(r) g_{ij}(r) 4\pi r^2 dr \qquad (2.17)$$

and

$$Z = \frac{P}{\rho kT} = 1 - \frac{\rho}{6kT} \sum_{i=1}^{m} \sum_{j=1}^{m} x_i x_j \int_0^\infty r\phi_{ij}'(r) g_{ij}(r) 4\pi r^2 dr \qquad (2.18)$$

where U^{ig} is the ideal gas internal energy, ϕ' is the derivative of the intermolecular

potential function with respect to the distance r. In deriving Equation 2.17, pair wise

additivity of the intermolecular potential is assumed, that is, the total potential energy of

the system is given by summing all the pair wise potential energies of the molecules.

$$\Phi = \sum_{i=1}^{N} \sum_{j<i}^{N} \phi(r_{ij})$$
(2.19)

Another important equation in thermodynamic properties evaluation is the

compressibility equation, expressed as:

$$\frac{1}{kT}\left(\frac{\partial P}{\partial \rho}\right)_{T} = 1 - \rho \sum_{i}^{m} \sum_{j}^{m} x_{i} x_{j} \int_{0}^{\infty} c_{ij}(r) 4\pi r^{2} dr$$
(2.20)

where $c_{ij}(r)$ is the direct correlation function which measures the direct effect of molecule

i on molecule j.

Equations 2.17, 2.18 and 2.20 are useful in evaluating thermodynamic properties

of simple fluids. To do this, we need to know the radial distribution function $g_{ij}(r)$.

Unfortunately, expressions for $g_{ij}(r)$ are not easier to solve than the partition function

expression from where they were derived. However, they have physical interpretations,

and can even be measured experimentally. In real applications, rdf expressions are

approximated to obtain solvable equations that can be evaluated for thermodynamic

properties. These approximations are the basis of a number of molecular theories.

The total correlation function c(r), is another important statistical mechanics

expression that gives the total influence of molecule 1 on molecule 2 at distance r in a

given system. Percus-Yevick (1958) used this expression to suggest an approximate

theory for pure fluids. This has subsequently been extended to mixtures. Property calculations using these mixture equations of state are very complex (Hamad, 1988).

2.3.3 Molecular Theories

The energy and pressure equations presented in the previous sections are only valid for spherically symmetric fluids. For systems with angle dependent potentials such as polar fluids, minor changes are needed in the above equations. There were several attempts to make the distribution functions more useful (Kirkwood, 1935; Yvon,1935; Born and Green, 1946). These have resulted to integral and integro-differential equations that are also complicated (Boublik et al., 1980). A comprehensive discussion of these approximations is given by Hamad (1988).

To avoid the above complexities, molecular theories are derived to use known pure fluid properties to develop models for predicting mixture properties. In these methods, approximations are made to the N-body integral equations to render them solvable. Among the existing molecular theories, the five principal ones (Gubbins, 1989) are: (1) corresponding states theory, (2) perturbation and cluster expansion theory, (3) integral equations theory, (4) density functional theory and (5) lattice models. The first three of these theories will be discussed briefly due to their relevance to this work.

2.3.3.1 The corresponding states theory

Corresponding states theory employs both theoretical and empirical means to develop models for pure fluids and fluid mixtures. It is based on fluids with identical form of intermolecular potential energy function which can be represented in the following form:

$$\phi_{ij} = \varepsilon_{ij} f\left(\frac{r}{\sigma_{ij}}\right) \qquad (2.21)$$

where ϕ_{ij} is the interaction energy between a molecule of type i and a molecule of type j. ε_{ij} is the corresponding potential well depth. The functional form f of the reduced intermolecular separation r is common for all molecular pairs. σ_{ij} is the collision diameter of molecules i and j. Lennard-Jones fluid Equation 2.8 is a good example of such fluids, (Harismiadis et al., 1991).

In an one-fluid corresponding states theory, mixture properties are considered equal to that of a single hypothetical fluid. The composition dependent molecular parameters of this hypothetical fluid is obtained by applying semiempirical mixing rules on the pure component properties.

2.3.3.2 Perturbation and cluster expansion theory

Simple fluid models such as hard spheres and Lennard-Jones fluids are idealized cases. Due to the simplicity of their application in theoretical studies, thermodynamic

properties of these fluids are well investigated. It is this resource that is exploited in perturbation theory to study real fluids.

In perturbation theory, the properties of a real fluid is considered to consist of two parts, the reference contribution and the perturbation contribution. Simple fluid models (such as hard-sphere fluid, Lennard-Jones fluids, etc.) are used to account for the reference contribution, while additional effects are treated as perturbations of the reference.

Developing real fluid equations of state via the perturbation approach involves: mathematical expansion of the configurational partition function of the original system around a reference system of known properties. Accuracy of the resulting model depends on the closeness of the original system to the reference.

2.3.3.3 Integral equations theory

Theories have been developed to simplify evaluation of the pair radial distribution function Equation 2.16. These are the Yvon-Born-Green YBG, the Hypernetted chain HNC and the Percus-Yevic PY theories.

In the YBG theory, Equation 2.16 is differentiated and simplified to the following form (Reed and Gubbins, 1973).

$$kT\frac{\partial g(r_{12})}{\partial r_1} + \frac{\partial \phi(r_{12})}{\partial r_1}g(r_{12}) + \rho \int \frac{\partial \phi(r_{13})}{\partial r_1}g_{(3)}dr_3 = 0 \tag{2.22}$$

This is an exact equation with all the quantities known except $g_{(3)}$, the triplet correlation function. Kirkwood (1935) first made Equation 2.22 of practical use by introducing the superposition assumption. This assumes the triplet correlation function to be the product of the three pair correlation functions, that is,

$$g_{(3)}\left(r_{12}, r_{13}, r_{23}\right) = g\left(r_{12}\right)g\left(r_{13}\right)g\left(r_{23}\right) \tag{2.23}$$

Equation 2.22 has been converted to an integral equation which has been solved numerically. Comparison of thermodynamics property prediction from this model and from molecular simulation shows that Equation 2.22 is only good at low densities (Reed and Gubbins, 1973). This points to the validity of superposition principle only at this condition.

Hypernetted-chain HNC and Percus-Yevick PY (Percus-Yevick, 1958) theories were developed to avoid the sensitivity of Equation 2.23 to small errors in the superposition assumption. These two theories use a less sensitive total correlation function which measures the total effect of molecule 1 on molecule 2 at separation r_{12} as follows:

$$h\left(r_{12}\right) = g\left(r_{12}\right) - 1 \tag{2.24}$$

This principle resulted to improved pair correlation functions over the YBG theory. Reed and Gubbins (1973) have presented details of the derivations.

The improved equations are as follows:

(i) For HNC,

$$\ln g(r_{12}) + \frac{\phi(r_{12})}{kT} = \rho \int [g(r_{23}) - 1] \left[g(r_{13}) - \ln g(r_{13}) - 1 - \frac{\phi(r_{13})}{kT} \right] dr_3 \qquad (2.25)$$

(ii) For PY,

$$g(r_{12}) \exp\left[\frac{\phi(r_{12})}{kT} \right] = 1 + \rho \int [g(r_{23}) - 1] g(r_{13}) \left[1 - \exp\left(\frac{\phi(r_{13})}{kT} \right) \right] dr_3 \qquad (2.26)$$

Equations 2.25 and 2.26 give results closer to molecular simulation than YBG. However, they are not reliable at high densities too. HNC overpredicts the compressibility factor while PY underpredicts it.

2.4 Consistency of Thermodynamics Mixture Models

2.4.1 Consistency of pcf Equations

If an approximate theory of g(r) is used to calculate pressure using the pressure Equation (2.18) and the compressibility Equation (2.20), different values will be obtained. This difference is due to the inaccuracy in the approximations used (Reed and Gubbins, 1973). One cause of such inaccuracy is inconsistency in the approximations. To develop accurate models, researchers are continuously striving to improve these approximations.

Rowlinson (1965), suggested a self consistent approximation in which the direct correlation function (dcf) was expressed in terms of unknown function ψ, which for

mixtures depend on temperature T, density ρ and mole fraction x_i of component i. The Rowlinson expression is:

$$c_{SC}(r;\rho,T) = c_{PY}(r;\rho,T) + d(r;\rho,T) \qquad (2.27)$$

where c_{PY} is the Percus-Yevick approximation, which for a mixture can be obtained from

$$c(r) = g_{ij}(r)\left(1 - exp\left(\frac{\phi_{ij}}{kT}\right)\right) \qquad (2.28)$$

and d in Equation 2.27, is given by

$$d(r;\rho,T) = \psi(\rho,T,x_i)\left[g_{ij}(r)e^{\phi/kT} - 1 - \ln g_{ij}(r) - \frac{\Phi}{kT}\right] \qquad (2.29)$$

This self consistent equation gave values for hard sphere fourth and fifth virial coefficients that are very close to the exact values (Watts and Henderson, 1969), which are shown in Table 2.2.

Hamad (1994) applied the basic calculus principle of the equality of mixed second derivative on the canonical and grand canonical ensemble partition functions (PF) to arrive at the following consistency criterion.

$$\frac{\partial^2 \ln PF}{\partial S_{ij}^{(p)} \partial S_{mn}^{(q)}} = \frac{\partial^2 \ln PF}{\partial S_{mn}^{(q)} \partial S_{ij}^{(p)}} \qquad (2.30)$$

where $S_{ij}^{(p)}$ is unlike interaction parameter with p and q running over all parameter types and i, j running over all components.

TABLE 2.2. Fourth and fifth virial coefficients of hard spheres (Watts and Henderson, 1969).

	PY_P	PY_C	SC	Exact value
B_4/b_o^3	0.2500	0.2969	0.2824	0.2869
B_5/b_o^4	0.0859	0.1211	0.1188	$0.1102 \pm .0003$

For binary hard spheres mixture of independent parameters (σ_{11}, σ_{12}, and σ_{22}), the consistency equation reduces to the following:

$$x_1 \sigma_{11}^2 \frac{\partial g_{11}(\sigma_{11})}{\partial \sigma_{12}} - 2x_2 \sigma_{12}^2 \frac{\partial g_{12}(\sigma_{12})}{\partial \sigma_{11}} = 0 \tag{2.31}$$

and

$$x_2 \sigma_{22}^2 \frac{\partial g_{22}(\sigma_{22})}{\partial \sigma_{12}} - 2x_1 \sigma_{12}^2 \frac{\partial g_{12}(\sigma_{12})}{\partial \sigma_{22}} = 0 \tag{2.32}$$

The factor 2 in the second terms of Equation 2.31 and Equation 2.32 were omitted in the original work of Hamad (1994) due to typographical error (Hamad, 1995).

For dependent size parameters, the consistency equation takes the form:

$$x_1 \sigma_{11}^2 \frac{\partial g_{11}(\sigma_{11})}{\partial \sigma_{22}} + 2x_1 x_2 \left(\frac{\partial \sigma_{12}}{\partial \sigma_{11}} \right) \sigma_{12}^2 \frac{\partial g_{12}(\sigma_{12})}{\partial \sigma_{11}}$$
$$- x_2^2 \sigma_{22}^2 \frac{\partial g_{22}(\sigma_{22})}{\partial \sigma_{11}} - 2x_1 x_2 \left(\frac{\partial \sigma_{12}}{\partial \sigma_{22}} \right) \sigma_{12}^2 \frac{\partial g_{12}(\sigma_{12})}{\partial \sigma_{11}} = 0 \tag{2.33}$$

Using the above consistency equations, Hamad (1994) showed that the virial equation for the commonly used Percus-Yevick approximation for mixture pcf is inconsistent.

Hamad and Mansoori (1989) have derived relations among integrals of rdf of mixtures in the canonical ensemble. The derived relations are useful in reducing the assumptions usually made in rdf approximations. It can as well be used to test the approximate theories of radial distribution functions.

2.4.2 Mixture virial coefficients

Virial mixture theories constitute a powerful tool for representing the behavior of mixtures. They can accurately predict the thermodynamic properties of mixtures with large molecular parameter difference (Hamad, 1988). The usefulness of virial equations of state results from their strong basis in statistical mechanics. There are also exact statistical mechanics expressions relating the experimentally measurable virial coefficients to intermolecular interactions.

For pure hard sphere fluids, exact virial coefficients are known up to the tenth virial (Kratky, 1977; Santos et al., 1995). The situation is, however, different for mixtures. For the simple case of mixture of additive hard spheres, exact analytical results are known only up to third virial.

For an m component mixture of additive hard spheres, the third virial coefficient is given by (Prausnitz, 1986):

$$C_{mix} = \tfrac{1}{3}\sum_i\sum_j\sum_k x_i x_j x_k C_{ijk} \qquad (2.34)$$

Exact expression for the coefficients C_{ijk} is given as (Kihara and Miyoshi, 1975):

$$C_{ijk} = \left(\frac{4\pi}{3}\right)^2 \left\{ \left(R_i^3 R_j^3 + R_i^3 R_k^3 + R_j^3 R_k^3\right)/\,3 + 3R_i^2 R_j^2 R_k^2 + \right\}$$
$$\left\{ R_i^3\left(R_j^2 R_k + R_j R_k^2\right) + R_j^3\left(R_i^2 R_k + R_i R_k^2\right) + R_k^3\left(R_i^2 R_j + R_i R_j^2\right)\right\} \qquad (2.35)$$

where $R_i = \sigma_{ii}/2$ is the collision radius of component i, the mixture third virial is given by

Equation 2.34. Fourth virial coefficient for mixture of hard spheres has also been calculated using a combination of analytical and numerical techniques. A result of this calculation for mixture of size ratio ranging from 1.67 to 3.0 gave accuracy within 0.01% of the exact value (Rigby and Smith, 1963).

Expressions for virial coefficients become even more difficult for non-spherical bodies. For convex body mixtures, the second virial coefficient is given by (Boublik, 1986):

$$B_{12} = \tfrac{1}{2}\left(v_1 + v_2 + R_1 S_2 + R_2 S_1\right) \tag{2.36}$$

where v_i is the volume of molecule and S_i is its surface area.

Kihara and Miyoshi (1975) have given mixture third virial coefficient of the same form as that in Equation 2.35 for non-spherical bodies. The $R_i^2 R_j^2 R_k^2$ term is, however, replaced by G_{ijk} whose value lies within the range $S_i S_j S_k \leq G_{ijk} \leq R_i^2 R_j^2 R_k^2$. Boublik (1986) suggested the following as an approximate expression for G_{ijk}:

$$G_{ijk} = \left(\frac{4\pi}{3}\right)\left(R_i^2 S_j S_k + R_j^2 S_i S_k + R_k^2 S_i S_j\right) \tag{2.37}$$

In a manner analogous to developing expressions for second and third virial coefficients, Boublik (1986) also suggested an expression for the fourth virial coefficient. The accuracy of 3rd and 4th virial coefficients for convex body mixtures could not be evaluated due to lack of exact results.

2.4.3 Exact limits on mixture models and excess properties

Fluid phase equilibria are among the most important thermodynamic properties directly used in the design and control of industrial chemical processes. In developing mixture models for phase equilibrium and other thermodynamic property calculations, researchers usually incorporate known limiting conditions for these functions. Composition limits are the ones commonly used. A symmetric quadratic dependence of mixture second virial on composition ensures (at least composition wise) that the limits of pure components are satisfied as the density approaches zero. Satisfaction of composition limits at low density alone is, however, not a sufficient condition for the consistency of a model.

Starting from the relation between the partition function and total Gibbs energy, Hamad (1995) derived a general condition for identical component limit of excess Gibbs energy mixture models. For a binary mixture with pairwise additivity, this reduces to the following:

$$\frac{\partial G^E}{\partial S_{ij}} = \sum_k \sum_l \frac{N_k(N_l - \delta_{kl})}{1 + \delta_{ij}} \left\langle \frac{\partial \phi_{kl}}{\partial S_{ij}} \right\rangle - \sum_i x_i \frac{N(N-1)}{2} \left\langle \frac{\partial \phi_{ij}}{\partial S_{ij}} \right\rangle_i \qquad (2.38)$$

where G^E is the excess Gibbs energy, S_{ij} is any parameter of intermolecular potential energy, δ_{ij} is the Kronecker delta, ϕ_{ij} is intermolecular energy between pair i,j and the angled brackets stand for expectation value.

Equation 2.38 reduces to the following multicomponent equations for independent energy parameters.

$$\frac{\partial G^E}{\partial \varepsilon_{ij}} = 2x_i x_j \, U_r / \varepsilon \qquad i \neq j \qquad (2.39)$$

and

$$\frac{\partial G^E}{\partial \varepsilon_{ii}} = -x_i \left(1 - x_i\right) U_r / \varepsilon \qquad (2.40)$$

with

$$U_r = U(T, P) - U^{ig}(T) \qquad (2.41)$$

where U_r, U and U^{ig} are the residual, total and ideal gas internal energies, respectively. x_i is the mole fraction of component i, and ε is the total interaction energy. In this derivation, it is assumed that the total number of particles is large, that is, $N \gg 1$.

For size parameter, Hamad (1995) obtained the following:

$$\sigma_{ii} \frac{\partial G^E}{\partial \sigma_{ii}} = 3NkT(Z-1)x_i \left[\sum_{k \neq i} 2x_k \frac{\partial \sigma_{ik}}{\partial \sigma_{ii}} - 1 + x_i \right] \qquad (2.42)$$

where Z is the compressibility factor (PV/NkT).

In the limit of infinite size ratio $(v_2/v_1 \rightarrow \infty)$, when species of a component becomes point molecules, Hamad (1995) obtained the limit of G^E for a binary mixture as follows.

$$G^E = kT\left(x_1 \ln\gamma_1 + x_2 \ln\gamma_2\right) \qquad (2.43)$$

where γ_i are activity coefficients given by:

$$ln\gamma_1 = ln\left[x_1 + x_2z_2\left(1 - v_2\,x_2/v\right)\right]$$ (2.44)

$$ln\gamma_2 = \frac{v_2x_1}{v - x_2v_2} + \Delta G_2$$ (2.45)

v_i is the molar volume of component i, and v is the mixture molar volume. The Gibbs

energy change is given by

$$\Delta G_2 = G_2(T,P_2) - G_2(T,P) = \int_{P_2}^{P} \rho_2 dp$$ (2.46)

where z_2, G_2, P_2 are properties of pure component 2 evaluated at mixture temperature T;

and $\rho_2 = N_2/V = x_2/v$.

Using the above equations, Hamad (1995) compared the limits of G^E models and

the expected exact values at these limits. This test revealed that even popular models such

as NRTL and UNIQUAC do not satisfy these conditions, major modifications are,

therefore, required especially in the size dependencies. Therefore, Hamad (1995)

suggested some exact statistical thermodynamics restrictions for mixture models in the

limits of infinite size ratio, identical components and independent components. He also

proposed the following simple mixture model which will satisfy all the restrictions.

$$A_r = \sum_i x_i A_{ir}\left(\{x_i\}s_{ij}, T, v, \omega_{ij}, \ldots\right)$$ (2.47)

where A_r is the residual Helmhotz free energy for the mixture, A_{ir} is the residual

Helmhotz free energy for pure component i, s_{ij} is the intermolecular interaction parameter

(for example collision diameter σ_{ij}, interaction energy ε_{ij},), ω_{ij} is the accentric factor, T is the absolute temperature, and v is the mixture molar volume. The fundamental difference between Equation 2.47 and the van der Waals two fluid theory is that A_{ir} is evaluated on a theoretical basis that can satisfy all the given restrictions.

2.5 Application of fluid models to polymer systems

Equations of state and mixture models that satisfactorily describe the properties of mixtures of simple spherical molecules are generally inaccurate in describing the systems of chain molecules such as polymers and polymer mixtures. This is due to the additional complexities of the latter which is caused by their highly entangled nature. For flexible liquid polymer chains, there is a large number of degrees of freedom due to the different possibilities in motions and orientations of segments, coupled with inter- and intramolecular interactions. These explain the difficulty in exact statistical mechanics treatment of chain molecules. Therefore, drastic idealizations and statistical mechanics approximations are necessary in developing equations of state for polymer fluids (Schwerzer and Curro, 1988; Chiew, 1990).

Despite the above drawbacks, researchers have developed theoretical and semiempirical models whose predictions compares favorably with experimental data of simple fluids and polymer systems. Several dense fluids equations of state have been developed based on the simplifying ideas of the Prigogine's theory.

The Prigogine's theory (Prigogine et al., 1953; Prigogine, 1957) is a corresponding states theory in which it was assumed that the effect of density on external

rotational and vibrational motion of the molecules is the same as its effect on translational motion. Following this assumption, the rotational and vibrational parts of the partition function (PF) were factored into external parts that are density dependent, and internal part that is independent of density. The density-dependent part is due to molecular rotations, low frequency vibrations and intermolecular motions such as bond bending and bond rotations that cause structural changes. The density-independent internal parts arising for instance from high frequency low amplitude vibrations have no effect on intermolecular interactions.

To approximate the unknown density dependence of the external rotational and vibrational motions for large molecules, a parameter c was defined as one third of the total number of external (density-dependent) degrees of freedom. The value of c is unity for spherical molecules (for example, argon) and small molecules with approximately spherical shape (for example methane). Using this assumption and the cell model, which accounts for the effect of repulsive forces, Prigogine obtained the following partition function for chain molecules (Vimalchand and Donohue, 1989):

$$Q = \frac{Q_{comb}}{\Lambda^{3Nc}} \left[g\upsilon_s^* \left(\tilde{\upsilon}^{\frac{1}{3}} - 1 \right)^3 \right]^{Nc} exp\left(\frac{Ncf(\tilde{\upsilon})}{\tilde{T}} \right) \tag{2.48}$$

where Q_{comb} is the combinatorial factor that accounts for number of distinguishable arrangements of the segments of molecules in the system, ϕ is the mean intermolecular potential energy, N is the total number of molecules in the system, g is a geometric

constant, υ_s^* is volume of segments, $\tilde{\upsilon}$ is reduced volume of segments. $\tilde{T}$ is the reduced temperature which is given by:

$$\tilde{T} = \frac{T}{T^*} = \frac{ckT}{\varepsilon q} \tag{2.49}$$

where k is the Boltzmann constant, ε is the interaction energy per unit external surface area, q is the surface area of a molecule and T the absolute temperature.

Several theories were developed from Prigogine's theory which include the Flory's theory, (Flory, 1956), the perturbed hard chain theory PHCT (Beret and Prausnitz, 1975; Donohue and Prausnitz, 1978), the chain of rotators theory COR (Chien et al., 1983).

In the Flory's theory, the concept of free volume was used to account for intermolecular interactions. A simple generalization of van der Waals attractive term was used for the r-mer chain. This can simply be written as (Vimalchand and Donohue 1989):

$$\frac{\phi}{2kT} = \frac{\varepsilon q}{kT} \cdot \frac{1}{\tilde{\upsilon}} \tag{2.50}$$

which results to the following partition function (Flory, 1956):

$$Q = \frac{Q_{comb}}{\Lambda^{3Nc}} \left[g\upsilon_s^* \left(\tilde{\upsilon}^{\frac{1}{3}} - 1 \right)^3 \right]^{Nc} exp\left(\frac{Nc}{\tilde{\upsilon}\tilde{T}} \right) \tag{2.51}$$

All the terms retain their connotations as defined in Equation 2.48.

The above perturbed hard chain theories differ from Prigogine's theory and the Flory's theory in the approximations used for density-dependent degrees of freedom and

the expressions for repulsive and attractive interactions. In the PHCT theory (Beret and Prausnitz, 1975), the Prigogine's theory of chain molecules and the perturbed hard chain theory for small molecules were used to develop a more accurate theory of wider applicability. The partition function of this theory is:

$$Q = \frac{V^N}{N! \Lambda^{3N}} \left(\frac{v_f}{v}\right)^{Nc} exp\left(\frac{-N\phi}{2kT}\right) \tag{2.52}$$

where v is the system volume, v_f is the free volume determined from the Carnahan-Starling expression for hard spheres molecules.

In deriving the PHCT, (Donohue and Prausnitz, 1978), considered the effects of rotational and vibrational degrees of freedom on the repulsive and attractive forces between molecules. These effects, which were treated as equivalent to those of translational motions, resulted to the following partition function:

$$Q = \frac{V^N}{N! \Lambda^{3N}} \left(\frac{v_f}{v}\right)^{Nc} exp\left(\frac{-\phi}{2ckT}\right)^{Nc} \tag{2.53}$$

where all the terms retain their previous meanings.

Vimalchand and Donohue (1989) have compared these theories of chain molecules comprehensively.

In simple molecular fluids, the attractive forces are much weaker than the repulsive forces. The structure of such fluids are, therefore, basically determined by the repulsive forces. In modeling such fluids, it is, therefore, natural to use athermal hard body fluids as reference. For simple molecules that are approximately spherically symmetric, hard spheres fluid is the useful reference, while for polymers, hard-sphere-

chains equations of state are the most convenient reference equations. These equations of state are simple, and they explain some significant features of real chain-like fluids (Song et al., 1994). Several of these equations are available in the literature (Boublik et al., 1990; Chiew, 1990; Yethiraj and Hall, 1993; Bokis and Donohue, 1992; Phan et al, 1993; Song et al., 1994; Hino et al., 1994).

As in the case for simple molecules, researchers have also simulated chain molecules (Gao and Weiner, 1989; Honnell and Hall, 1989; Denlinger and Hall, 1990; Muller and Binder, 1995; Chang and Sandler, 1994). These molecular simulation results serve as a reliable reference for testing models of chain molecules.

Song et al. (1994a) used three parameters (segment number r, defined as number of single hard spheres per chain, segment size σ, and non-bonded segment pair interaction energy ε), and modified hard-sphere-chains equation of state of Chiew (1990) to develop an engineering-oriented equation of state. This perturbed-hard-sphere-chains (PHSC) equation of state is applicable to simple fluids (r = 1) and polymers. It gives excellent predictions of thermodynamic properties of several simple fluids (normal and branched alkanes, aromatics, chlorinated hydrocarbons, etc.) with deviations less than about 5%. For the twenty two polymers with PHSC equation of state parameters as shown in Table 2.3, deviations of P-V-T properties from experimental values is in the range of 0.02 to 0.5% (Song et al., 1994a).

TABLE 2.3   PHSC Equation-of-State Parameters for Common Polymers (Song et al., 1994a)

polymer	r/M (mol/g)	σ(Å)	ε/k (K)	% rms dev n	% rms dev ρ_liq
high density poly(ethylene)	0.03542	3.860	384.9	67	0.11
low-density poly(ethylene)	0.04945	3.413	336.7	61	0.12
iso-poly(propylene)	0.01410	5.456	551.4	45	0.19
iso-poly(1-butene)	0.02140	4.663	485.0	45	0.25
poly(isobutene)	0.01019	6.030	779.5	55	0.11
poly(4-methyl-1-pentene)	0.02113	4.687	446.1	126	0.25
poly(styrene)	0.01117	5.534	724.7	69	0.12
poly(o-methylstyrene)	0.01191	5.446	731.4	50	0.06
cis-1,4-poly(butadiene)	0.01499	5.264	611.8	156	0.05
poly(vinyl chloride)	0.00981	5.271	736.9	87	0.19
poly(ethylene glycol)	0.02981	3.766	405.7	68	0.12
poly(vinyl acetate)	0.02044	4.242	477.2	110	0.02
poly(methyl methacrylate)	0.01432	4.850	655.9	41	0.03
iso-poly(methyl methacrylate)	0.01580	4.662	629.4	93	0.13
poly(butyl methacrylate)	0.01899	4.550	510.8	168	0.18
poly(cyclohexyl methacrylate)	0.01482	4.889	607.2	90	0.11
poly(ethylene terephthalate)	0.05437	2.798	350.3	121	0.38
poly(carbonate)	0.02628	3.828	479.5	107	0.18
poly(ether ether ketone)	0.06690	2.580	322.8	126	0.47
poly(sulfone)	0.02401	3.912	530.5	149	0.09
poly(tetrafluoroethylene)	0.03753	2.516	192.8	21	0.29
poly(tetrahydrofuran)	0.01708	4.843	531.0	47	0.08

Chapter 3

Development of Consistent Mixture Models

3.1   Simple Molecules

3.1.1   Model Formulation

In developing mixture models, it is useful to introduce the concept of residual property. This is defined for any real system property X as:

$$X^r(T,V,N) = X(T,V,N) - X^{id}(T,V,N) \tag{3.1}$$

The importance of this is to separate the contribution of intermolecular forces from all other factors that contribute to the total system property. X^{id} is the system property value in the absence of intermolecular forces (ideal gas state).

For a canonical ensemble, the relationship between pressure and partition function can be obtained by differentiating the Helmotz free energy in Table 2.1 with respect to the system volume (at fixed temperature and number of particles).

$$P = -\left(\frac{\partial A}{\partial V}\right)_{T,N} \tag{3.2}$$

Multiplying Equation 3.2 by the system volume V and splitting into the form of Equation 3.1 gives (Reed and Gubbins, 1973):

$$PV = kTV\left(\frac{\partial \ln Q}{\partial V}\right)_{T,N} = (PV)^{ig} + (PV)^r \qquad (3.3)$$

where the ideal gas contribution to the total system energy is given by

$$(PV)^{ig} = NkT \qquad (3.4)$$

The term $(PV)^r$ comes from the force ($-d\phi/dr$) between a particular molecule and all others in a spherical shell distance r from the central molecule i (see Figure 3.1).

Change in pressure ΔP is the total force $[(-d\phi/dr)\rho g(r)4\pi r^2 dr]$/area at r. This simplifies to the following statistical mechanics expression (Reed and Gubbins, 1973):

$$P = \rho kT - \tfrac{2}{3}\pi\rho^2 \int_0^\infty \phi' g(r) r^3 dr \qquad (3.5)$$

where ϕ' is the derivative of the potential function with respect to the distance r. Equation 3.5 can be rewritten in the following form:

$$Z = 1 - \tfrac{2}{3}\pi\rho \int_0^\infty r\phi' g(r) r^2 dr \qquad (3.6)$$

When extended to a mixture of m components, Equation 3.6 becomes:

$$\rho(r) = \rho g(r)$$
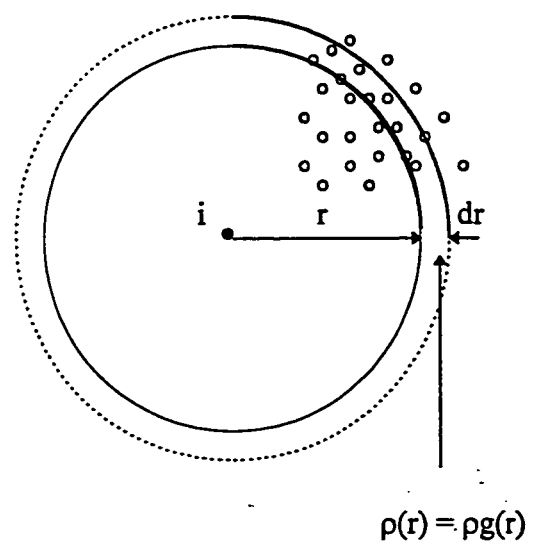
Figure 3.1 Configurational contribution of central molecule i (interacting with all other molecules) to increment of pressure in shell dr at r.

$$Z = 1 - \tfrac{2}{3}\pi\rho \sum_{i=1}^{m}\sum_{j=1}^{m} x_i x_j \int_0^\infty r\phi_{ij}'(r)g_{ij}(r)r^2 dr \tag{3.7}$$

where x_i, and x_j, are mole fractions of components i and j, respectively. r is the intermolecular separation, and g_{ij} is the pair correlation function.

The essence of starting with an equation of state in the present approach is to avoid dealing with the complex statistical mechanics part of Equation 3.7). Our expressions for compressibility factor Z are, therefore, written in three different equivalent forms as follows:

$$Z = 1 + \rho \sum_i \sum_j x_i x_j B_{ij} F_{ij} \tag{3.8}$$

$$Z = 1 + \rho \sum_i x_i \left(\sum_j x_j B_{ij} \right) H_i \tag{3.9}$$

$$Z = 1 + \rho \sum_i \sum_j x_i x_j B_{ij} G \tag{3.10}$$

where σ_{ij} is the collision diameter of molecules i and j. F_{ij}, H_i, and G are unknown functions of temperature, density, composition and molecular parameters. These can, therefore, be expressed in the following functional forms:

$$F_{ij} = F\left(\rho\sigma_{x_{ij}}, \frac{kT}{\varepsilon_{x_{ij}}}, \omega_{x_{ij}}, \cdots \right) \tag{3.11}$$

$$H_i = H\left(\rho\sigma_{x_u}, \frac{kT}{\varepsilon_{x_u}}, \omega_{x_u}, \cdots\right)$$ (3.12)

$$G(\rho g) = G\left(\rho\sigma_x, \frac{kT}{\varepsilon_x}, \omega_x, \cdots\right)$$ (3.13)

To meet the consistency criterion, Equation 3.8 to Equation 3.10 must reduce to the pure component values at the appropriate conditions (pure component limit, identical molecular parameter limit, etc.).

Each of the expressions for compressibility factor in Equations 3.8 to 3.10 has its particular advantage. The expression in the form of f_{ij}, (see Equation 3.8), besides being simple, is the most natural form since most intermolecular forces are pairwise additive. The most important advantage of Equation 3.9 is that it can easily be applied to evaluate mixture properties even if the pure components equations of state are different. This is highly desirable since researchers have developed accurate, but widely varying pure equations of state to describe specific substances or groups of substances. Finally, the functional form of G in Equation 3.10 preserves the density dependence of the pure equation of state in the mixture equation. This has some computational advantage. The functions F, H and G in Equations 3.11 to 3.13 are evaluated as *(Z-1)/B* from pure substance equation of state, with B as the second virial coefficient.

The first natural candidate to this approach is the hard-sphere fluid. Because, this is a very simple fluid model, and it considerably mimics real fluids especially at high temperatures and high densities where the fluid structure is mainly determined by

repulsive forces. Therefore F_{ij}, H_i, and G in Equations 3.10 to 3.12 are first evaluated for binary hard sphere fluid mixture. These are latter extended to multicomponent mixtures.

3.1.2 Evaluation of Parameters

3.1.2.1 Parameter F_{ij}

For the hard sphere fluid, due to the potential function as defined in Equation 2.5, it is only the size parameter that remains in Equations 3.11 to 3.13. Equation 3.10, therefore, simplifies to:

$$F_{ij} = F\left(\rho f_{ij}\right) \tag{3.14}$$

where f_{ij} represents three composition-dependent unknowns. Equation 3.14 is also expressed in another form to suit the proposed evaluation approach. The other functional form of Equation 3.14 is given as:

$$F_{ij} = F\left[\rho\left(x_1 f_{ij,1} + x_2 f_{ji,2}\right)\right] \tag{3.15}$$

The form of Equation 3.15 allows evaluation of $f_{ij,1}$ and $f_{ij,2}$, independent of the mixture composition.

The following strategies were employed in solving the above equations for f_{ij}.

(i)   The parameter f_{ij} was evaluated from the third virial coefficients derived from compressibility factor expressions of Equation 3.8 and Carnahan Starling Equation of state for hard spheres fluid given in Equation 3.16 (Mansoori et al., 1969; Boublik, 1970).

$$Z_{CS}^{hs} = \frac{6}{\pi \rho} \left[\frac{\xi_o}{1-\xi_3} + \frac{3\xi_1\xi_2}{(1-\xi_3)^2} + \frac{\xi_2^3(3-\xi_3)}{(1-\xi_3)^3} \right] \tag{3.16}$$

Equation 3.16 is the mixture version of Carnahan-Starling equation of state for pure hard spheres. Carnahan and Starling originally proposed this equation which resulted from the approximately recursive behavior of molecular dynamics results of the virial coefficients of hard spheres (Carnahan and Starling, 1969).

The sets of equations that resulted from the above formulations were difficult to solve analytically. The necessity of using numerical techniques to test this model limits its applicability.

(ii)   The pair correlation function for hard spheres mixture at contact is given by

$$g_{ij}^{hs}(\rho \sigma_{ij}) = \frac{1}{1-\xi_3} + \frac{3}{2}\frac{\sigma_i\sigma_j}{\sigma_{ij}}\frac{\xi_2}{(1-\xi_3)^2} + \frac{1}{2}\left(\frac{\sigma_i\sigma_j}{\sigma_{ij}}\right)^2\frac{\xi_2^2}{(1-\xi_3)^3} \tag{3.17}$$

where the system density ρ is given by:

$$\rho = \sum_{k=1}^{m} \rho_k \tag{3.18}$$

and

$$\xi_n = \pi/6 \sum_{k=1}^{m} \rho_k \sigma_{kk}^n \tag{3.19}$$

with the component density evaluated from Equation 3.16 as:

$$\rho_k = x_k \rho \qquad (3.20)$$

Equation 3.15 exhibits an approximate distinguishing factor between its three terms. This is more clearly expressed if Equation 3.15 is rewritten in the following form:

$$g_{ij}^{hs}(\rho\sigma_{ij}) = \left[\frac{\sigma_i\sigma_j}{\sigma_{ij}}\xi_2\right]^0 \frac{1}{1-\xi_3} + \left[\frac{\sigma_i\sigma_j}{\sigma_{ij}}\xi_2\right]^1 \frac{3}{2}\frac{1}{(1-\xi_3)^2} + \left[\frac{\sigma_i\sigma_j}{\sigma_{ij}}\xi_2\right]^2 \frac{1}{2}\frac{1}{(1-\xi_3)^3} \qquad (3.21)$$

f_{ij} was, therefore, taken as the distinguishing factor between the terms of the contact values for pair correlation functions of hard sphere mixtures. This value is thus given by:

$$f_{ij} = \left(\frac{\sigma_{ii}\sigma_{jj}}{\sigma_{ij}}\right)\sum_k x_k \sigma_{kk}^2 \qquad (3.22)$$

(iii)   The pressure of a mixture of hard spheres is given by (Reed and Gubbins, 1973):

$$P^{hs} = kT\sum_{i=1}^{r}\rho_k + \tfrac{2}{3}\pi k\sum_{i=1}^{r}\sum_{j=1}^{r}\rho_i\rho_j\sigma_{ij}^3 g_{ij}^{hs}(\sigma_{ij};\rho_i,...,\rho_r) \qquad (3.23)$$

where all the terms retain their previous meanings.

The compressibility factor expression from Equation 3.23 is similar in form to that from Equation 3.8. The model expression f_{ij} was, therefore, obtained by solving equations that result from equating equivalent terms from expansions of F_{ij} of Equation 3.8 and the pair correlation function of hard spheres, thus:

$$F_{ij}\left(\rho f_{ij}\right) = g_{ij}^{hs}\left(\rho \sigma_{ij}\right)$$

(3.24)

For a binary mixture, the values obtained for f_{ij} (see Appendix A). are:

$$f_{11} = \tfrac{2}{5}S_3 + \tfrac{3}{5}\sigma_1 S_2$$

(3.25)

$$f_{12} = \tfrac{2}{5}S_3 + \tfrac{3}{5}\left(\frac{\sigma_1 \sigma_2}{\sigma_{12}}\right)S_2$$

(3.26)

$$f_{22} = \tfrac{2}{5}S_3 + \tfrac{3}{5}\sigma_2 S_2$$

(3.27)

where the terms S_2 and S_3 are defined as:

$$S_2 = x_1\sigma_1^2 + x_2\sigma_2^2$$

(3.28)

$$S_3 = x_1\sigma_1^3 + x_2\sigma_2^3$$

(3.29)

(iv)   In Equation 3.15), $f_{ij,1}$ and $f_{ij,2}$ represent four unknowns. To solve for these unknowns, four independent equations are needed. These four equations were obtained in pairs using two different methods.

In the first approach, the four unknowns were solved from the equations that resulted from equating F_{ij} and g_{ij} as in (iii) above. For a binary mixture, this procedure gave the following expressions:

$$f_{11,1} = \tfrac{3}{5}\sigma_1\sigma_2^2 + \tfrac{2}{5}\sigma_2^3$$

(3.30)

$$f_{12,1} = \sigma_1^3 \left(\tfrac{2}{5} + \tfrac{1}{5}\sigma_{11}/\sigma_{12} \right) \tag{3.31}$$

$$f_{12,2} = \sigma_2^3 \left(\tfrac{2}{5} + \tfrac{1}{5}\sigma_1/\sigma_{12} \right) \tag{3.32}$$

$$f_{22,2} = \tfrac{1}{5}\sigma_1^2\sigma_2 + \tfrac{2}{5}\sigma_1^3 \tag{3.33}$$

On substituting Equations 3.30 to 3.31 back into Equation 3.14, the final equations simplify to the same form as that in Equations 3.25 to 3.27. This is expected since it is fundamentally the same model, and hence this serves as a check on our parameter evaluation strategy.

(v)   From statistical mechanics, the third virial coefficient of an m-component mixture C_{mix} is given by Equation 2.34. The coefficients C_{ijk} are related to pair potentials ϕ_{ij}, ϕ_{ik}, and ϕ_{jk} by:

$$C_{ijk} = \frac{-8\pi^2 N_A^2}{3} \int_0^\infty \int_0^\infty \int_{|r_{ij}-r_{ik}|}^{|r_{ij}+r_{ik}|} f_{ij}f_{ik}f_{jk}r_{ij}r_{ik}r_{jk}\,dr_{ij}\,dr_{ik}\,dr_{jk} \tag{3.34}$$

In Equation 3.34, the f terms are given by:

$$f_{lm} = exp\left(-\phi_{lm}/kT \right) - 1 \tag{3.35}$$

Similar expressions are also available for the fourth virial coefficient D_{mix} as:

$$D_{mix} = \sum_i^m \sum_j^m \sum_k^m \sum_l^m x_i x_j x_k x_l D_{ijkl} \tag{3.36}$$

In the second approach, the $f_{ij,1}$ and $f_{ij,2}$ terms were, therefore, evaluated by equating two corresponding terms from the third and fourth virial coefficients of Equation 3.8 and hard spheres compressibility equation. For the purpose of symmetry, terms C_{112}, and C_{122}, were the coefficients considered from the third virial coefficient, while D_{1112} and D_{1222} from the fourth virial were used to generate the second set of equations.

The above procedure resulted to four different roots. Three of these, unrealistically gave negative values of $f_{ij,1}$ and $f_{ij,2}$ for all size ratios of a binary mixture. The fourth model (see Appendix B) that always gave positive values of $f_{ij,1}$ and $f_{ij,2}$ is, however, complicated and can not be easily generalized to multicomponent mixtures. It has, therefore, not been considered any further (for generalization to multicomponent form) in this work. It was, however, tested for hard sphere fluids as will be seen later.

3.1.2.2 Parameter H_i

In a similar approach to section 3.1.2.1, H_i in Equation 3.9) is written in the following forms

$$H_i = H(\rho h_i)$$ (3.37)

and

$$H_i = H\left[\rho\left(x_1 h_{ij} + x_2 h_{ji}\right)\right]$$ (3.38)

Here also, for a binary mixture, Equation 3.37 involves two unknowns while Equation 3.38 consists of four unknowns. However, since H involves only one pure component

index i, for i = j we can readily see that h is a direct measure of the pure component molecular volume. Therefore,

$$h_{ii} = \sigma_{ii}^{3}$$

(3.39)

The following methods were, therefore, used to solve Equation 3.37 for h_i's:

(i)   In the first method employed, the parameter H_i was taken to be equivalent to the pair correlation function g_{ij}. A comparison of Equation 3.9 with Equation 3.45 justifies this assumption. Due to the difference in number of indices associated to H and g, equivalence of the two is not straight forward. The following scheme was, therefore, used for a binary mixture to retain consistency in composition dependence.

$$x_1^2 \sigma_{11}^3 g_{11} + x_1 x_2 \sigma_{12}^3 g_{12} = \left(x_1^2 \sigma_{11}^3 + x_1 x_2 \sigma_{12}^3\right) H_1$$

(3.40)

and

$$x_2^2 \sigma_{22}^3 g_{22} + x_1 x_2 \sigma_{12}^3 g_{12} = \left(x_2^2 \sigma_{22}^3 + x_1 x_2 \sigma_{12}^3\right) H_2$$

(3.41)

Note that for hard spheres, $\sigma_{21} = \sigma_{12} = (\sigma_{11} + \sigma_{22})/2$. Due to the definition in Equation 3.39, only two unknowns are left in Equation 3.38.

On solving Equation 3.40 and Equation 3.41 according to Equation 3.37, the following expressions for h_1 and h_2 were obtained.

$$h_1 = \tfrac{2}{3} S_3 + \tfrac{3}{3} \sigma_1 S_2 \frac{\left(x_1 \sigma_1^3 + x_2 \sigma_2 \sigma_{12}^2\right)}{\left(x_1 \sigma_1^3 + x_2 \sigma_{12}^3\right)}$$

(3.42)

and

$$h_2 = \tfrac{2}{3}S_3 + \tfrac{3}{5}\sigma_2 S_2 \frac{\left(x_1\sigma_1^3 + x_2\sigma_1\sigma_{12}^2\right)}{\left(x_2\sigma_2^3 + x_1\sigma_{12}^3\right)} \tag{3.43}$$

where S_2 and S_3 are as defined in Equation 3.28 and Equation 3.29. It should be noted that solution of Equations 3.40 and 3.41 using the functional form of H_i defined in Equation 3.38 gave exactly the same results as in Equations 3.42 and 3.43 above.

(ii)   In the second method, the unknowns in Equation 3.37 were solved from two coefficients (C_{112} and C_{122}) of the third virial of Equation 3.9 and the corresponding terms from hard spheres equation of state. Applying this procedure to a binary mixture yielded the following results.

$$h_{12} = \frac{\sigma_2^3\left(35\sigma_1^4 + 124\sigma_1^3\sigma_2 + 78\sigma_1^2\sigma_2^2 + 4\sigma_1\sigma_2^3 - \sigma_2^4\right)}{5\left(\sigma_1^4 + 8\sigma_1^3\sigma_2 + 30\sigma_1^2\sigma_2^2 + 8\sigma_1\sigma_2^3 + \sigma_2^4\right)} \tag{3.44}$$

and

$$h_{21} = \frac{\sigma_1^3\left(35\sigma_2^4 + 124\sigma_1\sigma_2^3 + 78\sigma_1^2\sigma_2^2 + 4\sigma_1^3\sigma_2 - \sigma_1^4\right)}{5\left(\sigma_1^4 + 8\sigma_1^3\sigma_2 + 30\sigma_1^2\sigma_2^2 + 8\sigma_1\sigma_2^3 + \sigma_2^4\right)} \tag{3.45}$$

3.1.2.3 Parameter G

The third form of our model representation as shown in Equation 3.10 is different from the pair correlation function. This unindexed model parameter is evaluated for the whole mixture before multiplying out by the summation term. This makes the model simpler to apply. The following methods were used to solve for the model parameter g.

(1)   An equivalent form of Equation 3.23 in pair correlation function is:

$$Z = 1 + \frac{\pi}{6} \rho \sum_i \sum_j x_i x_j \sigma_{ij}^3 g_{ij} \tag{3.46}$$

Expanding Equation 3.10 and Equation 3.46 with respect to density ρ, and substituting the previously evaluated function f_{ij} for $\partial g_{ij}/\partial \rho$, g was obtained as follows for a binary mixture:

$$g = \tfrac{2}{5} S_1 + \tfrac{3}{5} S_2 \frac{\sum \sum x_i x_j \sigma_{ij}^3 \left(\sigma_{ii} \sigma_{jj} / \sigma_{ij} \right)}{\sum \sum x_i x_j \sigma_{ij}^3} \tag{3.47}$$

(ii) Finally, g was taken to be the mixture packing fractions given by:

$$g = \sum_k x_k \sigma_{kk}^3 \tag{3.48}$$

3.2 Chain Molecules

The interaction particle theory has been very useful in developing equations of state for chain molecules (Schweizer and Curror, 1988; Chiew, 1990; Chiew, 1991; Malakhov and Brun, 1992; Thomas and Donohue, 1993). In the interaction particle theory, a chain molecule is considered to consist of several interacting particles or sites (see Figure 3.1). This interaction can originate from chain connectivity (bond between particles of a chain) and attractive and repulsive interactions.

In developing mixture models for chain molecules, we start from a general expression for compressibility factor for hard chains

$$Z = 1 + 2\pi / 3 \, \rho_c \sum_i \sum_j x_i x_j \sigma_{ij}^3 r_i r_j g_{ij} \qquad (3.49)$$

where ρ_c is the chain density and σ_{ij} is the collision diameter of sites i and j. x_i and x_j are the mole fractions of sites i and j. r_i and r_j are the chain lengths of components i and j, and g_{ij} is the pair correlation function of the sites.

Combining the binary third virial coefficient of Kihara (Hirschfelder et al., 1964) with the consistency conditions, (see Equations 2.31 to 2.33), Hamad, (1995) approximated the coefficients of density expansion of g_{ij} as follows:

$$g_{ij} = 1 + \pi\rho / 6 \, (5 / 2b_{ij}) \qquad (3.50)$$

The terms appearing in Equation 3.50 are exact and the remaining higher order terms have been neglected since their contribution to g_{ij} is small.

1
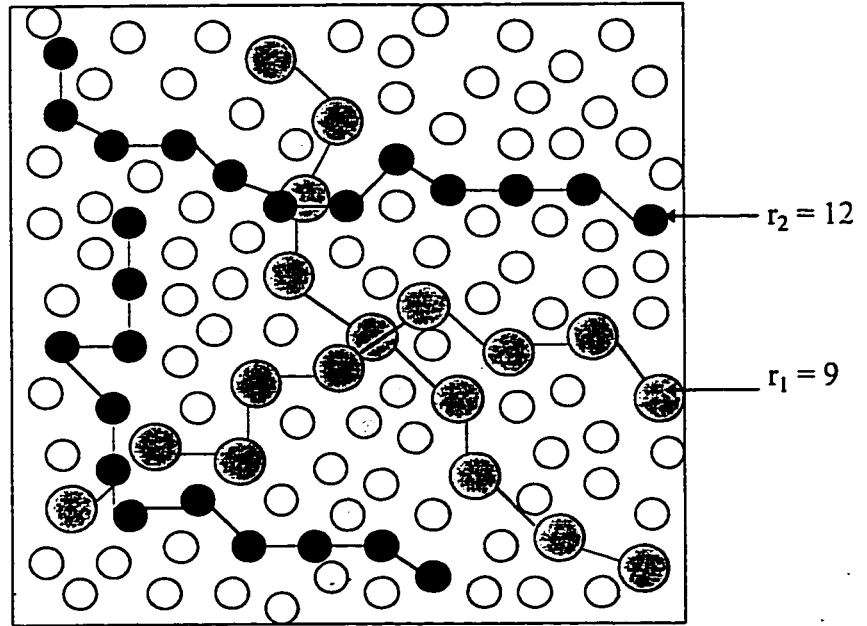
Figure 3.2 A system of interacting sites in a polymer solution ⑥ solvent molecules; ● sites of polymer 1;⊛ sites of polymer 2).

In Equation 3.50 b_{ij} is the composition-dependent mixture volume parameter given by the summation $\sum_k x_k c_{ij,k}$. The terms $c_{ij,k}$ are calculated from mixing rule.

Substituting the expression for b_{ij} and Equation 3.50 into the consistency equations yielded Equations 3.51 and 3.52. It should be noted that this method was previously used by Hamad, (1995) to derive equation of state for nonadditive hard spheres. Same approach is used here to develop the mixing rule for chain molecules.

$$\sigma_{11}^2 \frac{\partial c_{11,2}}{\partial \sigma_{22}} + \sigma_{12}^2 \left(\frac{\partial c_{12,1}}{\partial \sigma_{22}} - \frac{\partial c_{12,1}}{\partial \sigma_{11}} \right) = 0 \tag{3.51}$$

and

$$\sigma_{22}^2 \frac{\partial c_{22,1}}{\partial \sigma_{11}} + \sigma_{12}^2 \left(\frac{\partial c_{12,2}}{\partial \sigma_{11}} - \frac{\partial c_{12,2}}{\partial \sigma_{22}} \right) = 0 \tag{3.52}$$

Equations 3.51 and 3.52 were converted to ordinary differential equations, and solved for the parameters $c_{ij,k}$ (see Appendix C). This resulted to the following mixing rule.

$$c_{12,1} = \left(\sigma_{11}^2 / 20\sigma_{12}^2 \right) \left[r_1^2 \sigma_{11}^3 (1 + r_2) + 2r_1 r_2 \sigma_{11}^2 \sigma_{22} (1 + 4r_1) + r_1 r_2 \sigma_{11} \sigma_{22}^2 (5 + 3r_1) \right] \tag{3.53}$$

$$c_{12,2} = \left(\sigma_{22}^2 / 20\sigma_{12}^2 \right) \left[r_2^2 \sigma_{22}^3 (1 + r_1) + 2r_1 r_2 \sigma_{11} \sigma_{22}^2 (1 + 4r_2) + r_1 r_2 \sigma_{11}^2 \sigma_{22} (5 + 3r_2) \right] \tag{3.54}$$

$$c_{11,2} = \left(r_1 / 20 \right) \left[r_1 \sigma_{11}^3 (1 - r_2) + \sigma_{11}^2 \sigma_{22} \left\{ 5r_1(1 - r_2) - 2r_2(1 - r_1) \right\} + \right.$$
$$\left. r_2 \sigma_{11} \sigma_{22}^2 (13r_1 - 1) + r_2 \sigma_2^3 (5 + 3r_1) \right] \tag{3.55}$$

$$c_{22,1} = (r_2/20)\left[r_2\sigma_{22}^3(1-r_1) + \sigma_{11}\sigma_{22}^2\{5r_2(1-r_1)-2r_1(1-r_2)\} + \right.$$
$$\left. r_1\sigma_{11}^2\sigma_{22}(13r_2-1) + r_1\sigma_{11}^3(5+3r_2)\right] \tag{3.56}$$

where σ_{ij} are the collision diameters of the corresponding sites, r_i is the chain length (number of sites in chain i).

In the limiting case of unbonded hard spheres, $r_1 = r_2 = 1$ and $\sigma_{12} = (\sigma_{11} + \sigma_{22})/2$, Equation 3.53 to Equation 3.56 reduce to a set of equations which simplify to the expressions derived by Hamad (1995).

For reasonably long chain molecules ($r_1 \gg 1$ and $r_2 \gg 1$), Equation 3.53 to Equation 3.56 can reasonably be approximated to the following:

$$c_{12,1} = r_1^2 r_2\left(\sigma_{11}^2/12\sigma_{12}^2\right)\left[\sigma_{11}^3 + 8\sigma_{11}^2\sigma_{22} + 3\sigma_{11}\sigma_{22}^2\right] \tag{3.57}$$

$$c_{12,2} = r_1 r_2^2\left(\sigma_{22}^2/12\sigma_{12}^2\right)\left[\sigma_{22}^3 + 8\sigma_{11}\sigma_{22}^2 + 3\sigma_{11}^2\sigma_{22}\right] \tag{3.58}$$

$$c_{11,2} = \left(r_1^2 r_2/12\right)\left[-\sigma_{11}^3 - 3\sigma_{11}^2\sigma_{22} + 13\sigma_{11}\sigma_{22}^2 + 3\sigma_{22}^3\right] \tag{3.59}$$

$$c_{22,1} = \left(r_1 r_2^2/12\right)\left[-\sigma_{22}^3 - 3\sigma_{11}\sigma_{22}^2 + 13\sigma_{11}^2\sigma_{22} + 3\sigma_{11}^3\right] \tag{3.60}$$

Note that in arriving at Equation 3.57 to Equation 3.60, coefficients in Equation 3.53 to Equation 3.56 were adjusted to reproduce correct limiting values of $c_{ij,k}$.

CHAPTER 4

MODELS VALIDATION AND TESTING

4.1   Mixture Models for Simple Molecules

4.1.1   Introduction

This chapter presents all the mixture models for simple molecules (developed in chapter 4) in their generalized form. The generalized forms of these models are applicable to multicomponent systems. The developed models are used to predict properties of both hypothetical (hard sphere and Lennard-Jones) and real fluids. The predicted properties of model fluids are compared to some simulation data since these data are exact for the model fluid chosen. For real mixtures, experimental data are used as the basis for our model evaluation. In both cases we have compared the predictions of the newly developed models with other models in the literature.

4.1.2   Generalized Mixture Model

The general representation of our mixture models are summarized as follows.

(i)   For the model based on the approximate distinguishing value of the pair correlation function (hence forth referred to as model DVPCF), the compressibility factor is given by:

ʃ

$$Z = 1 + \pi/6\, \rho \sum_{i=1}^{m}\sum_{j=1}^{m} x_i x_j \sigma_{ij}^3 F_{ij}\left(\rho f_{ij}\right) \tag{4.1}$$

with

$$f_{ij} = \left(\sigma_{ii}\sigma_{jj}/\sigma_{ij}\right)\sum_{k=1}^{m} x_k \sigma_{kk}^2 \tag{4.2}$$

(ii)   The single indexed H_i model based on pair correlation functions of Equation 3.9 and Equation 3.46 and solved according to Equation 3.37 is referred to as model H1. The compressibility factor for this model is given by:

$$Z = 1 + \rho \sum_{i=1}^{m} x_i \left(\sum_{j=1}^{m} x_j \sigma_{ij}^3\right) H_i\left[\rho\left(x_1\sigma_{11}^3 + x_2 h_{ij}\right)\right] \tag{4.3}$$

where

$$h_{ij} = \frac{\sigma_{ij}^3\left(\overline{C}_{ij}/5 + \sigma_{ii}^3\sigma_{jj}^3\right) - \sigma_{jj}^3\left(\overline{C}_{ij}/5 + \sigma_{ij}^6\right)}{\sigma_{ij}^6 - \sigma_{ii}^3\sigma_{jj}^3} \tag{4.4}$$

The parameters $\overline{C}_{ij}$ and $\overline{C}_{ij}$ in Equation 4.4 are given by:

$$\overline{C}_{ij} = \sigma_{ii}^3\left(\sigma_{ii}^3 - 18\sigma_{ii}\sigma_{ij}^2 + 32\sigma_{ij}^3\right) \tag{4.5}$$

and

$$\overline{C}_{ij} = \sigma_{jj}^3\left(\sigma_{jj}^3 - 18\sigma_{jj}\sigma_{ij}^2 + 32\sigma_{ij}^3\right) \tag{4.6}$$

(iii)   The model formulated as in (ii) above and solved according to Equation 3.37 is referred to as model H2 with the following compressibility expression.

$$Z = 1 + \rho \sum_{i=1}^{m} x_i \left(\sum_{j=1}^{m} x_j \sigma_{ij}^3\right) H_i\left[\rho\left(h_i\right)\right] \tag{4.7}$$

where

$$h_i = \sum_{j=1}^{m} x_j \sigma_{ij}^3 f_{ij} \left/ \sum_{j=1}^{m} x_j \sigma_{ij}^3 \right.$$ (4.8)

where the parameter f_{ij} is as given in Equation 4.9.

(iv)   The general form of model fij (Equations 3.25 to 3.29) that is also applicable to non-additive hard spheres was obtained with the same procedure as in deriving Equations 3.25 to 3.29 but using the contact value of the following pair correlation function for non-additive hard spheres. This resulted to the following equation.

$$f_{ij} = \sum_{k=1}^{m} x_k c_{ij,k}$$ (4.9)

The term $c_{ij,k}$ in Equation 4.9 was obtained by expanding the pair correlation function Hamad (1995). The resulting expression interms of the exact third virial coefficient is (Kihara, 1943):

$$c_{ij,k} = \frac{1}{60\sigma_{ij}^2} \cdot \frac{\partial C_{ij,k}}{\partial \sigma_{ij}} \cdot \frac{1}{(\pi N_A/6)^2}$$ (4.9a)

where $C_{ij,k}$ are the coefficients of the third virial coefficient. σ_{ij} is the collision diameter of molecular pair i and j. N_A is the Avogadro's number.

If s is the maximum of the three collision diameters (σ_{ij}, σ_{ik} and σ_{jk}), then, for

$\sigma_{ij} + \sigma_{ik} + \sigma_{jk} \geq 2s$:

$$c_{ij,k} = \frac{1}{5\sigma_{ij}} (\sigma_{ik} + \sigma_{jk} - \sigma_{ij})^2 \left[\sigma_{ij} (\sigma_{ij} + 2\sigma_{ik} + 2\sigma_{jk}) - 3(\sigma_{ik} - \sigma_{jk})^2 \right]$$ (4.10)

and for $\sigma_{ij} + \sigma_{ik} + \sigma_{jk} < 2s$, $c_{ij,k}$ is given by

$$c_{ij,k} = \frac{16}{5s^2}\left(1 - \frac{\partial s}{\partial \sigma_{ij}}\right)\sigma_{ik}^3\sigma_{jk}^3 \qquad (4.11)$$

(v)   For model G1 (obtained by taking hard sphere packing fraction as the unindexed parameter g):

$$Z = 1 + \rho\sum\sum x_i x_j \sigma_{ij}^3 G[\rho(g)] \qquad (4.12)$$

with $g = \sum x_k \sigma_{kk}^3$

(vi)   For model G2 which was obtained from expansion of Equation 3.10 and Equation 3.46 with respect to density, the generalized expression for compressibility factor Z is the same as that in G1 where g is given by:

$$g = \frac{\displaystyle\sum_i^m\sum_j^m x_i x_j \sigma_{ij}^3 f_{ij}}{\displaystyle\sum_i^m\sum_j^m x_i x_j \sigma_{ij}^3} \qquad (4.13)$$

The parameter f_{ij} is as defined in model H2 above.

All the above models including models B1 (presented in Appendix B) and model D1 Equation 4.3 to Equation 4.4, reduce to the correct pure component compressibility in the limit of identical molecular parameters (size and energy). The models also satisfy the low pressure (ideal gas) limit. Models D1 (see Equations 4.3 to 4.4) and B1 were not generalized due to their complexity.

4.1.3 Mixtures of (additive) Hard Spheres

Figures 4.1 through 4.6 show the predictions of compressibility factor of a binary equimolar hard sphere fluid with size ratio $\sigma_2/\sigma_1 = 3.0$. These predictions are compared with the corresponding values calculated using the Mansoori-Carnahan-Starling-Leland MCSL equation of state (Mansoori et al., 1971), the van der Waals one fluid theory, and molecular simulation data (Alder, 1964). From these figures, it is clear that at the stated size ratio, all the developed models satisfactorily agree with the simulation data within the tested mixture density range. Model f_{ij} shows the best results with an average deviation of 0.62% from the simulation data. The maximum calculated error for this model occurs at a packing fraction ($\xi = \pi/6 \sum x_i \sigma_{ii}^3$) of 0.44. At this point Z is underpredicted by about 1.1%. For mixture densities up to 0.44, model f_{ij} under predicts Z. At a density of 0.51, however, the compressibility factor is over predicted. As it will be seen later, the model generally over predicts Z at mixture densities greater than about 0.45 even at high compositions of the smaller component. It should be noted that this density is close to the freezing density, the only phase transition (fluid-solid) for hard spheres which occurs at a density of about 0.50 (Fries and Hansen, 1983). The MCSL equation is very accurate because it is specific to the hard sphere mixtures, and cannot be used for other mixtures. The new models are general, therefore, they can be used for mixtures other than hard spheres.
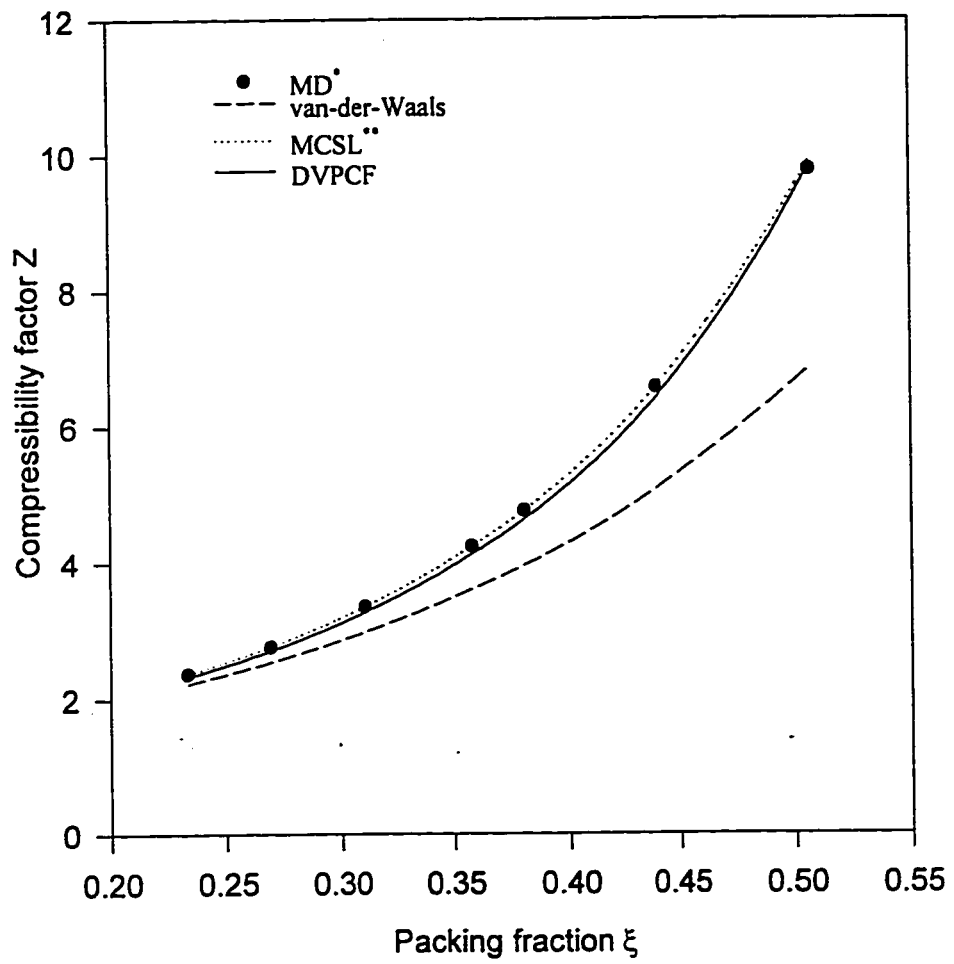
Figure 4.1   Compressibility factor of equimolar mixture of binary hard sphere fluid (σ_2/σ_1=3.0) using model DVPCF (* :- Simulation results of Alder, 1964; ** :- from Mansoori et al., 1971).
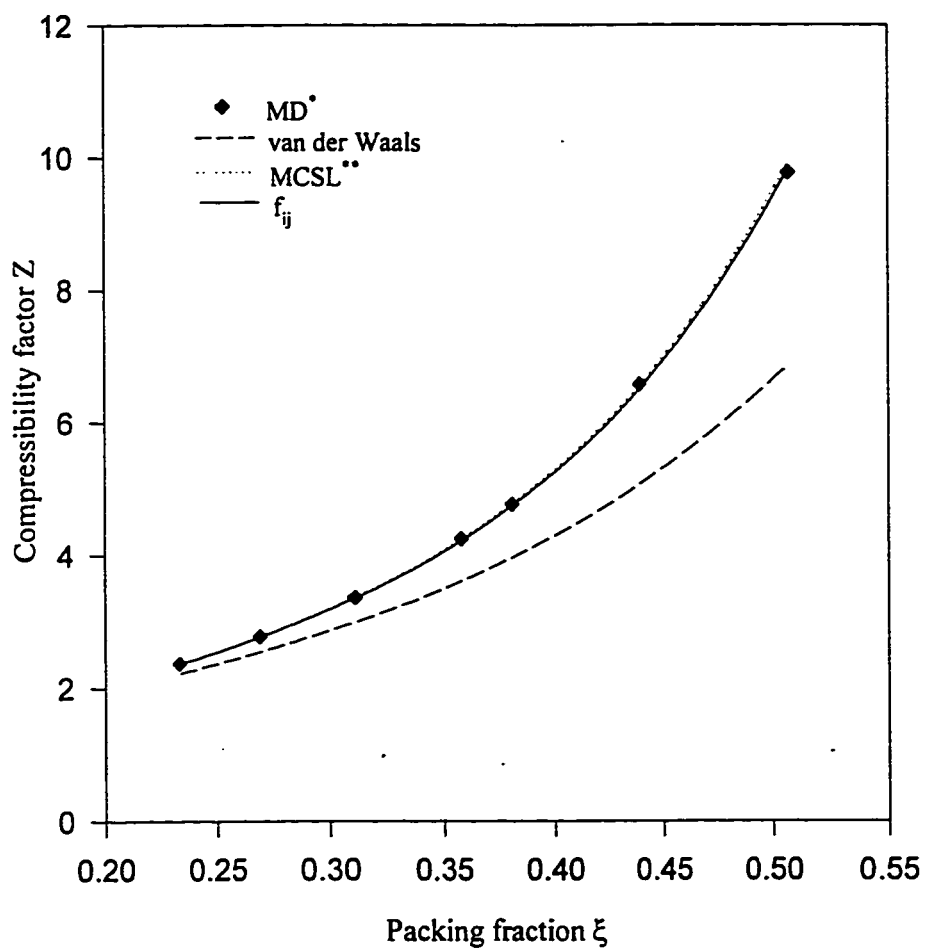
Figure 4.2   Compressibility factor of equimolar mixture of binary hard sphere fluid (σ_2/σ_1=3.0) using model f_{ij} (* :- Simulation results of Alder, 1964; ** :- from Mansoori et al., 1971).

f
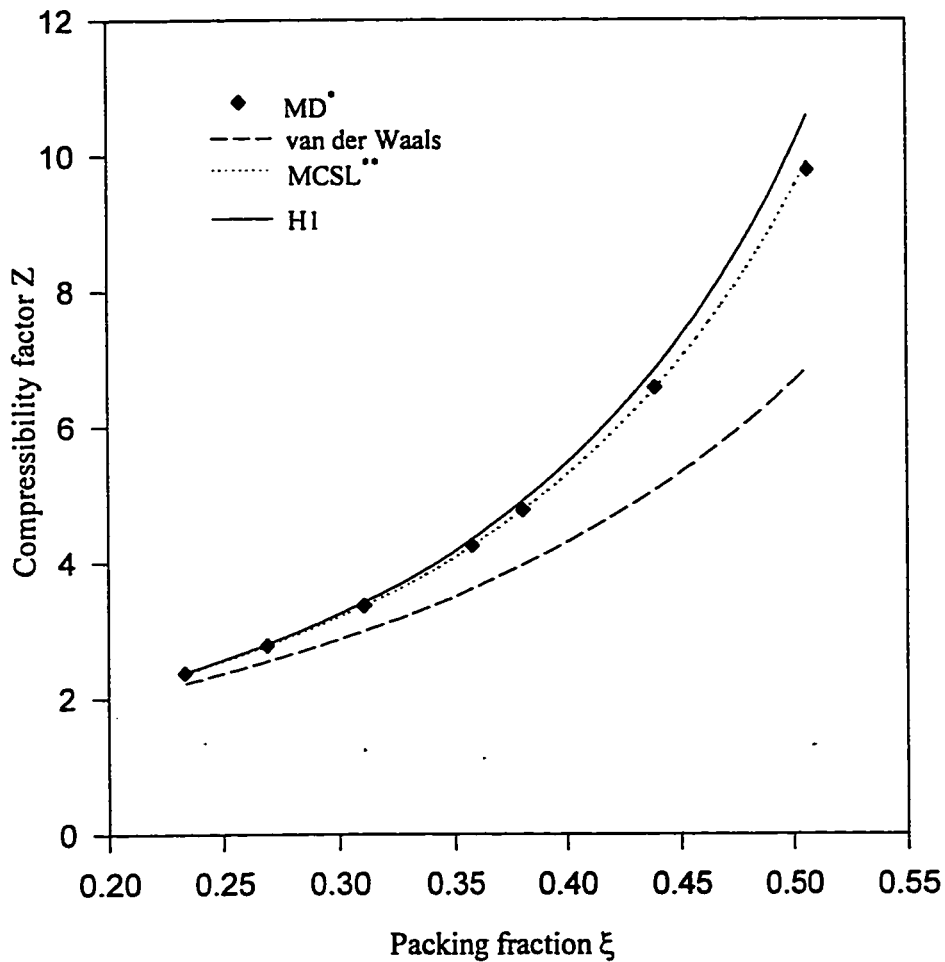
Figure 4.3   Compressibility factor of equimolar mixture of binary hard sphere fluid $(\sigma_2/\sigma_1=3.0)$ using model H1 (* :- Simulation results of Alder, 1964; ** :- from Mansoori et al., 1971).
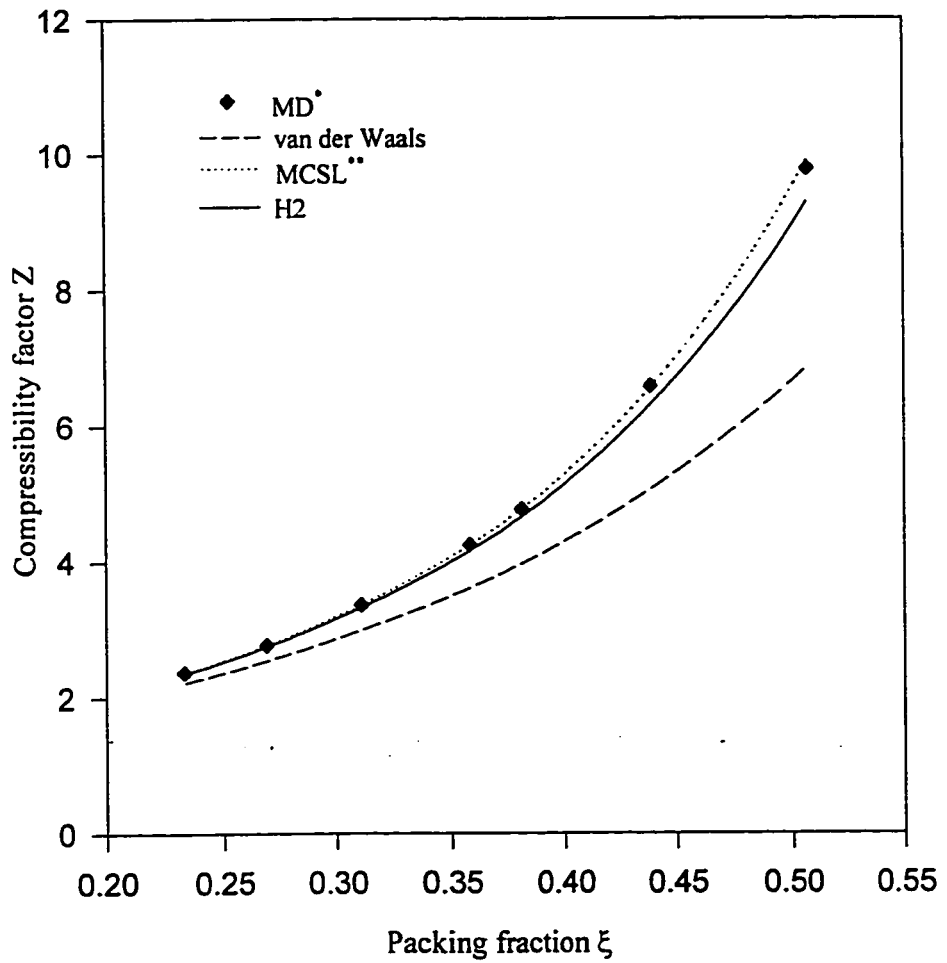
Figure 4.4   Compressibility factor of equimolar mixture of binary hard sphere fluid $(\sigma_2/\sigma_1=3.0)$ using model H2 (* :- Simulation results of Alder, 1964; ** :- from Mansoori et al., 1971).
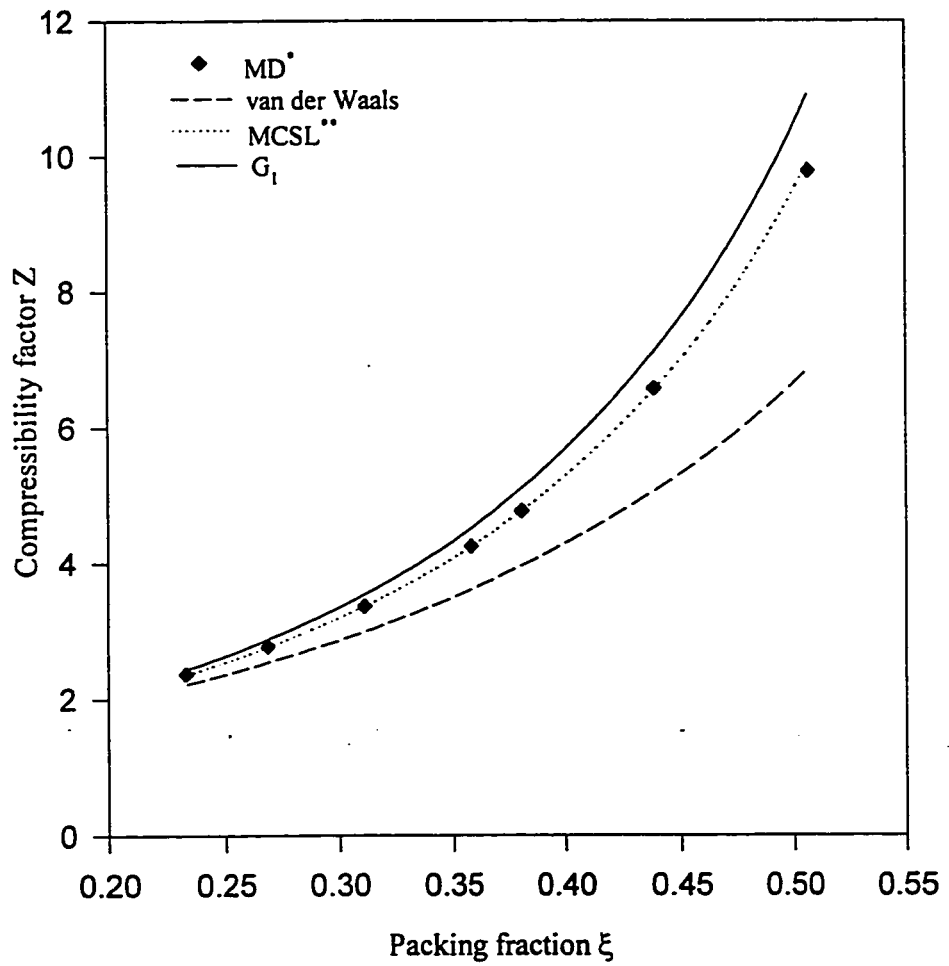
Figure 4.5   Compressibility factor of equimolar mixture of binary hard sphere fluid $(\sigma_2/\sigma_1 = 3.0)$ using model G1 (* :- Simulation results of Alder, 1964; ** :- from Mansoori et al., 1971).
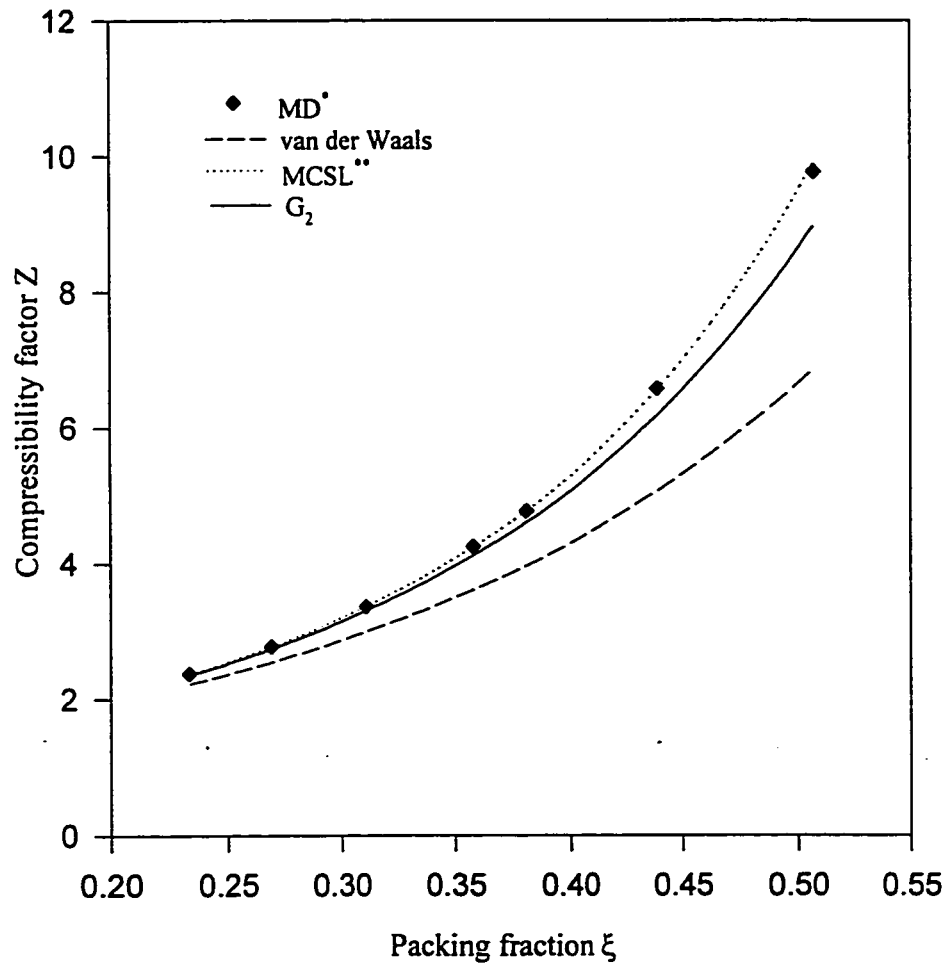
Figure 4.6   Compressibility factor of equimolar mixture of binary hard sphere fluid ($\sigma_2/\sigma_1 = 3.0$) using model G2 (* :- Simulation results of Alder, 1964; ** :- from Mansoori et al., 1971).

The superiority of model f_{ij} is attributable to the fact that, unlike H_i and G models, it fully accounts for all pair wise interactions in F_{ij}.

Expressions for B1 and D1 were not generalized to multicomponent form due to their complexity. Nonetheless, these two models predict hard spheres mixture compressibility factor satisfactorily. As shown in Figure 4.7, the models predict much more accurately than the van der Waals one fluid theory. The accuracy of the models decreases at higher density (packing fraction).

In Figure 4.8, we have tested our model DVPCF against the accurate Mansoori-Carnahan-Starling-Leland (MCSL) equation of state model (Mansoori et al., 1971) at different packing fractions and mole fractions. There is a reasonable agreement between the two models. The deviation shown is a strong function of the packing fraction used. In the region of low mole fraction of the smaller component, model DVPCF slightly underpredicts the MCSL model. This trend has, however, changed around $x_1 = 0.8$ for $\xi = 0.4$ and around $x_1 = 0.6$ for $\xi = 0.45$. For high packing fractions, the new model shows an inflection point in the low mole fraction region of the larger molecules. This is probably due to the factor $(1-\eta)^2$ that tends to zero in this region. This points to a limitation of the combination of this model with the Carnahan Starling (CS) equation. The CS equation is accurate but is known to behave incorrectly at high densities by predicting infinite pressure at a packing fraction of unity, while physically the infinite pressure occurs at the closest packing fraction of $(\pi\sqrt{2}/6)$ about 0.74. The combination of the new model with
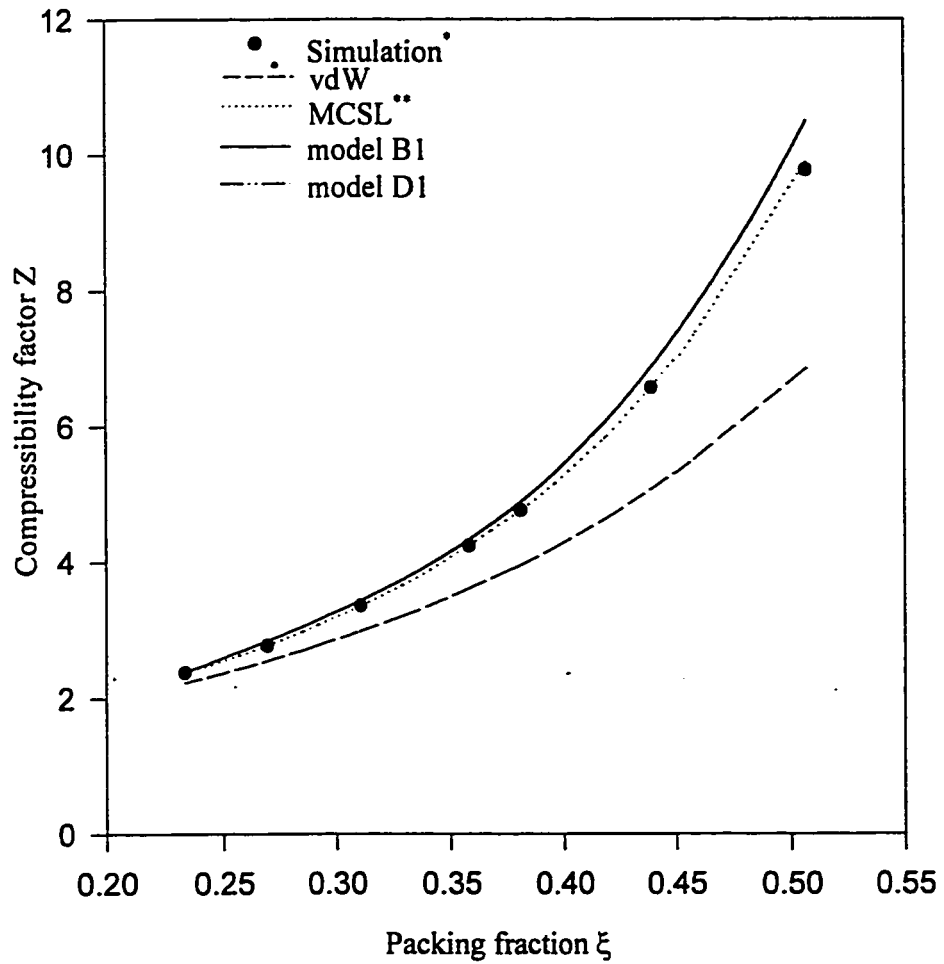
Figure 4.7 Compressibility factor of equimolar mixture of binary hard sphere fluid (σ_2/σ_1=3.0) using models B1 and D1 (* :- Simulation results of Alder, 1964; ** :- from Mansoori et al., 1971; there is overlap of predicted values of B1 and D1).

1
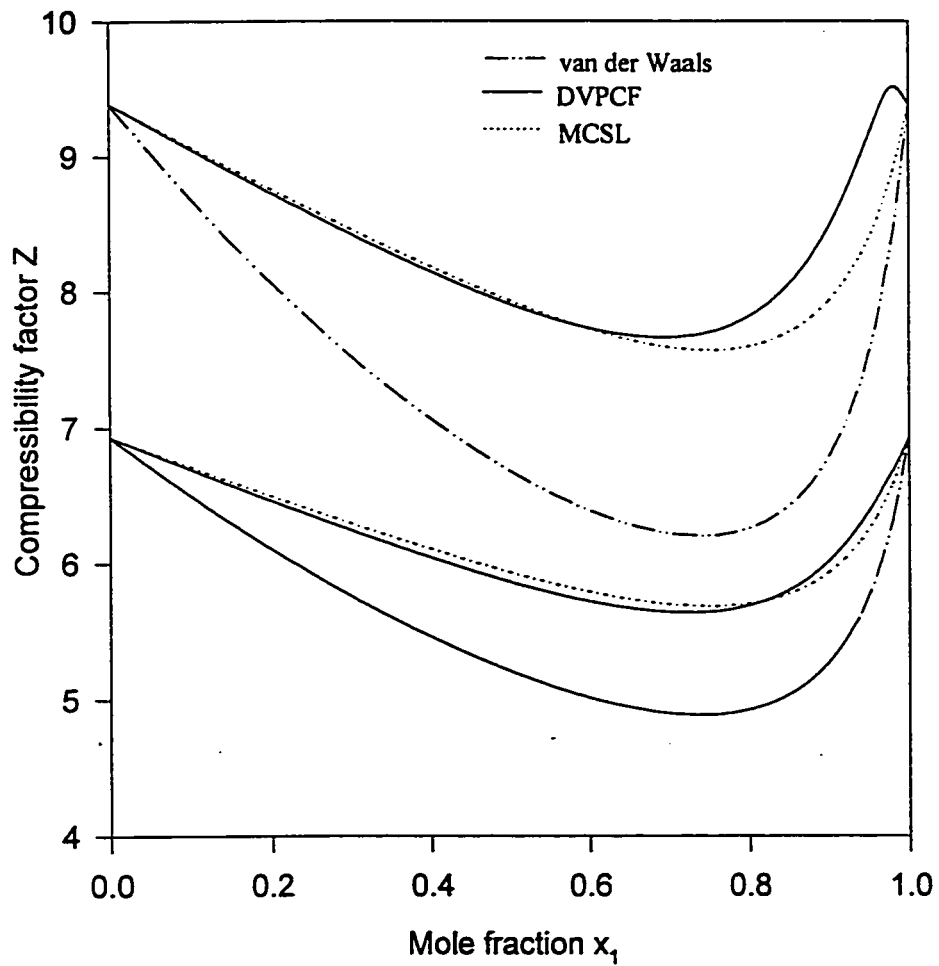
Figure 4.8 Compressibility factor as a function of mole fraction x_1 for binary hard spheres mixture using model DVPCF (σ_2/σ_1 = 2.0). The upper curves are for packing fraction ξ = 0.45, and the lower curves for ξ = 0.40.

the CS equation predicts infinite pressure for mixture packing fractions much less than unity. Except for the small region of its abnormal behavior, model DVPCF predicts more accurately than the van der Waals one-fluid model.

Generally, all the models show higher accuracy at lower densities. This is expected because the Carnahan-Starling pure equation of state which was used in evaluating the models' parameters agree almost exactly with molecular dynamics results for mixture densities up to about 0.5. Beyond this density, both Carnahan-Starling and other theories such as the self consistent approximation and the Percus-Yevick theories are not satisfactory (Reed and Gubbins, 1973).

Besides Figures 4.1 to 4.6, Tables 4.1 and 4.2 present further details of the deviations of our models from simulation data. It is clear, therefore, that for hard sphere fluids, all the mixture models perform much better than the van der Waals model. In spite of its relatively high errors, the van der Waals model is commonly used in science and engineering due to its simplicity. Although our models are more accurate than the van der Waals', evaluation of mixture properties using these models are almost equally tasking.

The MCSL mixture equation of state predicts the compressibility factor with the same accuracy as model f_{ij} and it is simple to use. This equation has, however, limited application since it can only be used for hard sphere mixture. It can, therefore, not be used to calculate fluid properties using the modified hard sphere theories that involve attractive forces.

Table 4.1 Compressibility factor of equimolar binary hard sphere mixture ($\sigma_2/\sigma_1 = 3$).

ξ	Z_{SIM} ($\pm 1\%$)	vdW	MCSL	f_{ij}	H1	H2	G1	G2
				Deviation of Model (%)				
0.2333	2.37	- 6.2160	-0.091	- 0.372	0.391	- 0.715	2.832	- 0.956
0.2692	2.77	- 8.1810	0.067	- 0.337	0.838	- 0.889	3.825	- 1.271
0.3106	3.36	- 11.194	-0.121	- 0.684	1.121	- 1.577	4.661	- 2.185
0.3583	4.24	- 14.886	0.034	- 0.723	2.057	- 2.192	6.089	- 3.169
0.3808	4.76	- 16.868	0.075	- 0.767	2.574	- 2.592	6.750	- 3.792
0.4393	6.57	- 22.857	-0.066	- 1.059	4.084	- 4.137	8.250	- 6.089
0.5068	9.77	- 29.856	1.294	0.398	8.468	- 5.043	11.693	- 8.317
Average Deviation[+]				< 1%	2.79	2.449	6.3	3.683
Average Deviation[++]				< 1%	3.703	1.910	7.085	3.230
Average Deviation[+++]				< 1%	2.948	2.248	6.508	3.469

+ for entries in the table using CS pure equation of state; ++ absolute average deviation using Sanchez (1994) EOS; +++ absolute average deviation using Kolafa EOS Boublík and Nezbeda (1986).

Table 4.2 Variation of hard sphere mixture compressibility factor with density and composition hard sphere mixture $(\sigma_{22}/\sigma_{11} = 2)$.

x1	$\rho\sigma_x^3$	Z_{MD}	Deviation of Model (%)						
			vdW	MCSL	f_{ij}	H1	H2	G1	G2
0.9500	0.45	8.71	-13.400	-3.56	-3.123	24.928	-5.283	0.125	-6.544
0.9500	0.50	11.5	-12.833	0.341	2.327	66.376	-1.919	4.783	-4.015
0.9500	0.55	16.4	-17.171	-0.626	5.591	177.541	-3.24	4.376	-6.553
0.8984	0.45	7.82	-13.487	1.3	1.571	25.702	-1.539	7.143	-3.209
0.8984	0.50	10.7	-17.596	1.247	3.054	47.702	-2.466	8.038	-5.066
0.8984	0.55	14.8	-21.071	2.953	8.706	99.75	-1.762	10.832	-5.836
0.8984	0.59	22.5	-34.067	-8.807	2.786	161.251	-13.6	-1.138	-18.697
0.8008	0.45	7.55	-17.128	0.615	0.427	16.12	-2.875	7.653	-4.689
0.8008	0.50	10.10	-20.353	2.544	3.390	29.489	-2.209	10.903	-5.021
0.8008	0.55	14.30	-26.620	1.582	4.858	47.802	-4.489	11.046	-8.658
Average Deviation[+]				2.607	4.203	72.456	6.388	12.904	10.511
Average Deviation[++]				2.607	20.104	137.912	3.726	16.998	8.082
Average Deviation[+++]				2.607	3.604	68.266	6.238	13.136	10.260

+ for entries in the table using CS pure equation of state; ++ absolute average deviation using Sanchez (1994) EOS; +++ absolute average deviation using Kolafa EOS Boublik and Nezbeda (1986).

The Sanchez' and the Kolafa's equations of state referenced in Tables 4.1 and 4.2 are given in Equations 4.14 and 4.15 respectively.

$$Z_{4,3} = \frac{1 + 1.024385\eta + 1.104537\eta^2 - 0.4611472\eta^3 - 0.7430382\eta^4}{1 - 2.975615\eta + 3.007000\eta^2 - 1.097758\eta^3} \tag{4.14}$$

$$Z = 1 + \frac{12\eta - 6\eta^2 + \eta^3 - 2\eta^4}{3(1-\eta)^3} \tag{4.15}$$

where η is the packing fraction. Subscripts 4, 3 on Z indicate the highest powers of the polynomials in the numerator and the denominator of the compressibility expression.

Sanchez (1994) derived Equation 4.14 using the Pade approximant theory (Pade, 1892). Boublik and Nezbeda (1986) reported Equation 4.15 as Kolafa equation of state. As shown in Tables 4.1 and 4.2, variation of the pure equation of state shows little effect on the accuracy of the predicted mixture properties. This is expected since all pure equations of state are known to be very accurate. Their major difference lies in their complexities.

From Table 4.2, it can be inferred that the models perform almost equally well at non-identical mixture compositions. The size, composition and reduced density values used in Table 4.2 present a more severe test of the models. This is because there are more of the smaller molecules in the mixture (higher x_1), hence, domination of the bigger molecules is highly reduced.

Figures 4.3 to 4.6 clearly show that deviation of models H1, H2, G1 and G2 increase with the mixture packing fraction. Since models H1 and H2 and models G1 and G2 deviate in an opposite manner, a combination of these two pairs can improve prediction results at high packing fractions. Table 4.3 compares the deviations of such a weighted model (H3), taken as $\tau H1 + (1-\tau)H2$ with models H1 and H2 in predicting the simulation data of Alder (1964). Note that this also applies to models G1 and G2. Table 4.4 therefore compares a similar model G3 to models G1 and G2 in predicting compressibility factor at high mixture packing fraction (simulation data are from Fries and Hansen, 1983). In both cases, varying τ can improve the prediction results up to four times. Note that maximum deviation in G3 remain consistently high. This always occurred at the highest packing fraction of the data ($\xi = 0.59$, $x_1 = 0.8984$), and at this point, both models underestimate the compressibility factor (see Table 4.5). The improvements obtained for the high packing fraction data is even more pronounced in H3 because predictions of model H1 are poor at these packing fractions. At $\xi = 0.59$, prediction errors in models H1 and H2 were reduced from about 70% and 4%, respectively, to less than 2% in H3.

TABLE 4.3 Compressibility factor of a mixture of hard spheres using model H3 ($x_1 = x_2 = 0.5$; $\sigma_{22}/\sigma_{11} = 2.0$).

τ	Absolute deviation of model H3 (%)	
	Average	Maximum
1 (H3 ≡ H1)	2.78	8.47
0.60	0.37	2.00
0.55	0.37	1.29
0.50	0.44	0.71
0.45	0.53	1.11
0.40	0.78	1.51
0 (H3 ≡ H2)	2.45	5.04

TABLE 4.4 Compressibility factor of a mixture of hard spheres using model G3 ($x_1 = x_2 = 0.5$; $\sigma_{22}/\sigma_{11} = 2.0$).

τ	Absolute deviation of model G3 (%)	
	Average	Maximum
1 (G3 $\equiv$ G1)	6.60	11.05
0.60	3.06	8.77
0.55	2.75	9.65
0.50	2.44	10.55
0.45	2.76	11.42
0.40	2.29	12.21
0 (G3 $\equiv$ G2)	6.83	18.70

TABLE 4.5 Improved compressibility factor prediction by model G3.

X_1	ξ	Z_{SIM}	Model deviation (%)		
			G1	G2	G3
0.9500	0.45	8.71	0.125	-6.544	-2.63
0.9500	0.50	11.50	4.783	-4.015	1.12
0.9500	0.55	16.40	4.376	-6.553	-0.21
0.8984	0.45	7.82	7.143	-3.209	2.80
0.8984	0.50	10.70	8.038	-5.066	2.48
0.8984	0.55	14.80	10.832	-5.836	3.67
0.8984	0.59	22.50	-1.138	-18.697	-8.77
0.8008	0.45	7.55.	7.653	-4.689	2.42
0.8008	0.50	10.10	10.903	-5.021	4.07
0.8008	0.55	14.30	11.046	-8.658	2.46
Absolute average deviation (%)			6.604	6.829	3.06

4.1.4 Mixtures of Non-additive Hard spheres (NAHS)

In additive hard sphere mixtures, the unlike particles' collision diameter σ_{ij} ($i \neq j$) is characterized only by the individual like particle collision diameters [$\sigma_{ij} = (\sigma_{ii} + \sigma_{jj})/2$]. For non-additive hard spheres, however, an additional non-additivity parameter Δ is required to fully describe the unlike particle collision diameter (see Figure 4.9) σ_{ij} =$(1+\Delta)(\sigma_{ii} + \sigma_{jj})/2$. Molecules with positive non-additivity have high repulsion. At sufficiently high densities, their mixtures become thermodynamically unstable, and they exhibit phase separation. Mixtures of molecules with negative non-additivity show association, and they do not phase separate.

Although non-additive hard spheres represent a simple fluid model, its distribution function resembles those of real fluids, hence it is widely used in perturbation theories (Jung and Jhon, 1994). Several observed phase behaviors in real mixtures have been attributed to non-additivity. The experimentally observed heterocordination in liquid alkali group IV alloys (Alblas et al., 1984) and aqueous electrolyte solutions (Gaminiti, 1982) are due to negative non-additivity. The homocoordination (phase segregation) observed in liquid alloys of Ti - Te (Ichigawa et al., 1974) and supercritical aqueous NaCl (Pitzer et al., 1985) are attributed to positive non-additivity. In fact at high pressures (~ 10^5 bar), even hydrogen-helium mixture exhibits phase separation due to positive non-additivity (Schouten et al., 1985).

$\Delta = -1/3$

σ_{12}

$\Delta = 0$ (additive HS)

σ_{12}

$\Delta = +2/3$

σ_{12}
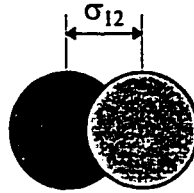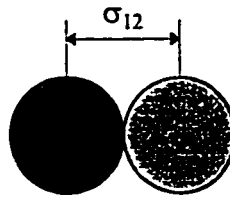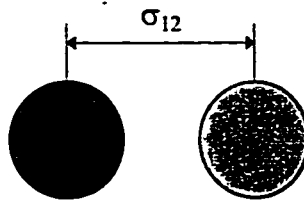
Figure 4.9 Unlike particle collision diameters of non-additive hard spheres.

4.1.4.1 Compressibility factor for non-additive hard spheres

Figures 4.10 to 4.21 show variation of compressibility factor with reduced density for our models at different compositions and non-additivity parameters. For the model f_{ij} (Figures 4.10 to 4.12), both at $x_1 = 0.1$ and $x_1 = 0.25$, the model agrees very well with the simulation data of Jung and Jhon (1994). For mixture densities up to 1.2, model f_{ij} predicts better than van der Waals 1-fluid model at higher deviations from additive hard spheres ($\Delta = -0.5$ and $\Delta = 0.3$) for both $x_1 = 0.1$ and $x_1 = 0.25$. At $\Delta = -0.1$, both f_{ij} and the vdW-1f model predict Z accurately. The later is known to be reliable for soft spheres. In the van der Waals model, the binary hard spheres mixture is represented by a single hypothetical fluid of size σ_x ($\sigma_x^3 = x_1^2\sigma_1^3 + 2x_1x_2\sigma_{12}^3 + x_2^2\sigma_2^3$). If vdW-1f reduced density ($\rho^* = \rho\sigma_x^3$) is taken as an independent variable, the fluid's compressibility factor expression has, therefore, no explicit dependence on Δ. This should correspond to compressibility for $\Delta = 0$, since at this value of Δ, for symmetric hard spheres, $\sigma_{12} = 1/2(\sigma_1+\sigma_2)(1+\Delta) = \sigma_1 = \sigma_2 = \sigma$, i.e. true one component fluid. This explains the accuracy of vdW-1f and our models at small deviations from additivity ($\Delta = -0.1$ in Figures 4.10 to 4.21) and it should apply to all models based on the theory of corresponding states.

Figures 4.12, 4.15, 4.18 and 4.21 clearly show that, for equimolar composition and equal molecular sizes, our models underpredict the compressibility factor at $\Delta = -0.5$ and overpredict it at $\Delta = 0.3$. The magnitudes of these deviations increase with the reduced density.
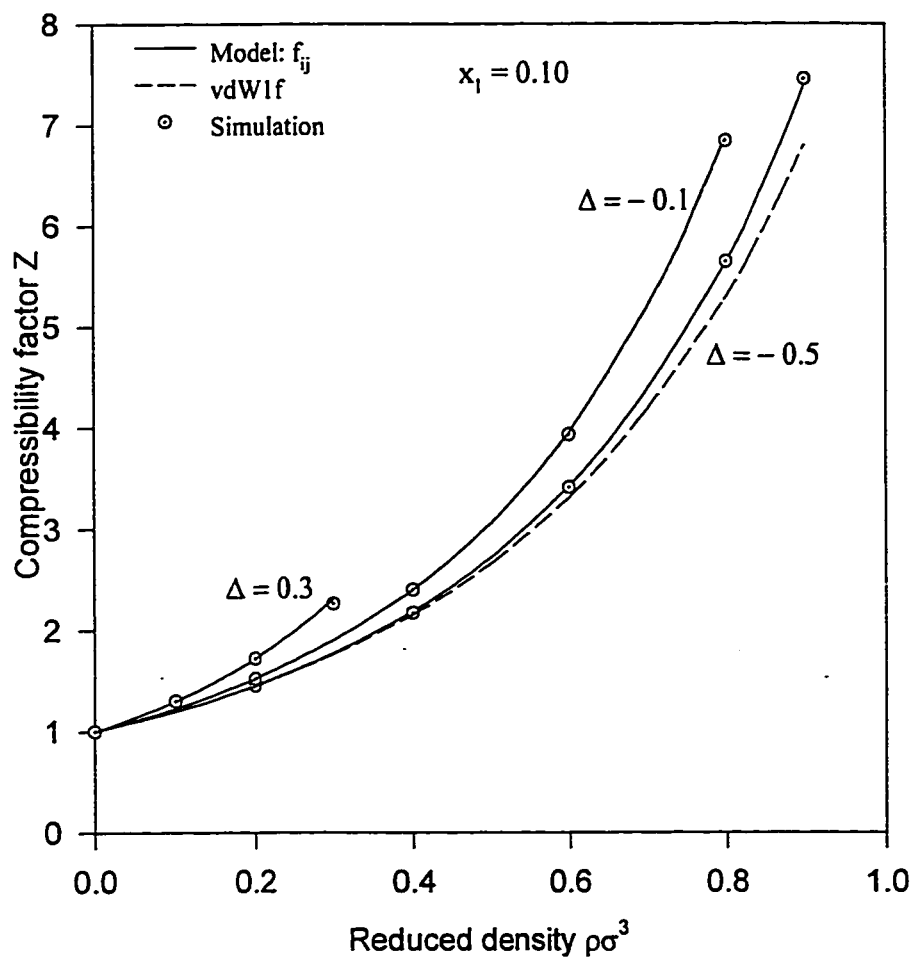
Figure 4.10 Effects of mixture density and Δ on the compressibility factor of symmetric NAHS for model f_{ij} at $x_1 = 0.1$. The points represent Monte Carlo simulation data from Jung and Jhon (1995). vdW-1f and f_{ij} overlap for $\Delta = 0.3$ and $- 0.1$.

i
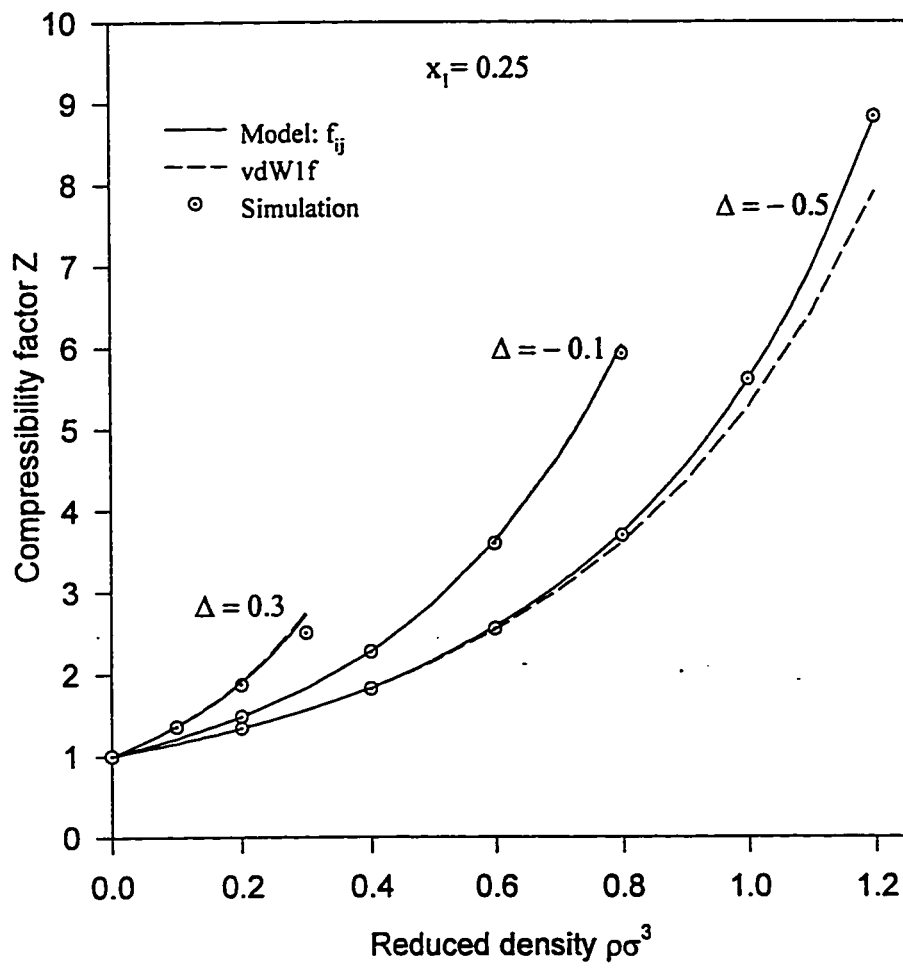
Figure 4.11 Effects of mixture density and Δ on the compressibility factor of symmetric NAHS for model f_{ij} at $x_1 = 0.25$. The points represent Monte Carlo simulation data from Jung and Jhon (1995). vdW-1f and f_{ij} overlap for Δ = 0.3 and - 0.1.
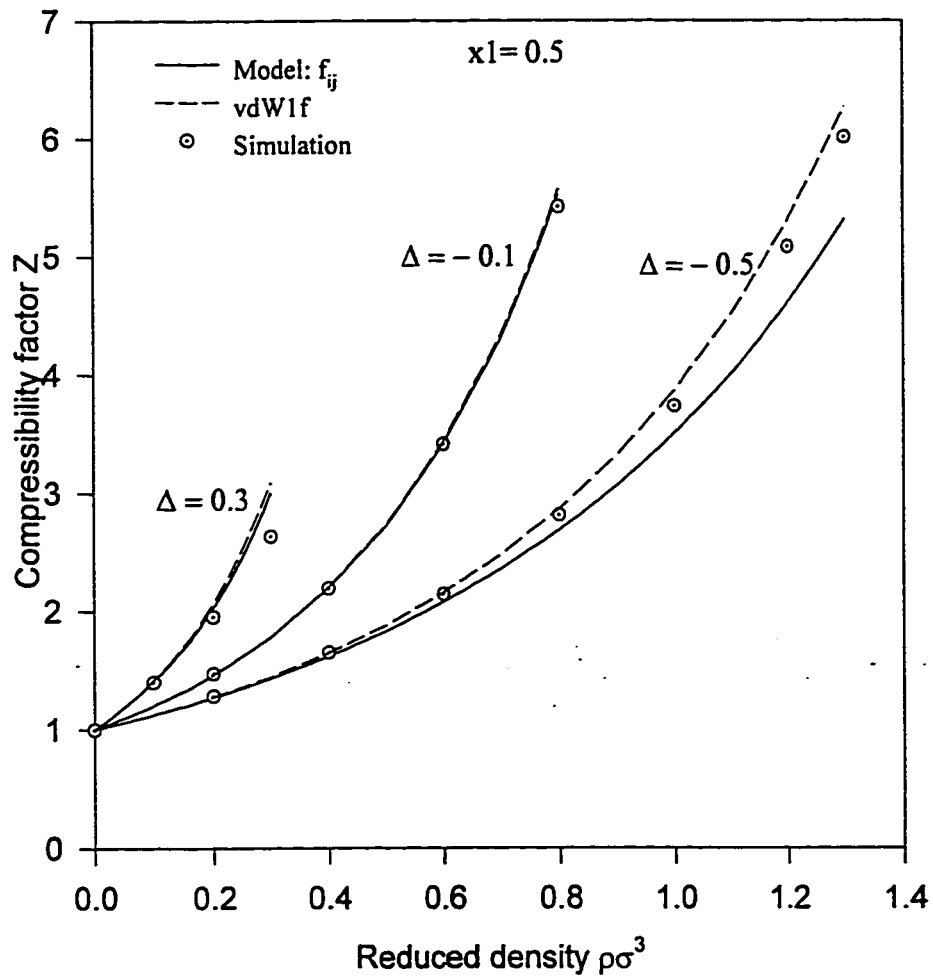
Figure 4.12 Effects of mixture density and Δ on the compressibility factor of symmetric NAHS for model f_{ij} at $x_1 = 0.50$. The points represent Monte Carlo simulation data from Jung and Jhon (1995). vdW-1f and f_{ij} overlap for $\Delta = -0.1$.
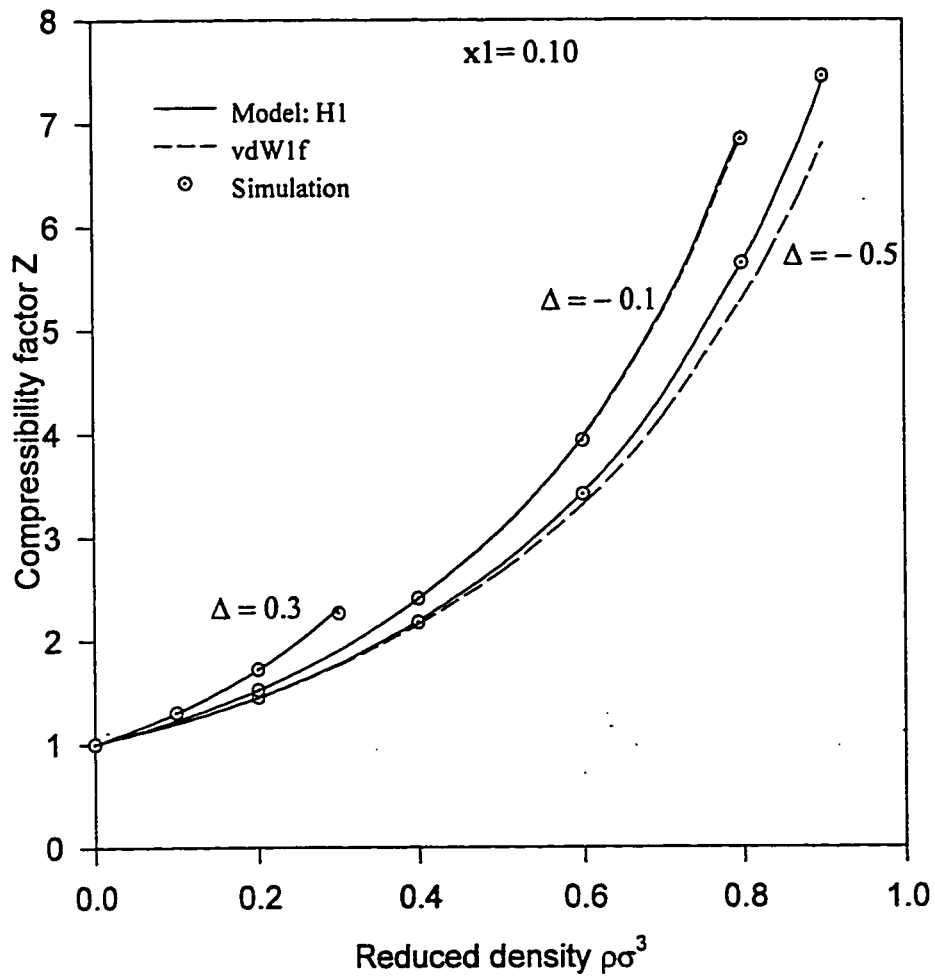
Figure 4.13 Effects of mixture density and Δ on the compressibility factor of symmetric NAHS for model H1 at $x_1 = 0.1$. The points represent Monte Carlo simulation data from Jung and Jhon (1995). vdW-1f and H1 overlap for $\Delta = 0.3$ and -0.1.
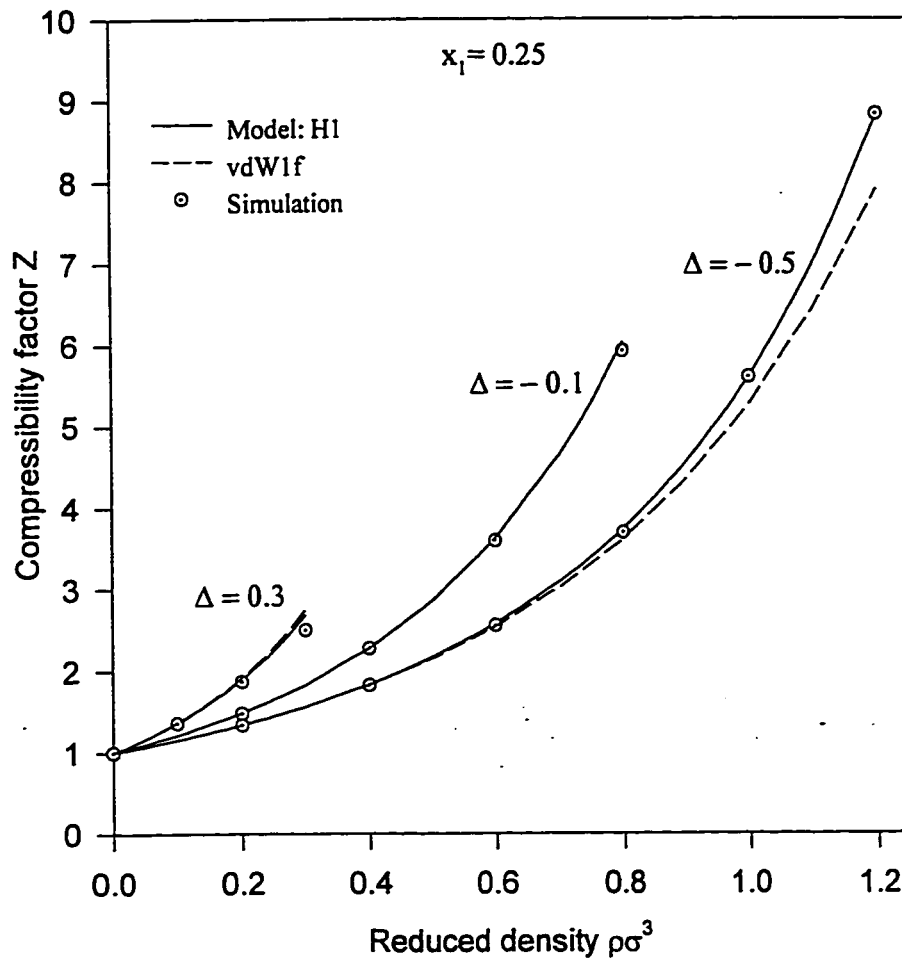
Figure 4.14 Effects of mixture density and Δ on the compressibility factor of symmetric NAHS for model H1 at x1= 0.25. The points represent Monte Carlo simulation data from Jung and Jhon (1995). vdW-1f and H1 overlap for Δ = - 0.1.
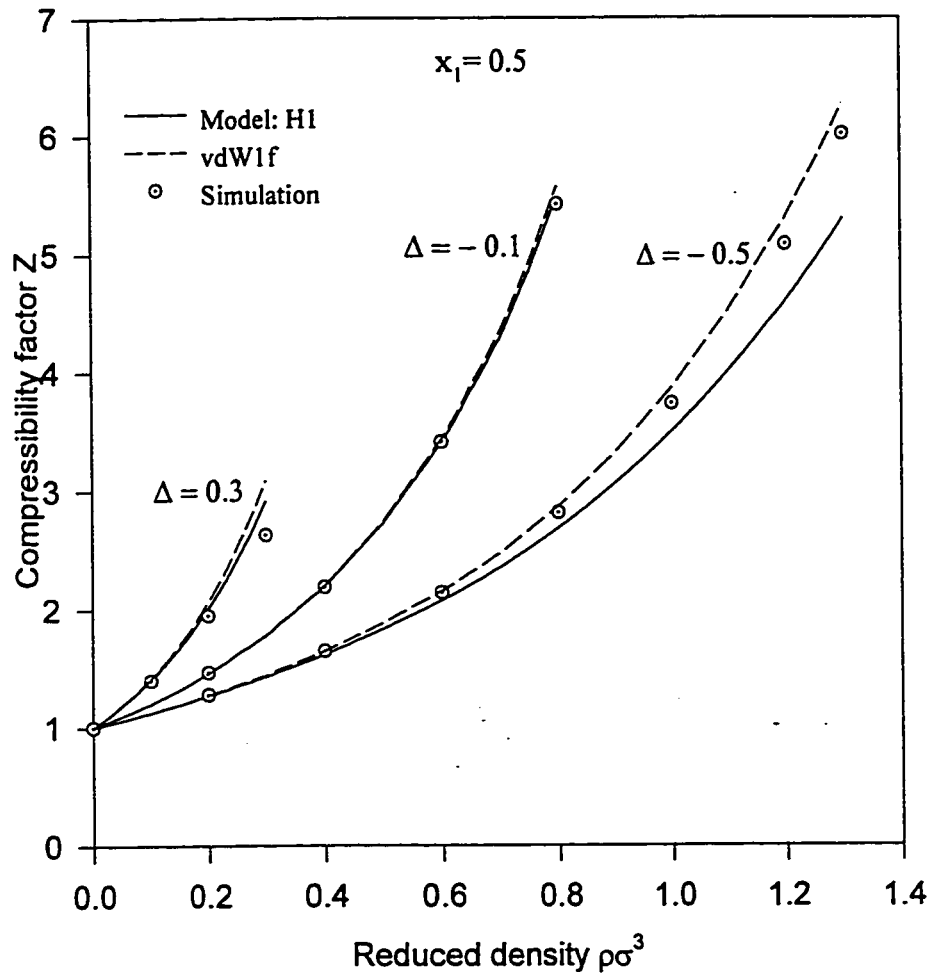
Figure 4.15 Effects of mixture density and Δ on the compressibility factor of symmetric NAHS for model H1 at x1= 0.50. The points represent Monte Carlo simulation data from Jung and Jhon (1995).
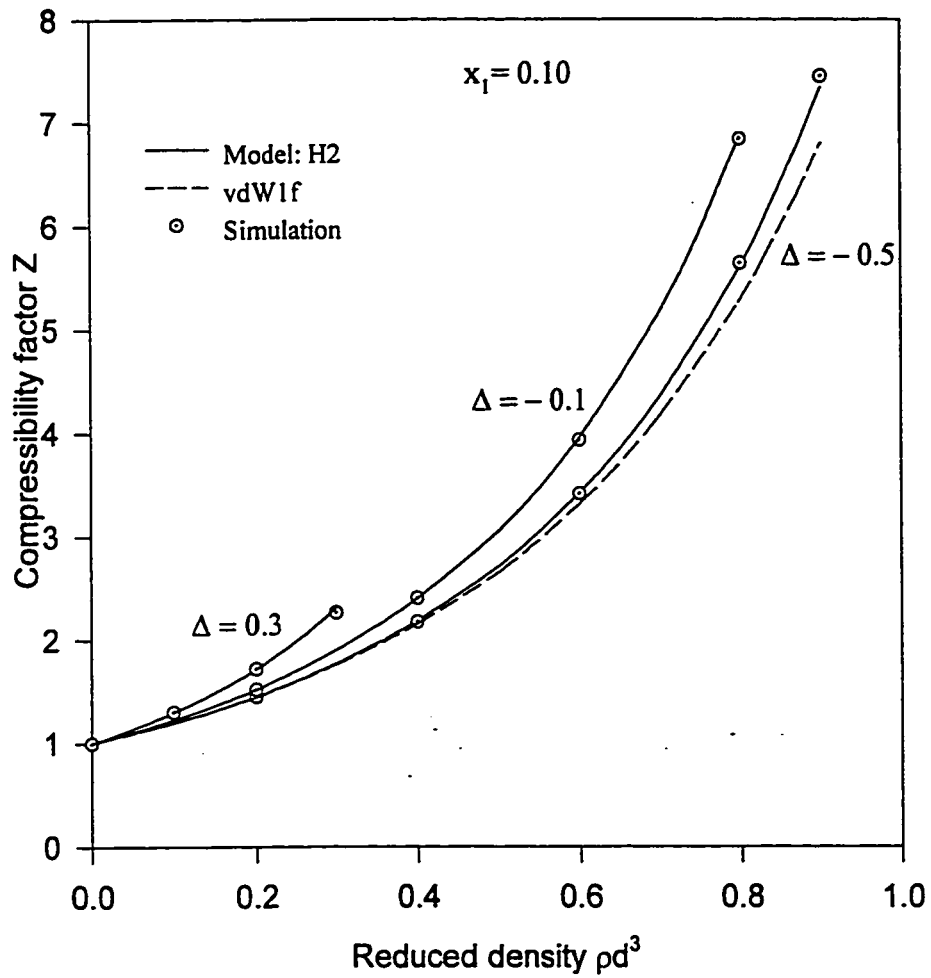
Figure 4.16 Effects of mixture density and Δ on the compressibility factor of symmetric NAHS for model H2 at x1= 0.1. The points represent Monte Carlo simulation data from Jung and Jhon (1995). vdW-1f and H2 overlap for Δ = 0.3 and - 0.1.
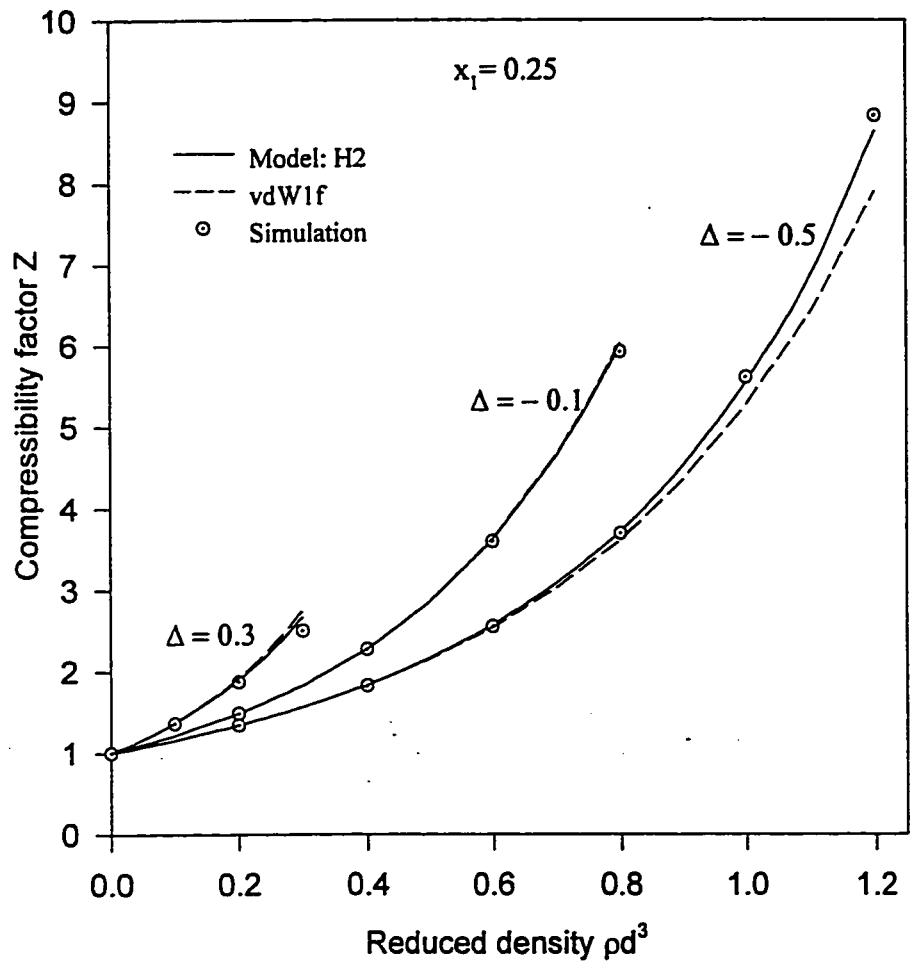
Figure 4.17 Effects of mixture density and Δ on the compressibility factor of symmetric NAHS for model H2 at x1= 0.25. The points represent Monte Carlo simulation data from Jung and Jhon (1995). vdW-1f and H2 overlap for Δ = - 0.1.
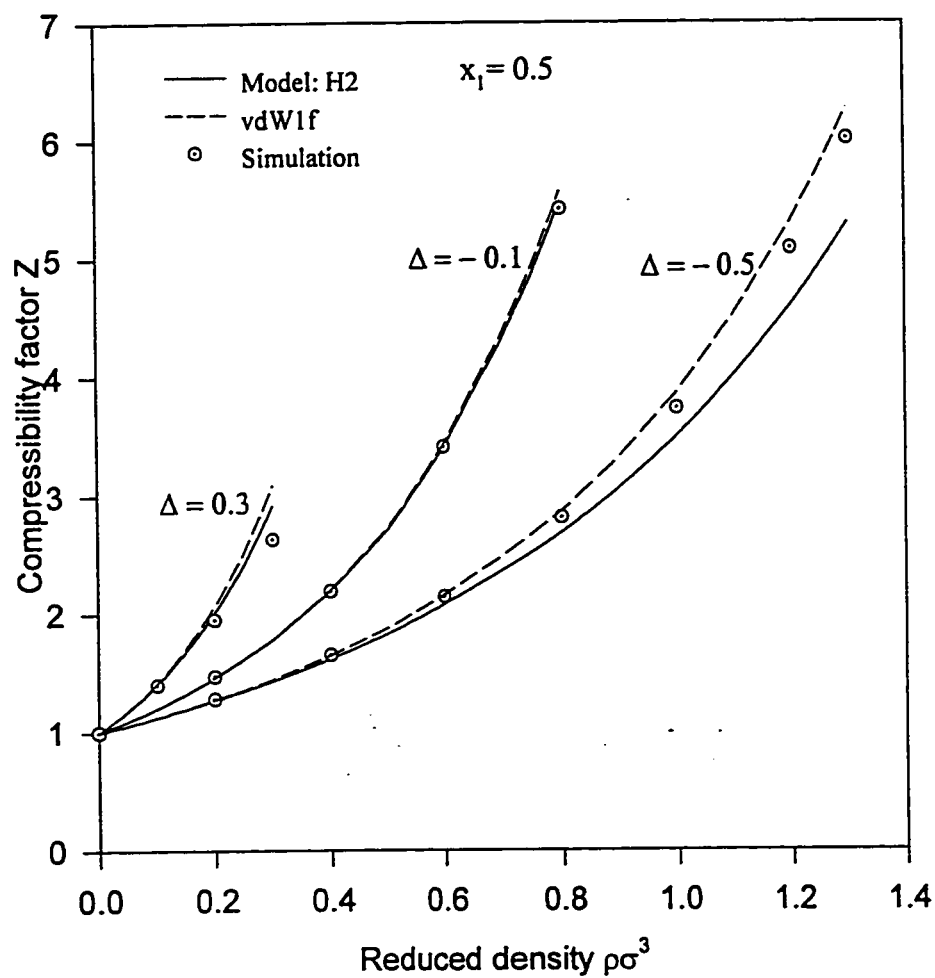
Figure 4.18 Effects of mixture density and Δ on the compressibility factor of symmetric NAHS for model H2 at x1= 0.50. The points represent Monte Carlo simulation data from Jung and Jhon (1995).
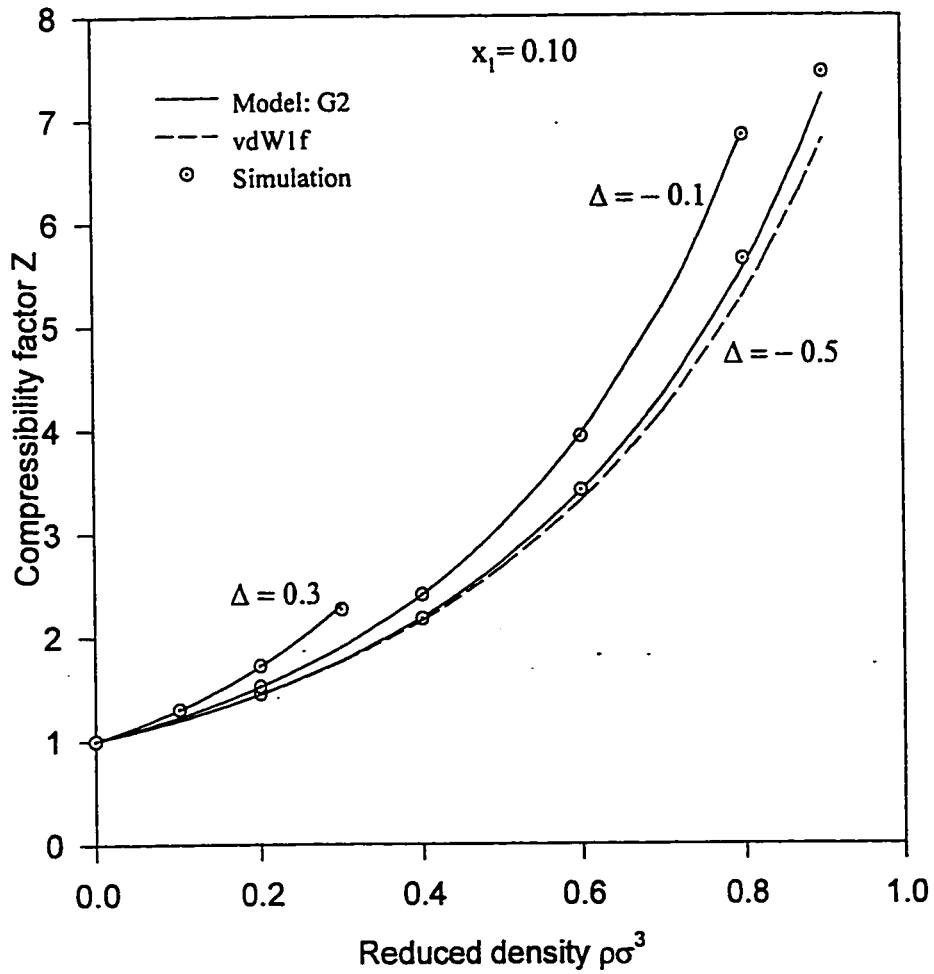
Figure 4.19 Effects of mixture density and Δ on the compressibility factor of NAHS for model G2 at $x_1 = 0.1$. The points represent Monte Carlo simulation data from Jung and Jhon (1995). vdW-1f and G2 overlap for $\Delta = 0.3$ and -0.1.
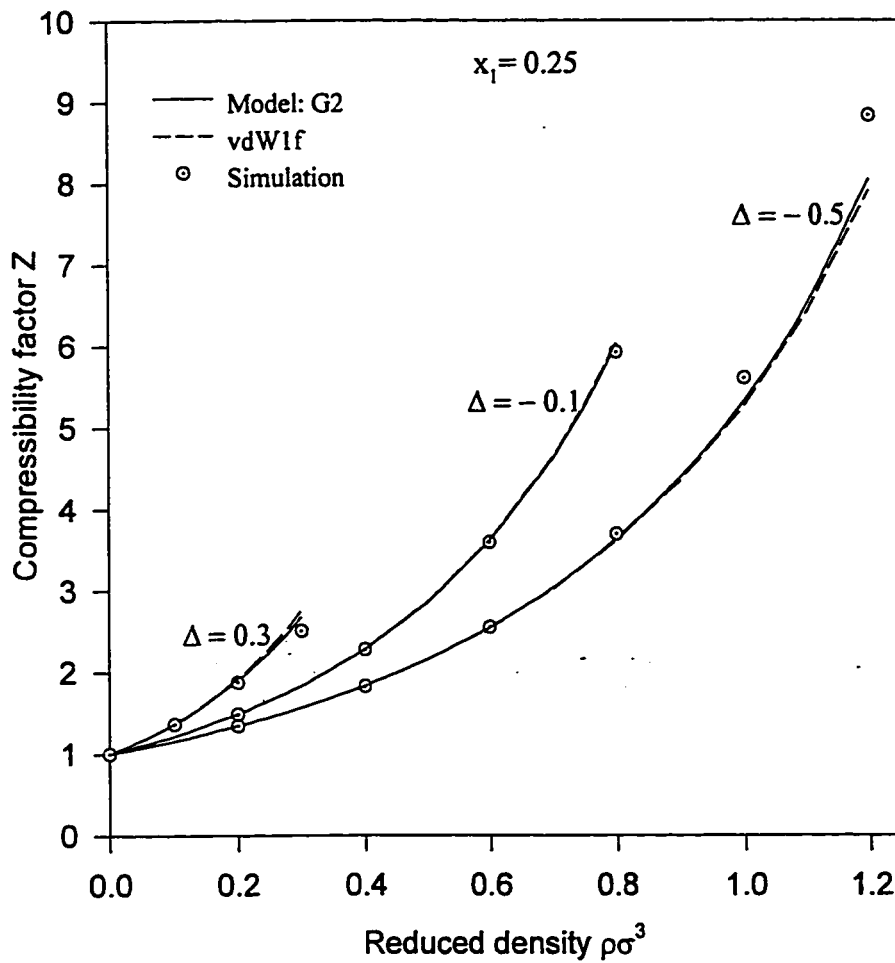
Fig. 4.20 Effects of mixture density and Δ on the compressibility factor of NAHS for model G2 at $x_1 = 0.25$. The points represent Monte Carlo simulation data from Jung and Jhon (1995). vdW-1f and G2 overlap for Δ = - 0.1.
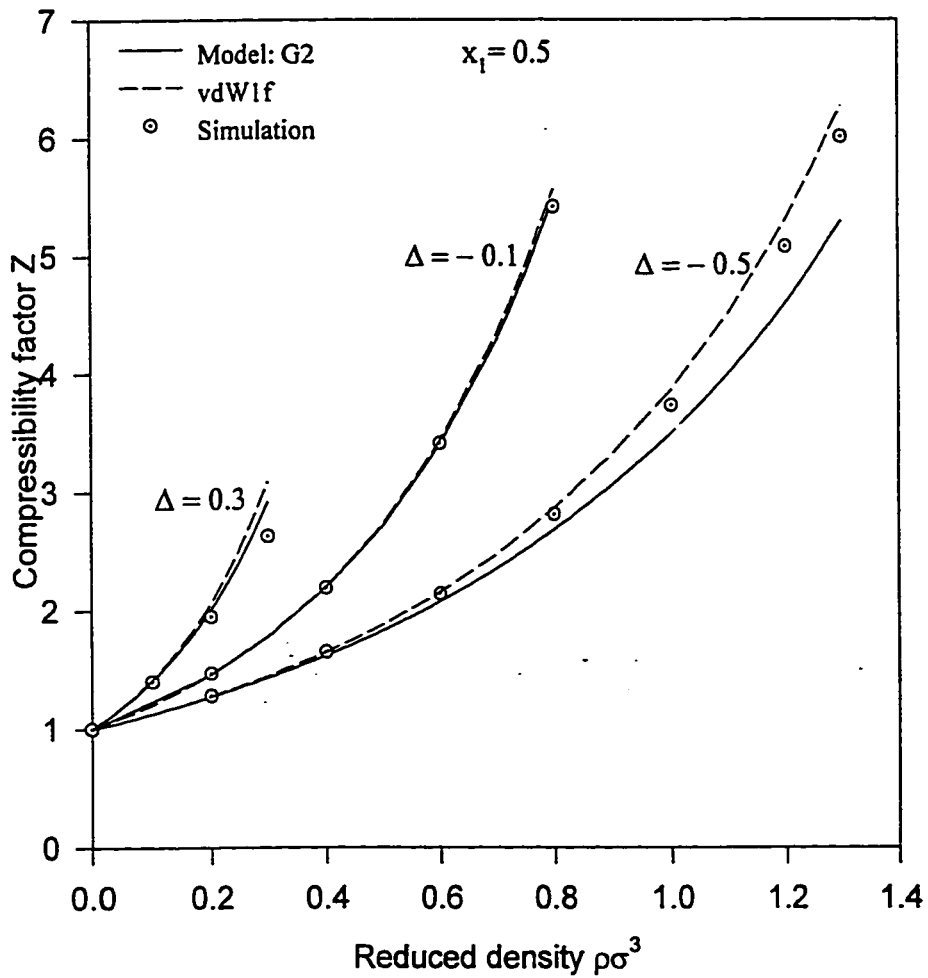
Figure 4.21 Effects of mixture density and Δ on the compressibility factor of NAHS for model G2 at $x_1 = 0.50$. The points represent Monte Carlo simulation data from Jung and Jhon (1995).

Bellone et al. (1986) have developed an accurate equation of state for symmetric non-additive hard spheres by parameterization of the Carnahan-Starling formula for hard spheres. Their equation is given by:

$$Z = 1 + \frac{4\eta_{eff}a_1 - 2\eta_{eff}^2 a_2}{\left(a_3 - a_4\eta_{eff}\right)^3}$$

(4.16)

where η_{eff} is the effective packing fraction $(\pi/12)\rho d^3[1+(1+\Delta)^3]$ of the mixture, a_i's are parameters related to Δ through constants b_i's as follows:

$$a_i = 1 + b_i\Delta \left(1+\Delta\right)^2$$

(4.17)

Equation 4.16 reproduced the simulation data of Ballone et al. (1986), and that of Adam and McDonald (1975) to an accuracy within the statistical error of these data (~5%). However, Equation 4.16 had to be fitted to simulation data to obtain the four constants.

4.1.4.2 Phase separation in non-additive hard spheres

Mixtures of non-additive hard spheres with positive non-additivity phase separate at high densities to minimize the system free energy. Spheres with highly positive non-additivity should separate at lower densities (due to their excessive repulsion) than those with lower value of positive non-additivity. The Helmholtz free energy for a mixture is given by:

$$\frac{A_{mix}}{RT} = \frac{A_{mix,r}}{RT} + \sum x_i \ln x_i$$ (4.18)

At low densities, the entropy terms $\sum x_i \ln x_i$ dominates the free energy, and the mixture remains homogeneous. The Helmholtz free energy can be obtained from compressibility factor as:

$$A = \int_0^\rho (Z-1)/\rho \, d\rho$$ (4.19)

Considering one of our models, say f_{ij}, and using Carnahan Starling equation of state, the reference free energy is given by

$$\frac{A_{mix,r}}{RT} = (2\pi/3)\rho \sum_i \sum_j x_i x_j \sigma_{ij}^3 F_A\left(f_{ij} \tfrac{x}{6} \rho\right)$$ (4.20)

where the function F_A is evaluated from Helmholtz free energy as follows:

$$F_A = \frac{1-(3/4)\eta}{(1-\eta)^2}$$ (4.21)

with $\eta = \rho\sigma^3$ for the symmetric equimolar system. Also, due to the symmetry, that is, $\sigma_{11} = \sigma_{22}$, the critical point, if it exists, must occur at points corresponding to equimolar mixture composition (that is $x_1 = x_2 = 0.5$). It must also satisfy the following condition.

$$\frac{\partial^2 A_{mix}}{\partial x_1^2}\bigg|_{T,P} = 0 \qquad\qquad (4.22)$$

Symmetry of the binary mixture also requires that for the two phases I and II in equilibrium, $x_1^I = x_2^{II}$ and $x_2^I = x_1^{II}$. This reduces the equilibrium condition to $\partial A_{mix}/\partial x_1|_{T,P} = 0$ for the coexistence curve between the two phases.

Figures 4.22 and 4.23 present phase diagrams for non-additive hard spheres ($\Delta = 0.2$) predicted by our mixture models. These are compared to the Monte Carlo simulation data of Amar (1989), MIX1 model of Melnyk and Sawford (1975) and the vdW-1f model. Figure 4.22 shows that models f_{ij} and H1 considerably underpredict the mixture densities at which phase separation occurs (compared to the simulation data), nonetheless these models are improvements over van der Waals' predictions. At the composition extremes ($x_1 < 0.05$ and $x_1 > 0.95$), however, the two models' predictions compare satisfactorily with the simulation data. Models DVPCF, H2, G1 and G2, on the other hand, overpredict the simulation data (see Figure 4.23). Our models could also not predict the flatness in the profile of the simulation data around $x_1 = 0.5$ due to the failure of the Helmholtz free energy expressions to give a flat turning point at this composition. The flat density profile is generally difficult to predict by simple theories. As shown in Figures 4.22 and 4.23, even the MIX1 model that uses hard spheres mixture as reference is not very satisfactory. In contrast to the other models, model f_{ij} shows a relatively flat region with density varying just between 0.36 to 0.3589 as the mole fraction x_1 increases from 0.3538 to 0.50.
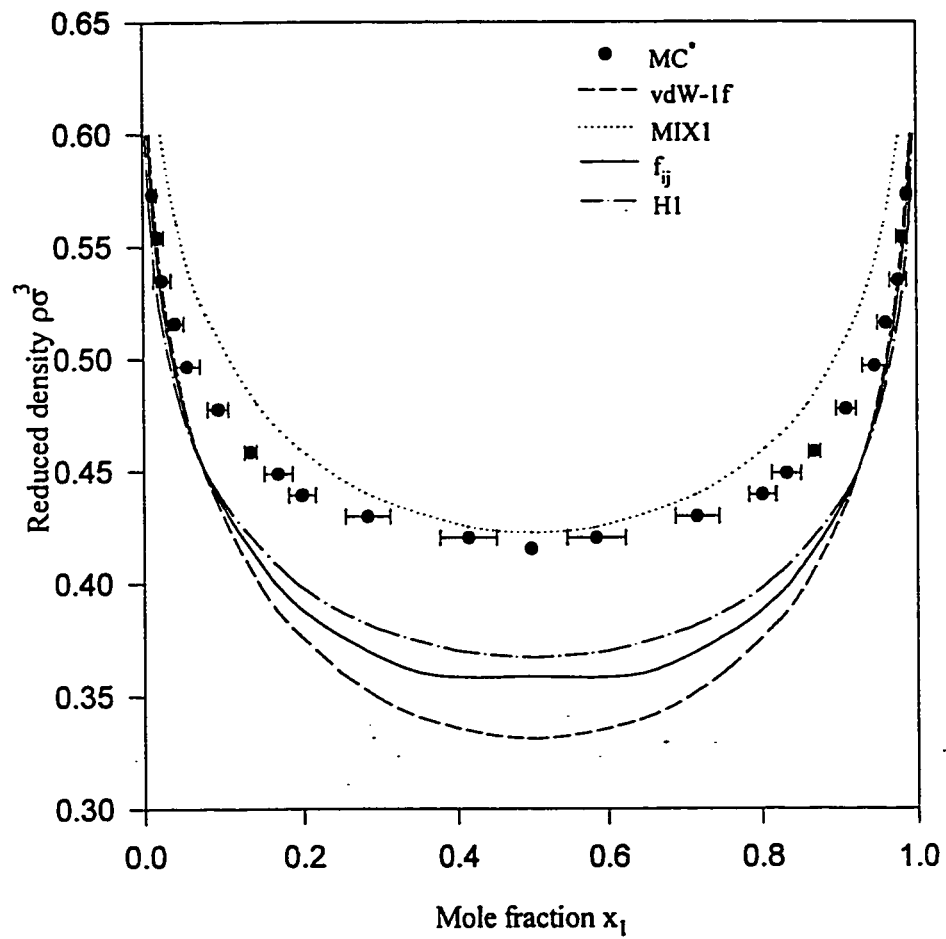
Figure 4.22 Phase diagram of a mixture of symmetric nonadditive hard sphere fluid system ($\Delta = 0.2$) for mixture models f_{ij} and H1 (*:-Monte Carlo results of Amar, 1989).
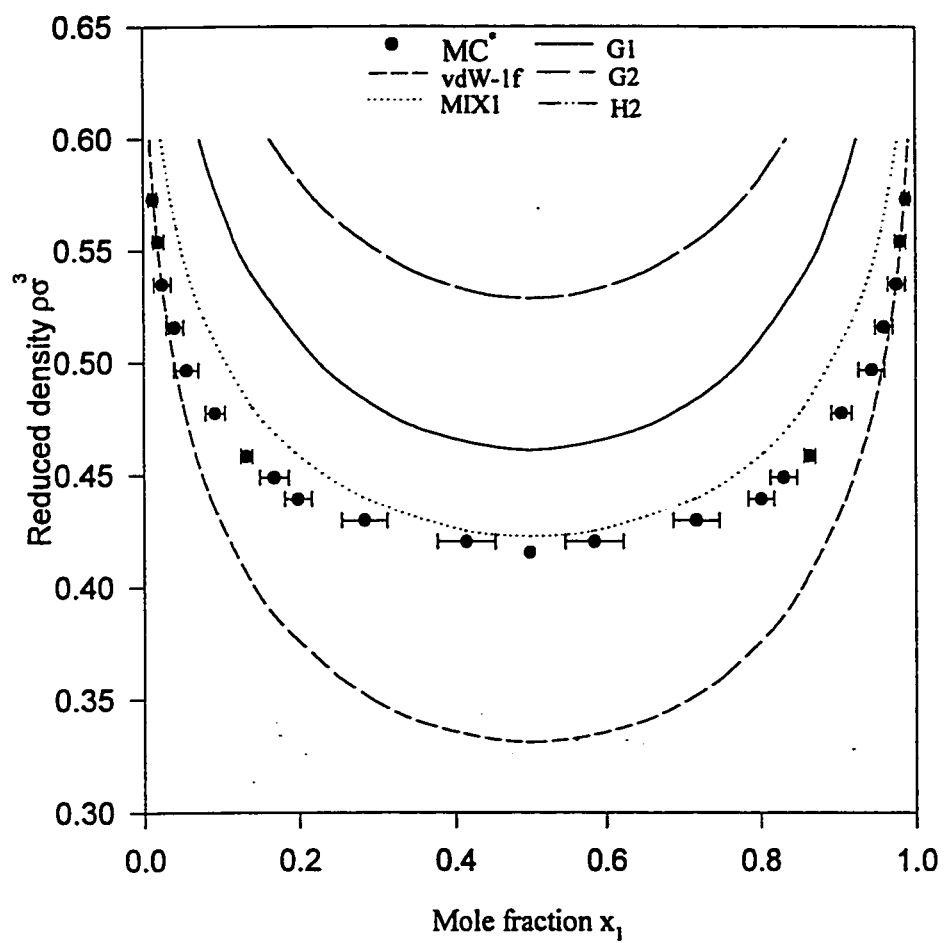
Figure 4.23   Phase diagram of a mixture of symmetric nonadditive hard sphere fluid system (Δ = 0.2) for mixture models H2, G1, and G2 (*:-Monte Carlo results of Amar, 1989). There is overlap of predictions by G2 and H2.
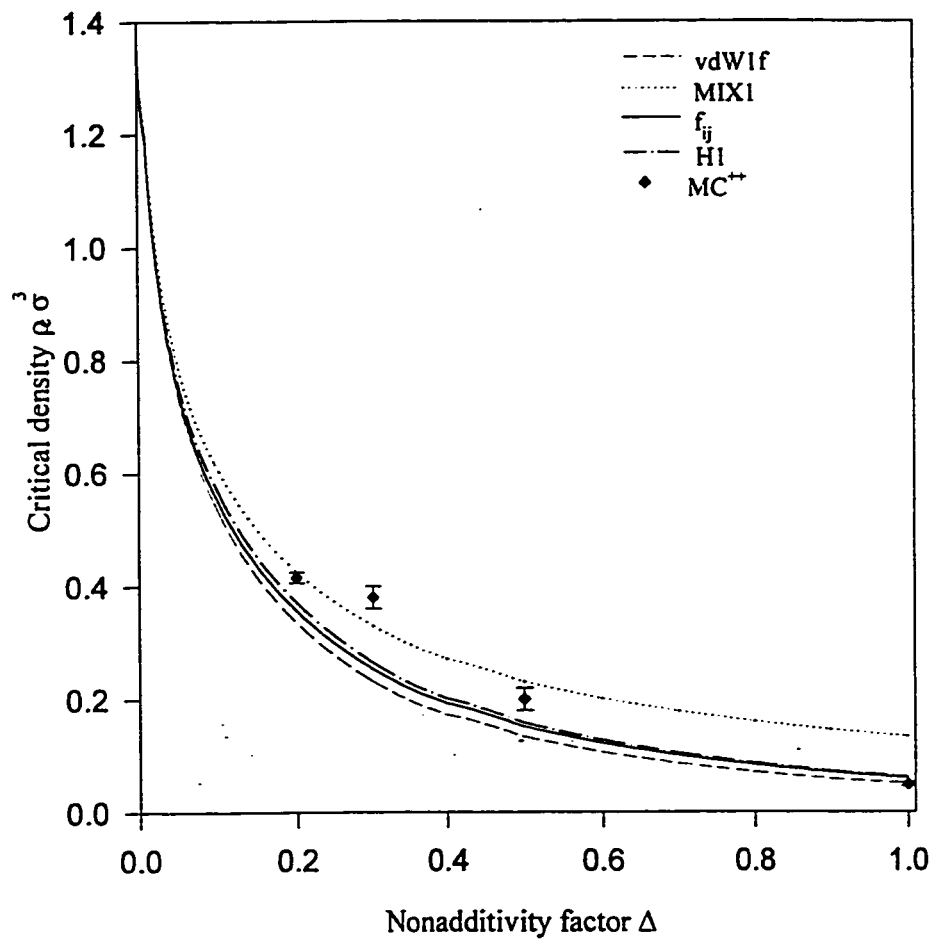
Figure 4.24   Coexistence curves for an equimolar mixture of symmetric nonadditive hard sphere fluid system for mixture models f_{ij}, H1, and DVPCF: (**:-Monte Carlo results as in Table 4.3).
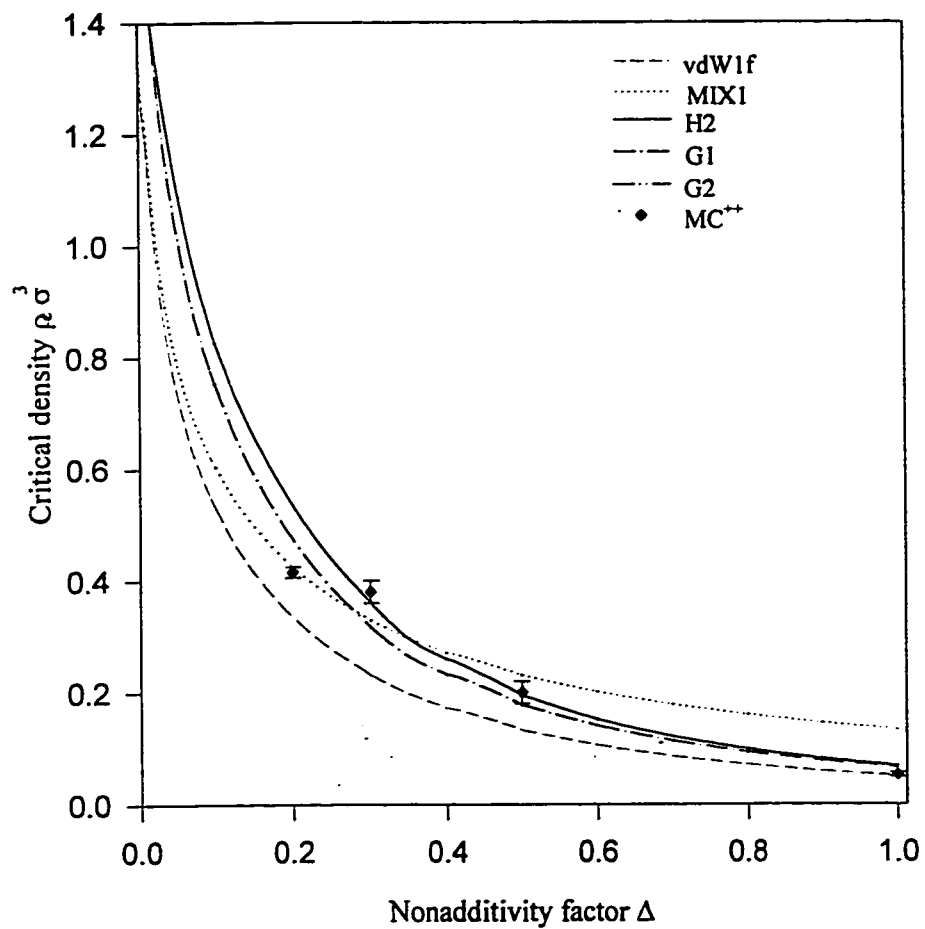
Figure 4.25 Coexistence curves for an equimolar mixture of symmetric nonadditive hard sphere fluid system for mixture models H2, G1 and G2 (**:-Monte Carlo results as in Table 4.3).

Using Equations 4.18 to 4.22, critical densities for our models were calculated at various values of the non-additivity parameter as shown in Figures 4.24 and 4.25. These figures show that our models are generally in better agreement with simulation data at high values of Δ when compared with van der Waals model. At lower deviations from non-additivity, models f_{ij} and H1 converge with the van der Waals and the MIX1 model into the solid region for pure hard spheres. The later occurs at a reduced density ($\rho\sigma^3$) of 1.033 (Jung et al., 1995). Note that the available simulation data as summarized in Table 4.6 does not extend to the region of Δ less than 0.20. MIX1 model is a first order perturbation equation of state using a multicomponent reference fluid. For starting with a multicomponent reference, MIX1 performs better than one component reference fluid models such as the vdW-1f and the Barker Henderson (BH) models Melnyk and Sawford, (1975). However, this applies only to the phase. behavior. It does not predict the compressibility factor correctly, even the second virial is not correct.

The model based on the distinguishing value of the pair correlation function (DVPCF) shows good agreement with simulation data at Δ greater than about 0.3. At Δ values lower than 0.3, however, the model deviates sharply from the vdW-1f, MIX1, f_{ij}, H1 models, and probably simulation results as shown in Figure 4.24. Models H2, G1 and G2 behave in a manner similar to DVPCF but to a lesser extent as shown in Figure 4.25 (on the scale of Figure 4.25, critical density predictions by models H2 and G2 are the same).

Table 4.6 Summary of simulation data for nonadiitive hard spheres (NAHS).

Nonadditivity Δ	Critical density $\rho\sigma^3$	Source
0.20	0.50 ± 0.02	Hoheisel, 1993
	0.42 ± 0.04	Melnyk and Sawford, 1975
	$0.415^{+\ 0.005}_{-\ 0.014}$	Amar, 1989
0.30	0.38 ± 0.02	Hoheisel, 1993
0.50	0.20 ± 0.02	Hoheisel, 1993
1.00	$0.0485 \pm 0.003 (N = 256)$	Ehrenberg et al., 1990
	$0.0488 \pm 0.003 (N = 256)$	Ehrenberg et al., 1990
	$0.0525 \pm 0.004 (N = 500)$	Ehrenberg et al., 1990

4.1.5 Mixture of Lennard-Jones Fluids

The Lennard-Jones potential is the simplest potential that possesses both the attractive and the repulsive properties of real fluids. For this reason it exhibits both the two first order transitions (liquid-vapor and fluid-solid) and the second order, the critical point. Lennard-Jones potential is, therefore, very useful in predicting the thermodynamic properties of rare gases and weakly anisotropic molecules such as methane, nitrogen and oxygen (Lee, 1988).

Lennard-Jones molecules account for attractive forces through an energy parameter ε. Considering a specific case, for example, model DVPCF, the quantity F_{ij} in Equation 4.1 is taken to depend on the parameter ε_{ij} through a dimensionless temperature as follows:

$$F_{ij} = F\left(\rho f_{ij}, \frac{kT}{\varepsilon_{ij}}\right) \qquad (4.23)$$

where ρf_{ij} is as defined in Equation 4.2, k is the Boltzmann constant, and T is the absolute temperature. This dependence gives the exact second virial coefficient. Note that the mean density approximation MDA also uses the same energy parameter dependence. The functional form of F given by:

$$F\left(\rho\sigma^3, \frac{kT}{\varepsilon}\right) = \left(\frac{Z_{pure} - 1}{\rho\sigma^3}\right) \qquad (4.24)$$

was obtained from the pure component equation of state or Z_{pure}, where σ is pure

component collision diameter. As shown in Equation 3.11, if the molecules are

characterized by other parameters, such as the accentric factor or polarity parameters,

then the appropriate values for the pair ij can also be used in evaluating F_{ij} after obtaining

F from the pure equation of state:

$$F_{ij} = F\left(\rho \frac{\sigma_{ii}\sigma_{jj}}{\sigma_{ij}} \sum_i x_i \sigma_{ii}^2, \frac{kT}{\varepsilon_{ij}} \right)$$ (4.25)

For a satisfactory evaluation of this model, we need to cover a wide molecular

parameter range. Therefore, we have used Lennard-Jones data from the work of Shukla et

al. (1986) in which they also presented results for molecular simulation and four other

models. This data covers the molecular size and energy ratios up to 2.0 and 4.5,

respectively. The reduced temperature T^* $(T^* = kT/\varepsilon)$ used was in the range 1.3 to 5.82

while the reduced density ρ^* $(\rho^* = \rho f_{ij})$ used was in the range of 0.425 to 0.90.

The equation of state of Johnson et al. (1993) was used for the pure Lennard-

Jones fluid. The reduced temperature range for this equation of state is $0.7 \le T^* \le 6.0$

while the density is in the range $0.1 \le \rho^* \le 1.25$. These values also form the

recommended range for use of our models with this pure equation of state. So only points

where all the individual temperatures $(T_{ii}^*, T_{jj}^*$ and $T_{ij}^*)$ and all the individual densities

$(\rho_{ii}^*, \rho_{jj}^*$ and $\rho_{ij}^*)$ fall within the given limits should be considered for use with our

models.

A comparison of model DVPCF with vdW-1f, MDA and WCA-LL-GH is presented in Table 4.7. Note that there are slight differences in the percentage error values of Table 4.7 and those reported earlier by Shukla et al. (1986). This is due to the more accurate equation of state of Johnson et al. (1993) for the pure fluid that was used instead of the equation of state of Nicolas et al. (1979) used by Shukla et al. (1986). Percentage errors in WCA-LL-GH are reported as given by Shukla et al. (1986) because they do not depend on the pure equation of state.

From Table 4.7, it is clear that vdW-1, MDA and WCA-LL-GH mostly underpredict the compressibility factor Z. On the contrary, our models mostly overpredict Z. Magnitudes of the average and maximum errors for our model are 3.3% and 8.6%, respectively. These values are lower than the corresponding values of 8.6% and 29.1% for vdW-1 theory and of 9.6% and 32.4% for MDA theory. The corresponding average and maximum errors for WCA-LL-GH theory are 3.7% and 9.5%, respectively. These values are quite close to the results for model DVPCF in spite of the more complex and involved form of the former. At higher size ratios, model DVPCF shows a major improvement in the accuracy of Z.

In a manner similar to the above, Table 4.8 present a summary of test for models f_{ij}, H1 and H2 for binary mixture of Lennard-Jones fluids with the energy parameters evaluated as in Equation 4.26.

$$F_{ij} = F\left(\rho f_{ij}, T_{ij}^{*}\right)$$
$$H_{I}1_{i} = H\left(h_{i}\rho, T_{i}^{*}\right) \tag{4.26}$$
$$H_{I}2_{i} = H\left(h_{i}\rho, kT\Big/\sum x_{i}\varepsilon_{ij}\right)$$

Table 4.7. Compressibility factors of Lennard-Jones fluids using model DVPCF.

$\varepsilon_2/\varepsilon_1$	σ_2/σ_1	$\rho\sigma_X^3$	Z_{MD} [•]	Deviation from Z_{MD} (%)			
				vdW-1	MDA [••]	WCA-LL-GH[+]	DVPCF
1.00	1.30	0.90	5.006	-3.9	-3.8	1.3	-1.6
1.00	2.00	0.90	5.682	-15.3	-15.3	-6.8	-3.1
1.50	1.00	0.90	4.944	0.4	0.1	1.4	0.1
1.50	1.30	0.90	5.177	-3.6	-3.8	1.1	0.1
1.50	2.00	0.90	5.976	-15.9	-16.1	-9.5	1.4
2.50	1.00	0.90	4.911	4.3	2.6	0.78	2.6
2.50	1.30	0.90	5.363	-3.9	-5.4	-1.0	1.8
2.50	2.00	0.90	6.522	-20.7	-21.7	-9.2	4.2
3.50	1.30	0.90	5.347	-3.3	-6.3	-0.2	4.3
3.50	2.00	0.90	6.790	-24.5	-26.4	-8.7	6.6
4.50	1.00	0.90	4.806	7.2	1.9	0.8	1.9
4.50	1.30	0.90	5.160	-1.2	-5.8	-0.54	8.6
4.50	2.00	0.90	6.988	-28.9	-31.5	-7.5	6.2
1.50	1.05	0.80	3.754	1.0	0.7	0.9	1.0
1.50	1.30	0.80	3.837	-1.0	-1.3	-0.9	2.0
1.50	1.55	0.80	4.102	-7.4	-7.6	-6.1	-0.3
1.50	2.00	0.80	4.449	-14.6	-14.7	-8.3	-0.2
2.50	1.05	0.80	3.754	0.5	-1.1	-0.1	-0.4
2.50	1.30	0.80	3.798	-1.1	-2.7	-1.1	3.2
2.50	1.55	0.80	3.928	-4.8	-6.3	-3.8	6.4
2.50	2.00	0.80	4.461	-16.9	-18.0	-9.4	5.3
3.50	1.05	0.80	3.572	2.9	-0.7	0.3	0.3
3.50	1.30	0.80	3.618	-0.2	-3.7	-0.9	5.1
3.50	1.55	0.80	3.988	-10.9	-13.9	-2.9	3.5
3.50	2.00	0.80	4.527	-23.4	-25.6	-9.0	5.8
4.50	1.05	0.80	3.316	6.5	0.5	-0.3	1.9
4.50	1.30	0.80	3.420	-0.5	-5.9	-0.8	5.9
4.50	1.55	0.80	3.644	-9.6	-14.3	-0.7	9.8
4.50	2.00	0.80	4.441	-29.1	-32.4	-7.7	7.9
1.50	1.30	0.68858	2.908	-2.6	-2.8	-1.1	-0.5
1.50	2.00	0.70863	3.313	-10.4	-10.5	-5.1	1.4
4.50	1.30	0.50000	1.161	-0.1	-3.7	-4.7	-1.6
4.50	2.00	0.42518	0.846	-7.7	-9.1	-8.3	-2.3
ABSOLUTE AVERAGE ERROR (%)				8.6	9.6	3.6	3.2
ABSOLUTE MAXIMUM ERROR (%)				29.2	32.4	9.5	9.8

Table 4.8. Compressibility factors of a binary Lennard-Jones fluid mixture using models f_{ij}, H1 and H2.

$\varepsilon_2/\varepsilon_1$	σ_2/σ_1	$\rho\sigma_x^3$	Deviation from Z_{MD} (%)				
			f_{ij}	H1	H2	H12*	H12+
1.00	1.30	0.90	-1.377	-0.481	-1.569	-1.415	-1.415
1.00	2.00	0.90	-1.537	2.415	-2.800	-1.217	-1.217
1.50	1.00	0.90	-0.007	-0.129	0.124	0.124	-0.109
1.50	1.30	0.90	-0.103	2.195	-0.935	-0.603	-0.128
1.50	2.00	0.90	2.096	8.967	-1.355	1.016	2.318
2.50	1.00	0.90	2.516	1.265	3.349	3.349	1.500
2.50	1.30	0.90	0.566	4.468	-0.609	0.027	0.127
2.50	2.00	0.90	3.582	14.247	-2.377	1.195	3.666
3.50	1.30	0.90	1.925	6.709	0.764	1.702	0.637
3.50	2.00	0.90	5.485	18.766	-2.045	2.612	5.580
4.50	1.00	0.90	1.848	-3.786	4.351	4.353	-2.735
4.50	1.30	0.90	5.075	10.416	4.054	5.333	2.665
4.50	2.00	0.90	5.843	20.523	-2.172	3.457	6.533
1.50	1.05	0.80	0.997	1.013	1.048	1.064	0.833
1.50	1.30	0.80	1.871	3.581	1.384	1.649	1.810
1.50	1.55	0.80	-0.189	3.174	-1.334	-0.588	-0.131
1.50	2.00	0.80	0.592	6.069	-1.854	0.049	0.849
2.50	1.05	0.80	-0.682	-2.055	0.044	0.083	-2.147
2.50	1.30	0.80	2.263	4.395	2.135	2.647	1.456
2.50	1.55	0.80	5.226	10.602	3.838	5.204	4.959
2.50	2.00	0.80	4.500	13.186	0.636	3.737	4.694
3.50	1.05	0.80	-0.069	-4.223	1.647	1.707	-3.911
3.50	1.30	0.80	3.238	4.513	4.060	4.824	0.923
3.50	1.55	0.80	0.943	6.779	0.104	1.969	-0.092
3.50	2.00	0.80	3.263	13.873	-1.170	2.984	3.191
4.50	1.05	0.80	1.462	-6.654	4.304	4.389	-5.706
4.50	1.30	0.80	3.081	2.623	5.104	6.138	-1.325
4.50	1.55	0.80	5.525	11.727	5.444	8.030	3.285
4.50	2.00	0.80	3.541	15.771	-1.253	4.073	3.152
1.50	1.30	0.68858	-0.536	0.504	-0.642	-0.456	-0.625
1.50	2.00	0.70863	2.347	6.635	0.833	2.354	2.706
4.50	1.30	0.50000	-1.655	-17.000	7.366	7.588	-10.092
4.50	2.00	0.42518	-0.901	-14.410	21.867	22.943	3.509
ABS. AVERAGE ERROR (%)			2.268	7.268	2.805	3.299	2.546
ABS. MAXIMUM ERROR (%)			5.843	20.523	21.867	22.943	10.092

*, +: linear combinations of models H1 and H2 with combining rules as explained in text

Again, these models show considerable improvement over the vdW-1f and the MDA models. Model f_{ij} predicts better than WCA-LL-GH as well. Models H1 and H2 are comparable to the WCA-LL-GH in terms of the average deviation. They, however, perform poorly at low system density and size and energy ratios.

At several of the parameter sets used in Tables 4.7 and 4.8, models H1 and H2 deviate differently from simulation data (while H1 under predict, H2 over predict). In the last two columns of Table 4.8 (denoted by H12* and H12$^+$), we have attempted improving the predictions by combining models H1 and H2. Column H12* represent a linear combination of H1 and H2 as [τH1 + (1-τ)H2] and a geometric average of their energy parameters $\left(T_i^* \times kT / \sum x_i \varepsilon_{ij} \right)^{\frac{1}{2}}$. The value of α used is 0.9 , and as seen in the table, model H2 is still better than the combined model. There are several useful ways of determining τ; one of this which uses molecular sizes for a binary mixture is given below.

$$\tau = \frac{\left(1 + \left(\sigma_2 / \sigma_1 \right)^n \right) / \left(\sigma_1 + \sigma_2 \right)}{\sum_k x_k \sigma_k^n} \qquad (4.27)$$

In this equation n can be adjusted to get the best value for τ subject to the condition that τ $\leq$ 1.0. In the last column of Table 4.8, instead of the geometric average of the energy terms, a weighted average with respect to α, $\left[\tau T_i^* + (1-\tau) kT / \sum x_i \varepsilon_{ij} \right]$ was used. Although the resulting model predicts better than both H1 and H2, the small difference does not justify the extra effort.

4.2   Mixtures of simple real molecules

Unlike hypothetical fluids, the intermolecular potentials of real fluids are not exactly known. There are accurate potentials for the noble gases (Aziz et al. 1983; Aziz and Slaman, 1986) because they are simple monatomic fluids. These molecules are also satisfactorily represented by the Lennard-Jones (12, 6) potential. Next to noble gases in spherical symmetry are the Quasi-spherical (tetrahedral) molecular fluids like methane and carbon tetrafluoride. Molecules such as carbon dioxide and ethane are distinctly non-spherical. They are nonetheless considered simple because they are relatively small in size and non-polar. Any good model for simple molecules should, therefore, give best predictions for noble gases followed by quasi-spherical and then non-spherical molecules.

In the test of our models for simple molecules, the accurate equation of state for non-polar fluids of Tao and Mason (1994) was used. This is a modified form of an earlier statistical mechanical analytical equation of state proposed by Song and Mason (1989) and by Ihm et al. (1991). The equation of state of Tao and Mason (1994) is written as:

$$\frac{P}{\rho kT} = 1 + (B - \alpha)\rho + \frac{\alpha\rho}{1 - \lambda b\rho} + A_1(\alpha - B)b\rho^2 \frac{\left(e^{\kappa T_c/T} - A_2\right)}{1 + 1.8(b\rho)^5} \qquad (4.28)$$

where ρ is the number density N/V, B is the second virial coefficient, α is a temperature dependent correction to the second virial (for softness of repulsion), T is absolute temperature, T_c is the critical temperature, $b\rho$ is the packing fraction, A_1, A_2, κ and λ are

constants correlated to the molecular properties. Note that ρ was missing in the second term of their original publication.

To demonstrate our mixture model using this equation of state, consider a specific case, for instance model f_{ij}. For real molecular system, this is easily written as:

$$Z = 1 + \rho \sum_i \sum_j x_i x_j B_{ij} F_{ij} \left(\rho f_{ij}, T \right) \tag{4.29}$$

The parameter F_{ij} is then evaluated from $(Z-1)/B\rho$ in the same manner as explained earlier in the previous section. The expression for F from Equation 4.28 is, therefore:

$$\frac{Z-1}{B\rho} = \left(1 - \alpha/B\right) + \frac{\alpha/B}{1 - \lambda(b\rho)} + A_1(b\rho)(\alpha/B - 1)\frac{\left(e^{\kappa T_c/T} - A_2\right)}{1 + 1.8(b\rho)^4} \tag{4.30}$$

where α and b are given as functions of Boyle volume v_B and non-dimentional temperature T/T_B. T_B is the Boyle temperature (Song and Mason, 1989; Song and Mason, 1990; Song and Mason, 1991; Song and Mason, 1992).

$$\alpha/v_B = a_1 \exp\left\{-c_1(T/T_B)\right\} + a_2 \left[1 - \exp\left\{-c_2(T/T_B)^{\frac{1}{4}}\right\}\right] \tag{4.31}$$

$$b/v_B = a_1 \left[1 - c_1(T/T_B)\right] \exp\left\{-c_1(T/T_B)\right\} + a_2 \left[1 - \left(1 + \frac{c_2}{4(T/T_B)^{\frac{1}{4}}}\right) \exp\left\{-c_2(T/T_B)^{\frac{1}{4}}\right\}\right] \tag{4.32}$$

where a_1, a_2, c_1 and c_2 are constants.

For computational simplicity, we have used the second virial expression of Pitzer and Curl (1957) which was later modified by Tsonopolous (1978). This is given by:

$$B = \left(P_c / RT_c\right)^{-1}\left[f^{(0)}(T_r) + \omega f^{(1)}(T_r)\right]$$

(4.33)

with

$$f^{(0)}(T_r) = 0.1445 - 0.330/T_r - 0.1385/T_r^2 - 0.0121/T_r^3 - 6.07 \times 10^{-4}/T_r^8$$

(4.34)

and

$$f^{(1)}(T_r) = 0.0637 + 0.331/T_r^2 - 0.423/T_r^3 - 0.008/T_r^8$$

(4.35)

where T_r is the reduced temperature (T/T_c), ω is the accentric factor and P_c is the critical pressure.

The terms in Equation 4.30 were, therefore, expressed in terms of T_s, T_r and ω (T_s = T/T_B) as follows.

$$\alpha = v_B \, f_1(T_s)$$

(4.36)

$$b = v_B \, f_2(T_s)$$

(4.37)

$$B = \left(P_c / RT_c\right)^{-1} f_3(T_r, \omega)$$

(4.38)

$$\alpha / B = f_4(T_s, T_r, \omega)$$

(4.39)

Substituting the above relationships into Equation 4.30 and extending it to mixtures gives the following expression for F_{ij}.

$$F_{ij} = 1 - f_i\left(T_{sij}, T_{rij}, \omega_{ij}\right) + \frac{f_i\left(T_{sij}, T_{rij}, \omega_{ij}\right)}{1 - \lambda_{ij}\left(b_{x_{ij}}\rho\right)} + \frac{A_i\left(b_{x_{ij}}\rho\right)\left[f_i\left(T_{sij}, T_{rij}, \omega_{ij}\right) - 1\right]\left[exp\left(\kappa/T_{rij}\right) - A_2\right]}{1 + 1.8\left(b_{x_{ij}}\rho\right)} \tag{4.40}$$

In evaluating F_{ij} from Equation 4.40, two different expressions were chosen for b_{xij}. Firstly, the volume parameter b taken proportional to the volume of molecules (σ^3). Secondly, the Boyle's volume v_B can be taken proportional to σ^3. After making each choice, application of the mixing rules in b_x is then straight forward (see Appendix D).

The noble gases have extensively been studied both theoretically and experimentally. The works of Sorokin (1969), Schouten et al. (1975), Barreiros et al. (1982), among several others constitute a rich reference data base. The predicted molar volumes of a binary mixture of 48.5 mole % Argon and 51.5 mole % Krypton using model f_{ij} are shown in Figures 4.26 and 4.27. The volume of molecules were taken to be proportional to an equal contribution of the molecular parameters v_B and b, that is $\sigma^3 \propto$ (v_B + b)/2. This combination was chosen because for all the experimental data range, the selection $\sigma^3 \propto v_B$ underpredicts the mixture volume while $\sigma^3 \propto b$ overpredicts it. The unlike pair collision diameter was calculated using the hard spheres formula. Geometric mean was used for the temperature while composition dependent pseudocritical pressure ($P_{c12} = x_1 P_{c1} + x_2 P_{c2}$) was used for the unlike pair critical parameters. As shown in the figures, the models satisfactorily predict the mixture volumes for all the experimental data range. The figures also show that the model under predict experimental data in the low
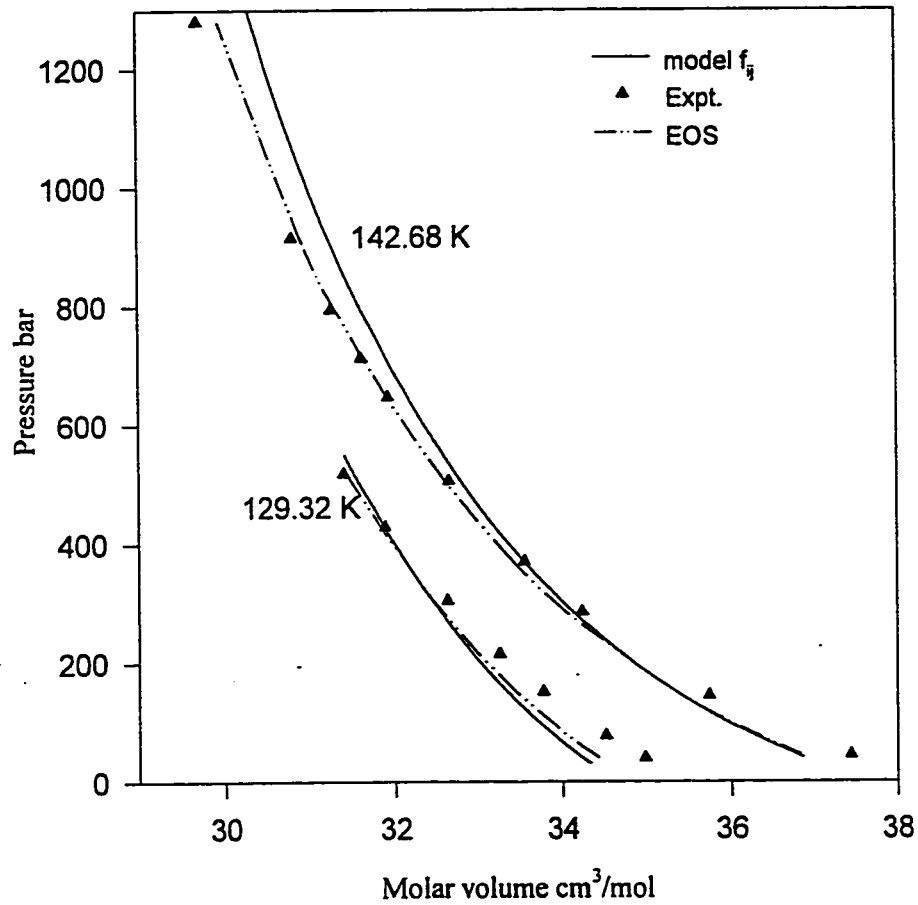
Figure 4.26 Prediction of molar volumes of a binary liquid mixture of argon and krypton with $x_{Ar} = 0.485$ at 129.32 K and 142.68 K for model f_{ij} (Points are experimental data of Barreiros et al., 1982; EOS is the equation of state of Ihm et al., 1992).
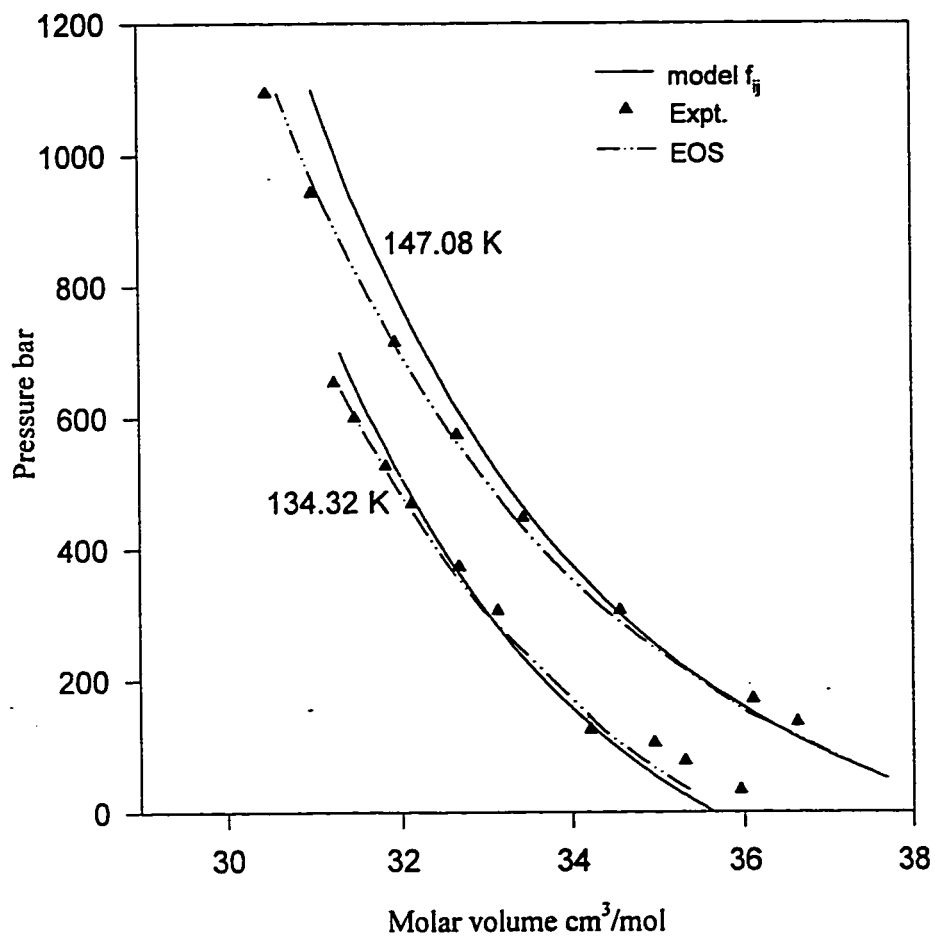
Figure 4.27   Prediction of molar volumes of a binary liquid mixture of argon and krypton with x_{Ar} = 0.485 at 134.32 K and 147.08 K for model f_{ij} (Points are experimental data of Barreiros et al., 1982; EOS is the equation of state of Ihm et al., 1992).
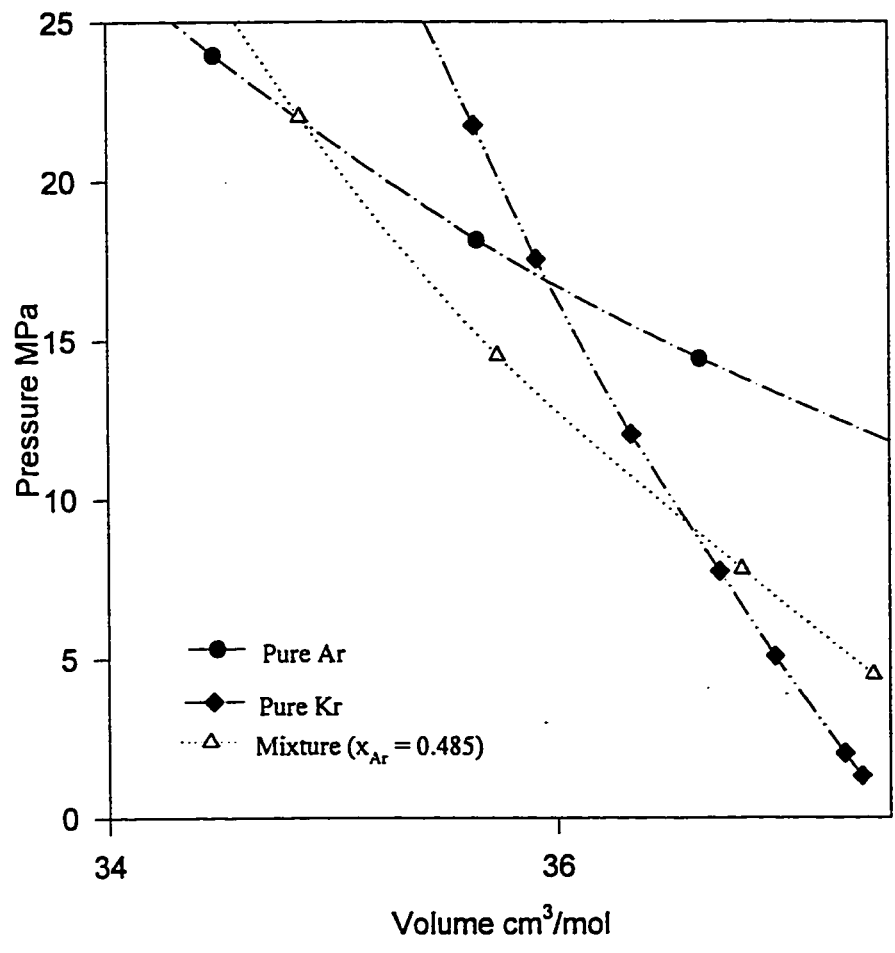
Figure 4.28   Experimental molar volumes of argon, krypton and their binary mixture using data of Berreiros et al. (1982).

pressure range and overpredict at high pressure for all the temperatures observed.

The mixture model f_{ij} shows a similar trend to the equation of state of Ihm et al. (1992). Both overpredict and underpredict experimental data in the same regions. At 142.68 K, predictions of the two equations are closest in the pressure range of about 50 to 220 bar (see Figure 4.26). In this region, it was experimentally observed that the mixture volume falls outside the two pure components' envelope as shown in Figure 4.28. This region also shows considerable skewness in the experimental excess volume versus mole fraction plots (Barreiros et al., 1982). Generally, the mixture equation of state of Ihm et al. (1992) predicts better than our models. Nonetheless, the predictions of our models are satisfactory with actual error of just 2.22% even at points of highest deviation. Naturally, it is expected that use of experimentally measured parameters such as the second virial coefficient (instead of correlations as used in the foregone calculations) will improve the prediction accuracy. This is demonstrated in calculating pure component volumes using the equation of state of Ihm et al. (1992). Using experimental second virial coefficient, they calculated the volume of pure saturated carbon dioxide with an error of 0.00% as compared to an error of - 0.63% using correlation for the second virial coefficient.

Table 4.9 compares the calculated and experiental molar volumes of the same Ar - Kr mixture (with same combination rules) using models H1, H2, G1 and G2. With the simple pseudocritical parameters used, only model H1 predicts accurately taking only parameter b as the molecular size. For the other models, however, use of arithmetic average of the two parameters was necessary. Even then predictions of models G1, and especially G2 are inaccurate.

TABLE 4.9   Predictions of the molar volumes of a binary mixture of 48.5 mole % argon and 51.5 mole % krypton.

T	P	Molar volume (cm^3/mol)					
(K)	(bar)	Expt.	f_{ij}	H1	H2	G1	G2
129.32	39.8	34.98	34.24	34.38	33.70	32.11	44.84
	214.7	33.25	32.94	33.16	32.54	31.02	41.96
	517.9	31.42	31.54	31.83	31.25	29.79	39.51
134.32	33.0	35.95	35.91	35.23	34.62	32.99	46.48
	372.5	32.68	32.57	32.82	32.30	30.81	41.06
	653.7	31.25	31.47	31.71	31.22	29.77	39.21
142.68	44.9	37.43	36.77	36.58	36.08	34.43	48.86
	647.5	31.93	32.16	32.29	31.90	30.45	39.93
	915.0	30.82	31.25	31.41	31.03	29.82	38.63
	1280.4	29.69	30.35	30.54	30.17	28.78	37.41
147.08	61.1	38.10	37.48	37.19	36.77	35.10	49.69
	447.6	33.45	33.54	33.56	33.21	31.73	41.85
	942.5	31.00	31.45	31.56	31.24	29.61	38.80
	1094.2	30.48	31.02	31.15	30.83	29.43	38.22

Table 4.10 presents the predictions of molar volumes of a binary mixture of Neon and Argon at different compositions using model f_{ij}. It is clear from the tables that the prediction errors are strong functions of both composition and pressure. Increasing composition of neon from 0.02686 to 0.1151 increases deviation of the model from 0.48% to 2.28% at 275.7 bar and from 1.28% to 3.10% at 551.4 bar. Also, for each composition, errors increase with pressure. Table 4.11 shows a trend similar to the above for a mixture of methane and carbon tetrafluoride at 298.15 K. For pressures up to about 110 bar, the model predicts quite good for all compositions. Above about 300 bars, however, the predictions are unsatisfactory, with the highest error occurring at equimolar composition. At high pressures, even the pure equation of state predicts with some significant error. The error for the larger component, CF_4 at about 353 bar is - 6.10%.

Carbon dioxide and ethane are distinctly non-spherical molecules but of relatively simple shapes. A binary mixture of these two compounds is of interest in natural gas liquefaction process since carbon dioxide can easily freeze and block pipes at cryogenic temperatures. A combination of the strong quadrupole moment in carbon dioxide coupled with the relatively weak one for ethane (Willis et al. 1984) makes this system a more severe test for mixture models compared to the previous cases. This mixture is known to form non-ideal solutions with azeotropes (Fredenslund and Mollerup, 1974).

TABLE 4.10 Prediction of molar volumes of a binary mixture of Neon and Argon at 121.36K for model f_{ij}.

Mole fraction of neon	Pressure (bar)	v (experimental) (cm^3/mol)	Error $100(v-v_{expt})/v_{expt}$
0	7.03	34.7374	-0.98
	206.79	31.6295	-0.22
	551.43	29.1591	0.57
0.0286	29.64	34.5765	-0.12
	275.71	30.9368	0.48
	551.43	28.9791	1.28
0.1511	110.29	34.3184	1.36
	275.71	31.0857	2.28
	551.43	28.6075	3.10
0.3501	190.93	35.8598	1.29
	344.64	30.8374	4.75
	551.43	28.0841	6.26
0.4662	201.62	37.9873	2.32
	344.64	31.5197	5.60
	551.43	27.8872	7.77

TABLE 4.11   Prediction of pressures of a binary mixture of
Methane and Carbontetraflouride at 298.15K using model H1.

Molefraction CH$_4$	P(expt) (bar)	Error 100(P-P$_{expt}$)/P$_{expt}$
1.0000000	18.02	-0.05
	114.26	-0.48
	273.79	1.64
0.749787	17.96	-0.04
	113.50	1.35
	301.76	13.09
0.500050	17.84	-0.06
	109.93	1.98
	319.17	15.06
0.2500066	17.66	-0.13
	104.06	1.23
	337.90	7.02
0.0000000	17.42	-0.25
	95.73	-0.56
	352.88	-6.10

The performance of models f_{ij} and H1 in predicting the molar volumes of carbon dioxide and ethane is shown in Table 4.12. Over the entire composition range, the saturated liquid volumes are predicted with a maximum absolute error of about 5% for both models. Model H1 always underpredicts the mixture volume while f_{ij} overpredicts. In these tests, The pseudocritical parameters (temperature, pressure, accentric factor and size) needed in evaluating our models' unlike pair (i ≠ j) parameters are as follows:

$$T_{cij} = \left(T_{cii}T_{cjj}\right)^{\frac{1}{2}}\left(1 - k_{ij}\right) \tag{4.41}$$

$$P_{cij} = \frac{4T_{cij}\left(p_{cii}V_{cii}/T_{cii} + p_{cjj}V_{cjj}/T_{cjj}\right)}{\left(V_{cii}^{\frac{1}{3}} + V_{cjj}^{\frac{1}{3}}\right)^{3}} \tag{4.42}$$

$$\omega_{ij} = 0.5\left(\omega_{ii} + \omega_{jj}\right) \tag{4.43}$$

where T_c's are the critical temperatures and k_{ij} is 0.08 for the pair CO_2 - C_2H_6 (Chueh and Prausnitz, 1967). P_c's and V_c's are the critical pressures and critical volumes respectively. ω is the accentric factor.

The above relationships have been found satisfactory, and are commonly used in virial calculations (Prausnitz and Gunn, 1958; McElroy and Fang, 1993; McElroy and Ababio, 1994). Use of the simpler pseudocritical combining rules gave results that are very close to Table 4.12 (difference between deviations from the two calculations was not more than about 0.2%). A wider prediction range for the carbon dioxide-ethane mixture for model f_{ij} is shown in Figure 4.29. For this, the maximum deviation is about 5% in the supercritical range.

TABLE 4.12   Prediction of molar volumes of molar volumes of a binary mixture of Carbondioxide and Ethane at 241.5K using models f_{ij} and H1.

Mole fraction CO$_2$	Pressure (bar)	v (expt) (cm^3/mol)	Deviation (%)	
			f_{ij}	H1
0	10.09	65.17	-0.63	-0.41
0.0832	12.05	63.80	0.53	-1.16
0.1711	13.63	62.51	1.33	-2.22
0.3047	15.18	59.90	3.02	-2.94
0.4594	16.10	56.87	3.87	-3.97
0.5604	16.38	54.06	5.08	-3.39
0.6330	16.46	52.26	5.03	-3.43
0.7145	16.36	49.93	4.99	-3.00
0.7996	16.10	47.06	5.14	-1.83
0.9098	15.16	43.44	.3.59	-0.90
1	13.41	40.72	-2.58	-1.65
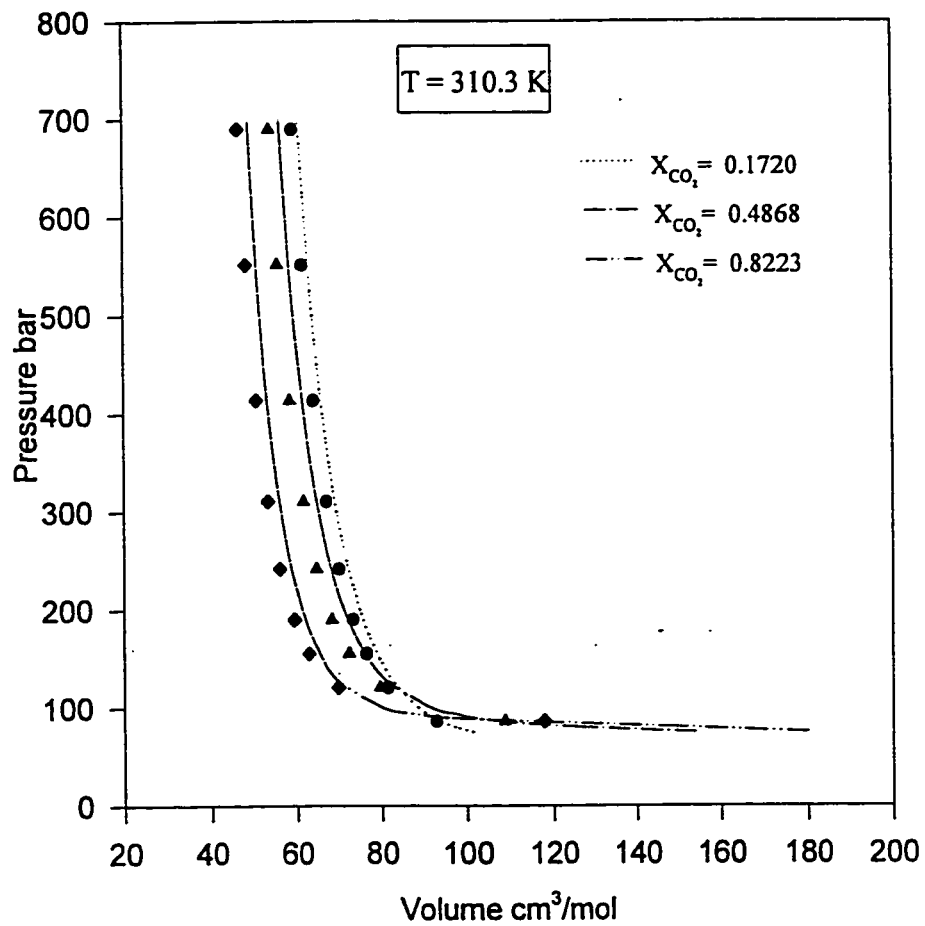
Figure 4.29   Molar volumes of supercritical binary mixture of carbondioxide and ethane predicted with model f_{ij}. Points are experimental data of Reamer et al. (1945).

CHAPTER 5

MODELS FOR PVT BEHAVIOR OF POLYMER SYSTEMS

5.1 Mixture models for polymer systems

Mixtures of different polymers or solutions of polymers in solvents are commonly referred to as polymer systems. Compared to simple molecules, polymer systems exhibit two unusual properties. For a mixture of two or more polymer species, there is a tendency for incompatibility emanating from the small entropy of mixing compared to that found with small molecules. This incompatibility can split the mixture into phases. The second abnormality is common in polymer solutions in solvents. Due to the large size difference between the polymer and solvent molecules, activity coefficient of the solvent/monomer molecules is considerably diminished. This latter property is important in solvent recovery and devolatilization of polymer products, while the former is important in polymer blending (Chao and Greenkorn, 1975).

Review of theoretical equations of state for hypothetical chain fluids was already presented in section 2.5. For real polymers, correlative equations of state are often used to describe their PVT behavior. One such commonly used empirical equations is the Tait equation (Tait, 1888). This is actually an isothermal compressibility equation rather than truly been an equation of state (Danner and High, 1993). Within limited ranges, such empirical equations can dependably be used to interpolate or extrapolate data to desired conditions. Alternatively, equations of state from statistical mechanics theory can be used

to correlate the experimental data. This later method gives equations of state whose parameters are useful in devising mixing rules to predict properties of polymer solutions (Danner and High, 1993).

5.2   Equations of state from average correlation functions

Theoretical equations of state for chain molecules can be developed from the knowledge of their molecular structure which is adequately described by intermolecular site-site correlation function. The intermolecular site-site correlation function $g_{\alpha\beta}(r)$ of molecular fluids is the probabilistic distribution of site α of one molecule and site β of another separated by a distance r. For long chains, this distribution results from the interaction of many force centers (see Figure 3.1). Therefore, it is more convenient to use the average values.

The average intermolecular correlation function g(r) is related to the site-site correlation function by (Chiew, 1991):

$$g(r) = \frac{1}{m^2} \sum_{\alpha=1}^{m} \sum_{\beta=1}^{m} g_{\alpha\beta}(r) \tag{5.1}$$

where g(r) is the average probability of finding two sites of different molecules at distance r apart, and m is the number of sites in a molecule (chain length).

The single index average correlation function $g_{\alpha}(r)$ is also of particular importance. This gives the average correlation between site α and all other sites. It is related to the site-site correlation function by:

$$g_\alpha(r) = \frac{1}{m}\sum_{\gamma=1}^{m} g_{\gamma\alpha}(r) \qquad (5.2)$$

For a polymer with different site types (copolymers), differentiating the canonical

partition function Q with respect to site-site interaction parameter $S_{\alpha\beta}^{(p)}$ and using the pair

correlation function of the ensemble gives:

$$\frac{\partial \ln Q}{\partial S_{\alpha\beta}^{(p)}} = -\frac{N\rho_c}{2kT}\sum_\alpha\sum_\beta \int \frac{\partial u_{\alpha\beta}}{\partial S_{\alpha\beta}^{(p)}} exp\left(-u_{\alpha\beta}/RT\right)\Bigg/ Q \qquad (5.3)$$

Substituting for the integrand and simplifying the resulting expression yields:

$$\frac{\partial \ln Q}{\partial S_{\alpha\beta}^{(p)}} = -2\pi N\rho_c\sum_\alpha\sum_\beta \left(S_{\alpha\beta}^{(p)}\right)^2 g_{\alpha\beta} \qquad (5.4)$$

If S is taken as the size parameter σ, for a homonuclear chain (homopolymer) ($\sigma_{\alpha\alpha} = \sigma_{\alpha\beta}$

$= \sigma_{\beta\beta} = \sigma$), substituting Equation 5.4 and the expression for lnQ from the partition

function relationship (lnQ = -A/NkT) simplifies to the following expression.

$$g(\sigma) = \frac{1}{2\pi\rho_c\sigma^2 m}\frac{\partial\left(A/NkT\right)}{\partial\sigma} \qquad (5.5)$$

where g(σ) is the average intermolecular site-site correlation function, A is the residual

Helmholtz energy, and m is the chain length. Density of sites in the system is given by:

$$\rho = \frac{N}{V} = m\rho_c \tag{5.6}$$

where N is the total number of sites and V is the volume of the system.

Equation 5.5 can be used to derive expressions for average correlation function from equations of state since the residual Helmholtz energy is given by:

$$\frac{A}{NkT} = \int_0^\rho \left(Z(\rho') - 1\right)\frac{d\rho'}{\rho'} \tag{5.7}$$

where Z is the compressibility factor, primes are used on the integrand to distinguish it from the limits.

5.3   Consistency of Pair Correlation Functions

Consistency of pair correlation functions is useful in deriving accurate equations of state and mixture models. Equations of state of athermal hard sphere chains are therefore tested for consistency. Average intermolecular pair correlation function were also evaluated based on Equation 5.5 derived earlier.

The equation of state of Chiew (1990) is given by:

$$g_{ij} = \left[\frac{1}{1-\eta} + \frac{3\eta}{(1-\eta)^2} + \frac{3\eta^2}{(1-\eta)^3}\right] - \frac{r-1}{r}\frac{1+\eta/2}{(1-\eta)^2} \tag{5.8}$$

This equation was tested according to the consistency conditions given in Equatios 3.52 to 3.53. The consistency condition was not satisfied.

Song et al. (1994) generalized Equation 5.8 using the Carnahan-Starling radial distribution function at contact. For pure copolymer system, they obtained the following equation.

$$g_{ij} = \frac{1}{1-\eta} + 3/2\frac{\xi_{ij}}{(1-\eta)^2} + 1/2\frac{\xi_{ij}^2}{(1-\eta)^3} \qquad (5.9)$$

where g_{ij} is the radial distribution function at contact between a sphere of diameter d_i and another of diameter d_j. The packing fractions η is $\rho/4\sum_i b_{ii}$ and ξ_{ij} are defined as follows.

$$\xi_{ij} = \rho/4\left[\frac{b_{ii}\,b_{jj}}{b_{ij}}\right]^{\frac{1}{3}}\sum_k b_{kk}^{\frac{2}{3}} \qquad (5.10)$$

Equation 5.9 is also not consistent with Equation 5.5. However, this was made consistent by adding another parameter F (that makes it consistent) and solving for the parameter. For a homopolymer $(i = j)$

$$g_{ii} = \frac{1}{1-\eta} + 3/2\frac{\xi_{ii}}{(1-\eta)^2} + F/2\frac{\xi_{ii}^2}{(1-\eta)^3} \qquad (5.11)$$

Using the approach of Hamad (1995) for hard spheres mixture, Equation 5.11 was substituted into the consistency equations to derive the following functional form of F for chain molecules.

$$F = 3/4 - \left[3/4 - f\left(\sigma^3\right)\right]R \qquad (5.12)$$

where

$$R = \left(\sum_{k=1}^{r} \sigma_k^3\right)^2 \Big/ \left(\sum_{k=1}^{r} \sigma_k^2\right)^3 \qquad (5.13)$$

Substituting Equations 5.12 and 5.13 into Equation 5.11, and solving the correlation function equation yields the following expressions for F.

(i)   For Carnahan-Starling equation,

$$g_{ii} = (1 - \eta/2)/(1 - \eta)^3 \qquad (5.14)$$

the function $f(\sigma^3)$ then equals unity. Therefore, $F(\sigma)$ becomes $(3-R)/2$, and the consistent pair correlation function at contact becomes:

$$g(\sigma) = \frac{1}{1-\eta} + 3/2 \frac{\eta}{(1-\eta)^2} + \frac{(3 - 1/\eta)\eta^2}{(1-\eta)^3} \qquad (5.15)$$

(ii)   For virial Percus-Yevick equation,

$$g_{ii} = (1 - \eta/4)/(1 - \eta)^2 \qquad (5.16)$$

This yields $f(\sigma^3) = 3(\eta-1)/4\eta$. From this, $F(\sigma) = 3R(\eta-1)/2\eta$. Therefore, the consistent pair correlation function at contact becomes:

$$g(\sigma) = \frac{1}{1-\eta} + 3/2 \frac{\eta}{(1-\eta)^2}(1 - 1/2\eta) \qquad (5.17)$$

(iii)   For compressibility Percus-Yevick equation,

$$g_{ii} = (1 + \eta/2 + \eta^2/4)/(1 - \eta)^3 \qquad (5.18)$$

gives $f(\sigma^3) = 3/2$. This results to $F(\sigma) = 3(1+R)/4$.

Therefore, consistent expressions for contact value radial distribution functions for homopolymers based on Carnahan-Starling (CS) and the virial Percus-Yevick (PY)

equations of state are given in Figures 5.1 and 5.2. The consistent CS equation gave almost identical results to the Percus-Yevick compressibility equation. These values are in good agreement with the predictions of the original equations. For the virial Percus-Yevick equation, the new consistent equation underpredict the compressibility factor at high packing fractions (see Fig. 5.2). At low packing fractions, all the equations are in good agreement.

5.4   PVT Behavior of Polymer Mixtures

PVT behavior of polymers is a necessary physical property that is directly used in the design and operation of polymer process equipment. It can also be used with calorimetric data to accurately estimate the enthalpy and entropy of polymers. This is necessary for energy-efficient design in high pressure (high power) operations (Isacescu et al., 1971).

There are several correlations for predicting the PVT behavior for pure polymers. These are mostly in the form of equations of state. Notable among these is the Tait equation, (Tait, 1888). This correlative equation is very accurate in the pressure and temperature range used to determine the equation's constants. Within this range, the average error of the equation (~ 0.1%) is less than most reported experimental errors. Due to this high accuracy, the Tait equation has been used to fit several pure polymer data (Danner and High, 1993; Rodgers, 1993).
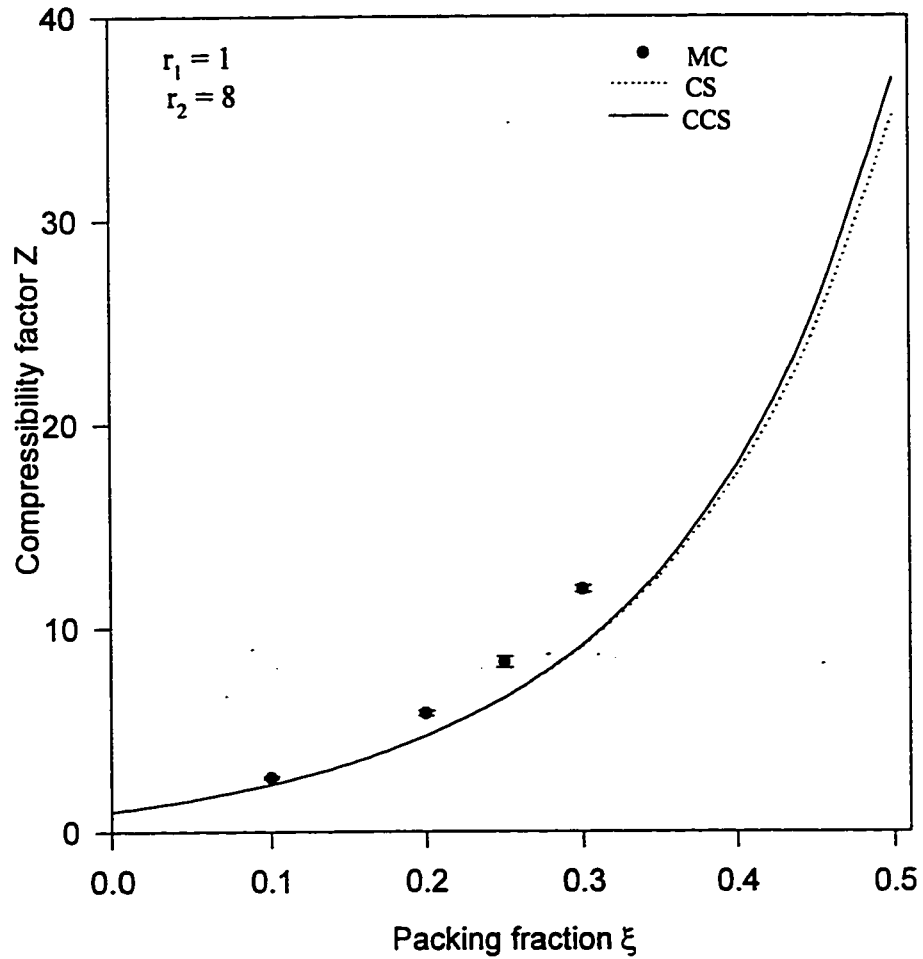
Figure 5.1 Compressibility vs packing fraction for an 8-mer/monomer mixture predicted using hard chain g_{ij} expressions based on Carnahan-Starling (CS) and corresponding consistent expression (CCS). Points are Monte Carlo data of Honnell and Hall (1991).
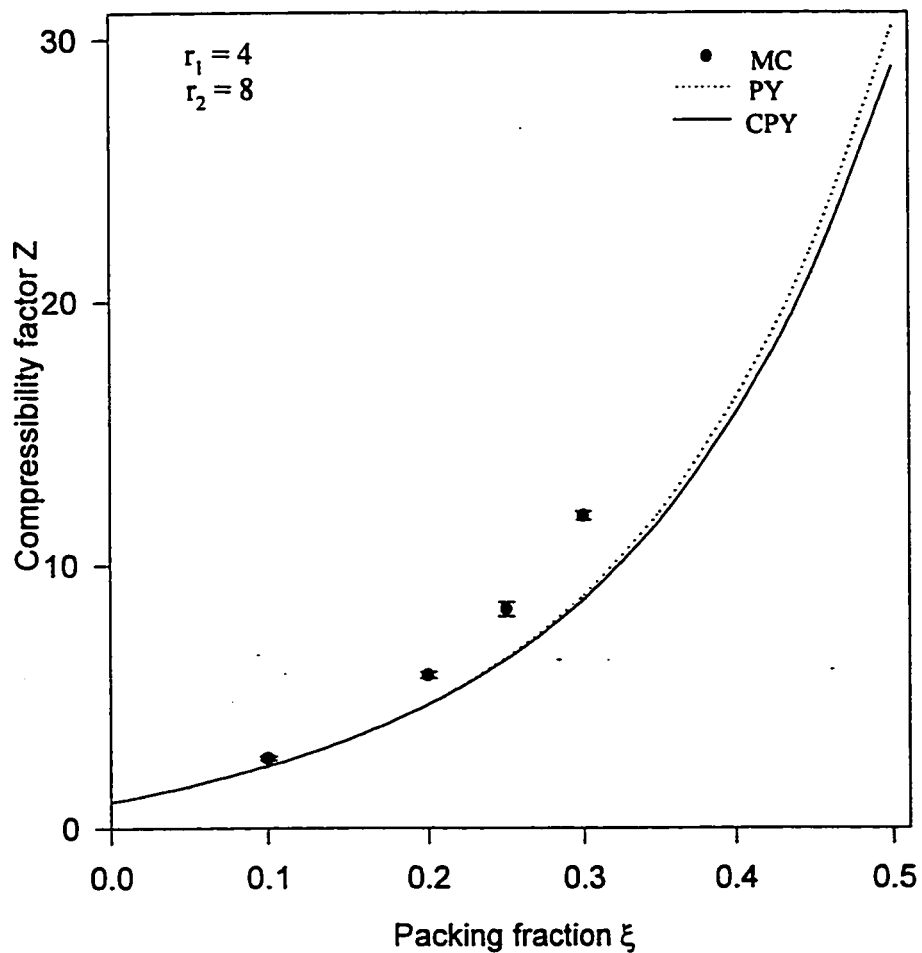
Figure 5.2 Compressibility vs packing fraction for an 8-mer/4-mer mixture predicted using hard chain g_{ij} expressions based on Percus-Yevick compressibility (PY) and corresponding consistent expression (CPY). Points are Monte Carlo data of Honnell and Hall (1991).

A major limitation of this method is the restriction of its use in only polymers for which the constants have been determined from experimental data. Thus, no method is available for predicting the constants from the molecular parameters of the polymer. As a result, the sensitivity of the constants with variation of molecular weight of the same polymer species is not known (Danner and High, 1993). In an attempt to extract molecular parameter information from the equation constants, a general equation of state for polymer mixture in the form of Equation 3.48 was used.

Noting that the molar volume $v = V/N$, and using density as a basis, Z in Equation 3.48 can be written as:

$$Z = PV/NRT = (P/RT)(V/m)(m/N) \qquad (5.19)$$

where m is the total mass of polymer in the system, N is the total number of molecules and V is the system volume.

The term m/N for a mixture is commonly defined as the weight average molecular weight of the polymer.

$$m/N = \sum_i M_i N_i / N = \sum_i M_i x_i = \overline{M} \qquad (5.20)$$

where M_i is the molecular weight of component i, N_i is the number of molecules of type i, x_i is the mole fraction of chains of type i, and $\overline{M}$ is the weight average molecular weight of the polymer mixture.

Substituting Equations 5.19 and 5.20 into Equation 3.48 and noting that for long chains, $1/\overline{M} \approx 0$, gives:

$$\frac{Pv}{RT} = \frac{4\pi}{6\overline{M}}\rho_c \sum \sum x_i x_j \sigma_{ij}^3 r_i r_j g_{ij} \tag{5.21}$$

where v is the volume per unit mass of the mixture.

In the limit of pure component, that is, $x_2 \rightarrow 0$, solving Equation 5.21 for the average correlation function of pure component 1, yields an expression that can be generalized to the following:

$$g_{ii} = (6/4\pi\rho_c)(Pv/RT)_i (M_i/r_i)(1/\sigma_{ii}^3 r_i) \tag{5.22}$$

where all the terms retain their previously defined meanings.

The terms in Equation 5.22 were deliberately grouped in the presented form because of the physical significance attached to each of them. The term M_i/r_i is proportional to the average weight of a repeat unit, while the term $\sigma_{ii}^3 r_i$ is a measure of the volume of a polymer molecule. These relationships are exact if the polymer is assumed to consist entirely of tangent hard sphere chains. Pv/RT can be obtained from accurate pure polymer equations of state as explained in what follows.

The Tait equation is generally written as:

$$V(P,T) = V(0,T)\{1 - C\ln[(B+P)/(B+P_0)]\} \tag{5.23}$$

where V(P,T) is the specific volume at pressure P and temperature T. V(0,T) is the specific volume at zero pressure and temperature T. B(T) is the Tait parameter for the specific polymer, C is a universal constant (numerically equal to 0.0894) for polymers, P and T are absolute pressure and temperature, respectively.

The term V(0,T) is given by polynomial or exponential functions of the form:

$$V(0,T) = A_0 + A_1 t + A_2 t^2 \qquad (5.24)$$

or

$$V(0,T) = V_0 \, exp(V_1 t) \qquad (5.25)$$

where A_0, A_1, and A_2, or V_0, V_1 are specific constants for a given polymer. B(T) in Equation 5.23 is also commonly written in the form of Equations 5.24 and 5.25 with the corresponding constants B_0, B_1 and B_2 for the quadratic form or just B_0 and B_1 for the exponential form (Rodgers, 1993).

The term (Pv/RT) in Equation 5.22 can be obtained from the Tait equation which can be rewritten as follows for $P_0 = 0$:

$$\frac{Pv}{RT} = \frac{PV(0,T)}{RT} \overline{M}\left[1 - C\ln(1 + P/B)\right] \qquad (5.26)$$

The zero-pressure term V(0,T) in Equation 5.23 can be factored into size and energy terms as follows:

$$V(0,T) = A_0 \left[1 + q_1(T - T_0) + q_2(T - T_0)^2\right] \qquad (5.27)$$

where A_0 is the volume term, and q_1 and q_2 are reciprocals of energy and energy squared.

In a similar manner (to the above development), the log term in the Tait equation can be factored into separate volume and energy contributions using the definition of $B(T)$ in the Tait equation as follows:

$$\frac{P}{B(T)} = \frac{PB_l/R}{B_l B_0/R} exp(B_l t)$$ (5.28)

where $B_l B_0/R$ was taken as molar density and A_0 as volume parameter of the polymer. Therefore, the following holds:

$$\frac{1/A_0}{B_l B_0/R} \propto \frac{M}{r}$$ (5.29)

where M is the molecular weight of polymer and r is its chain length.

Equation 5.19 was tested for some common polymers with repeat units as shown in Figure 5.3. From tabulated Tait equation parameters (Danner and High, 1993), and our fitted Tait equation for poly-4-hydroxystyrene using the pure polymer data (Luenga and Rubio, 1994), values of M/r were calculated according to Equation 5.29. These are presented in Table 5.1.

The fitted Tait parameters for the polymers given by Danner and High (1993) are general for the polymer type. Hence, their general dependence on polymer specie molecular weight is not known (Danner and High, 1993). In spite of this short coming, based on the knowledge of average range of molecular weights of such polymers that are

commonly encountered in the literature, it is clear that one cannot make meaningful conclusions from the calculated values of M/r (see Table 5.1) based on the repeat units shown in Figure 5.3.

5.5   Tait Equation for Mixtures

The failure of Equation 5.29 to give reasonable values for M/r means Equation 5.22 cannot give reliable values for pair correlation functions. This prompted the need for development of mixture version of the Tait equation from the existing form for pure polymers. To this end, Equation 5.23 was directly extended to mixtures as follows (for $P_0 = 0$):

$$V_{mix}(P,T) = \sum\sum x_i x_j V_{ij}(0,T)\left[1 - Cln\left(1 + P/B_{ij}\right)\right] \qquad (5.30)$$

The V(0,T) and the P/B(T) terms as written in Equation 5.27 and Equation 5.28 respectively, were similarly extended to mixtures as follows:

$$V_{ij}(0,T) = A_{0ij}\left[1 + q_{ij}^{(1)}(T - T_0) + q_{ij}^{(2)}(T - T_0)^2\right] \qquad (5.31)$$

and

$$\frac{P}{B_{ij}(T)} = \frac{b_{ij}}{R/PB_{1ij}}exp\left[B_{1ij}(T - T_0)\right] \qquad (5.32)$$

where the term $R/B_{1ij}B_{0ij}$ as in Equation 5.28 is simply represented by b_{ij}.

$$-\left(CH_2-CH\right)_n \qquad -\left(CH_2-CH_2\right)_n$$

$$\underset{\underset{CH_3}{\overset{|}{C=O}}}{\overset{|}{O}}$$

[PVAc]   **[P4HS]**

$$-\left(CH-CH_2\right)_n \qquad -\left(CH_2-CH_2\right)_n$$
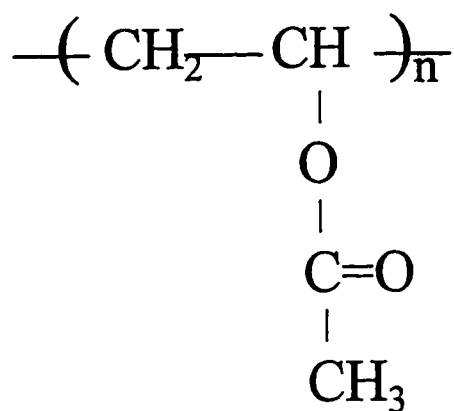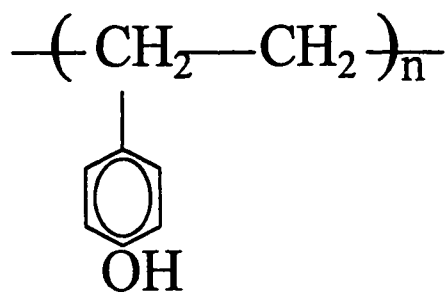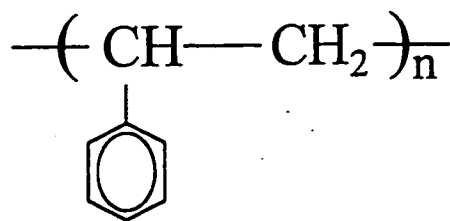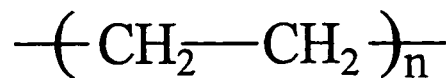
[PS]   **[PE]**

Figure 5.3   Structure of repeat units of some common polymers.

TABLE 5.1 Derived M/r parameters for some polymers[*]

Polymer	$\overline{M}_w$	$10^4 \times A_0$ (m³/kg)	$10^{-8} \times B_0$ (Pa)	$10^3 \times B_1$ (1/K)	M/r Eq.(5.19) (g/mol)
LDPE	-	11.615	1.9325	5.6839	17.6
PVAc	-	8.2832	1.8825	3.8774	11.4
HDPE	-	11.567	1.7867	4.7254	10.9
PS	-	9.3805	2.5001	4.1815	7.9
P4HS	≈6200	8.4295	2.5001	3.0780	3.1

[*] the values of A_0, B_0, B_1 for P4HS is from our fit while the rest are from Danner and High, 1993.

The advantage of writing Equations 5.27 and 5.28 in the form of Equations 5.31 and 5.32, respectively, for mixtures lies in the readily applicable mixing and combining rules in the latter. The term $q^{(1)}$ is inversely proportional to energy, while $q^{(2)}$ is inversely proportional to energy squared. Lorenz Berthelot's combining rules can, therefore, be readily applicable to the cross parameter. Thus

$$q_{ij}^{(n)} = \left(q_{ii}^{(n)} q_{jj}^{(n)} \right)^{1/2} \tag{5.33}$$

If need be, an additional characteristic binary constant can be used to account for deviations of $q_{ij}^{(n)}$ from the above geometric mean. In that case, the cross parameter will, therefore, be of the form:

$$q_{ij}^{(n)} = \left(1 - k_{ij} \right) \left(q_{ii}^{(n)} q_{jj}^{(n)} \right)^{1/2} \tag{5.34}$$

where k_{ij} is a characteristic binary constant (relating to energy or temperature).

The form of Equation 5.34 is not desirable since it introduces an additional parameter to the mixture equation. For the volume parameter, A_{0ij} and b_{ij}, the mixing rule especially developed for chain molecules (see Equations 3.56 to 3.59) was applied.

Equation 5.20 was tested using experimental data of Luengo et al. (1994) for a 50:50 (wt/wt) mixture of poly(4-hydroxystyrene) and poly(vinylacetate). The fitted Tait parameter for poly(vinylacetate) from Danner and High, (1993) was used. Since there was no such parameter for pure poly(4-hydroxystyrene) available, experimental parameters

for pure poly(4-hydroxystyrene) from Luengo et al. (1994) was used to fit Tait equation for the parameters. Much of the temperature for the experimental data of the mixture (75 to 200°C) falls outside the range for the pure poly(4-hydroxystyrene) (130 to 250°C). The validity of the fitted pure parameters outside the experimental temperature of the fit was, therefore, tested. In doing this, pure experimental data in the pressure range of (10 MPa to 100 Mpa) and a temperature range of 130 to 180°C was used to fit Tait equation. The fitted equation reproduced these data with an absolute average error of 0.10% and a maximum of 0.26%. The equation was then used to predict some experimentally available data in the temperature range 190 to 220°C which is outside the fit range. The 14 experimental data points predicted were reproduced with absolute average and maximum errors of 0.20% and 0.42% respectively. It is expected that the error in predicting pure polymer volumetric data at the mixture conditions will even give smaller errors because the temperature range of the mixture is closer to the range used in fitting the Tait equation than the temperature range in which the fit was tested. This justified the use of the fitted constants outside the range of the fit, despite a recommendation for the contrary (Danner and High, 1993).

The mixing rule for chain molecules can be applied to the volume parameter b according to the following equation.

$$b_{ij} = \sum_k x_k \; c_{ij,k} \qquad\qquad (5.35)$$

where the terms $c_{ij,k}$ are given by Equations 3.56 to 3.59.

To calculate the zero pressure volume term V(0,T), the following mixing rules were tested on the volume parameter A_{0ij}.

$$A_{0_{ij}} = 1/2 \left(A_{0_{ii}} A_{0_{jj}} \right)^{1/3} \sum_k A_{0_{kk}}^{1/3} \tag{5.36}$$

$$A_{0_{ij}} = 2 \left(A_{0_{ii}} A_{0_{jj}} \right)^{1/3} \sum_k x_k A_{0_{kk}}^{2/3} / \sum_k A_{0_{kk}}^{1/3} \tag{5.37}$$

$$A_{0_{ij}} = \left(A_{0_{ii}} A_{0_{jj}} \right)^{1/3} \sum_k x_k A_{0_{kk}}^{2/3} / \sum_k x_k A_{0_{kk}}^{1/3} \tag{5.38}$$

$$A_{0_{ij}} = \left(A_{0_{ii}} A_{0_{jj}} \right)^{1/3} \sum_k x_k A_{0_{kk}}^{1/3} \tag{5.39}$$

$$A_{0_{ij}} = 1/2 \sum_k A_{0_{kk}} \tag{5.40}$$

$$A_{0_{ij}} = \frac{2}{5} \sum_k x_k A_{0_{kk}} + \frac{3}{5} \frac{\left(A_{0_{ii}} A_{0_{jj}} \right)^{1/3}}{\frac{1}{2} \left(A_{0_{ii}}^{1/3} + A_{0_{jj}}^{1/3} \right)} \sum_k x_k A_{0_{kk}}^{1/3} \tag{5.41}$$

Using the above mixing rules, Equation 5.30 fairly predicted the mixture density within the same error range. Table 5.2 shows these errors for some representative experimental data points for the mixture of poly(4-hydroxystyrene) P4HS and poly(vinylacetate) PVAc.

The errors in Table 5.2 were reduced by factor of 1 to 2 by introducing an additional binary size parameter Δ. Therefore,

TABLE 5.4 Errors in predicting the densities of a mixture of poly(4-hydroxystyrene) and poly(vinylacetate).

P (MPa)	T (°C)	Percentage Deviation					
		Eq. (5.36)	Eq. (5.37)	Eq. (5.38)	Eq. (5.39)	Eq. (5.40)	Eq. (5.41)
10	100.5	-1.77	-1.71	-1.74	-1.74	-1.77	-1.74
60	160.2	-2.24	-2.18	-2.21	-2.21	-2.24	-2.16
100	190.8	-2.41	-2.35	-2.38	-2.38	-2.41	-2.33

$$A_{0_{ij}} = \left[(1 + \Delta)\left(A_{0_{ii}}^{1/3} + A_{0_{jj}}^{1/3}\right)/2 \right] \qquad (5.42)$$

Using a value of 0.06 for Δ reduced the errors in Table 5.2 to between - 0.05% and 0.50%. Even though this parameter (which resembles nonadditivity) improves the predictability of Equation 5.20, one cannot conclude that it originates from non-additivity. It could be due to other shape factors of the repeat units. For spherical chain repeat units, Δ is truly the non-additivity parameter.

A plot of the predicted volumes of a binary mixture of poly(4-hydroxystyrene) and poly(vinylacetate) using a value of 0.06 for Δ is shown in Figure 5.4. From this plot, it could be seen that accuracy of the predictions increases with both temperature and pressure. One possible reason for the increase in accuracy with temperature is due to the pure poly(4-hydroxystyrene) data used. This was at a temperature higher than the low temperature end of the mixture data. Another factor might be the dominant effect of repulsive forces on the molecular configuration (structure) of the system at high pressure and temperature. The predictions are generally accurate because even at the region of the highest deviations (low temperature and pressure), the percentage error is below 1.0%.

The parameter Δ is only related to the size of the polymer repeat units. In an analogous manner, one should expect an energy-related parameter also to improve the accuracy of the model. Surprisingly, however, addition of this parameter does not show any noticeable effect. The improvement achieved by using $k_{ij} = - 0.02$ in $q_{ij} = \sqrt{(q_{ii}q_{jj})}\,(1 - k_{ij})$ is less than the improvement due to Δ above. This suggests a similarity in the interaction energies of the sites of the two polymers.
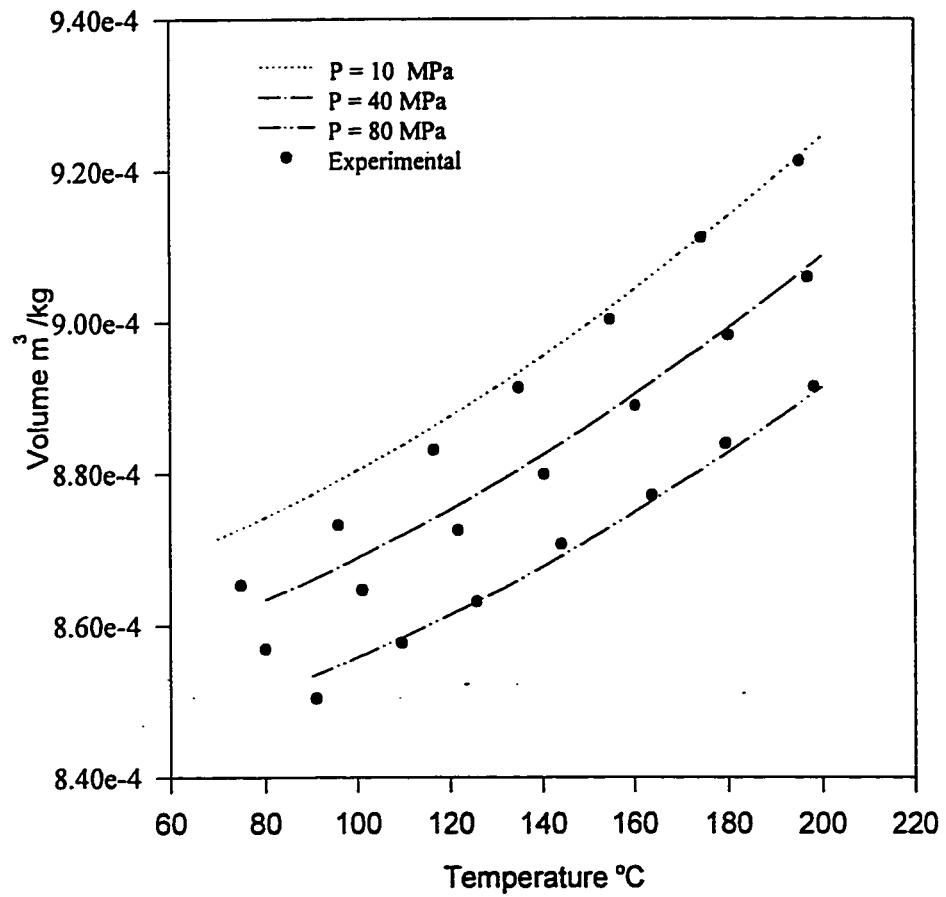
Figure 5.4   Density of binary mixture (50:50 w/w) of poly(4-hydroxystyrene) and poly(vinylacetate). The experimental data are from Luengo et al. (1994).

CHAPTER 6

CONCLUSIONS AND RECOMMENDATIONS

6.1   CONCLUSIONS

Consistent mixture models for simple molecules were developed from the following:

(i)   Approximate distinguishing values between pair correlation for hard spheres.

(ii)   Expansion of the pair correlation for hard core molecules.

(iii) Third and fourth virial coefficients for hard core molecules.

All the models were validated and tested for. mixtures of additive hard spheres, non-additive hard spheres, Lennard-Jones fluid and simple real fluids. Based on these tests, the model based on the expansion of the pair correlation function was on overall the best.

For additive hard spheres, the models accurately predicted the mixture compressibility factors. The model predictions were much better than the van der Waals one fluid and the mean density approximation theories, and it was very close to the accurate Mansoori-Carnahan-Starling-Leland equation for hard sphere mixtures. There was generally slight decrease in accuracy of the H and G models at high packing fractions. In this region, models H1 and G1 overpredicted the compressibility factors while models H2 and G2 underpredicted. Therefore, linear combinations of models H1 and H2 and of models G1 and G2 predicted accurately even at high packing fractions.

For non-additive hard spheres, the models were found quite satisfactory for symmetric mixtures between Δ (non-additivity parameter) values of - 0.5 to + 0.3. Their accuracy, however, decreased at higher values of the non-additivity. Except for the flat region at the critical point, the models correctly predicted the trend of the phase boundary. However, the quantitative values were generally not quite satisfactory.

For Lennard-Jones fluids, models f_{ij}, DVPCF and H2 predicted compressibility factor with average deviations of about 3%, about three times better than the van der Waals and the mean density approximations. Except at the highest regions of the test parameter (size ratios of 2.0 and energy ratios of 4.5), model H1 was also satisfactory. Here also, due to the opposite prediction trends, combinations of models H1 and H2 and of models G1 and G2 gave good results even at the high size and energy ratio regions.

The models also performed satisfactorily for mixtures of argon-krypton, neon-argon, methane-tetrafluoromethane, and carbon dioxide-ethane. Deviations from experimental data were generally within 5% except at high pressures where deviations of up to 15% was observed for model H1.

For chain molecules, a consistent mixing rule was developed from third virial coefficient and consistency equations. Tait equation of state for pure polymers was also extended to mixtures. The extended mixture equation was tested with the developed mixing rules for chain molecules. It closely predicted the experimental polymer mixture data for poly(4-hydroxystyrene) and poly(vinylacetate) with a maximum deviation of about 1.0%. The predicted results were more accurate at high temperatures and high pressures of the polymer mixture.

6.2 RECOMMENDATIONS

Although the developed models were generalized for multicomponent mixtures, they were only tested with binary experimental data. This models should, therefore, be tested for at least ternary and quartenary mixtures to find their accuracy for such mixtures. This is necessary since there may be build up or fortuitous cancellation of the binary pair errors. This will certainly depend on the molecular properties of the pure substances involved.

Due to the scarcity of volumetric data for polymer mixtures, our polymers mixture model was only compared to one set of experimental data. Pressure-Volume-Temperature experiments for polymer mixtures are, therefore, recommended to complement the existing huge pure polymer data base in the enhancement of modeling in this field. At relatively high temperatures, measurements could be made for polymers in their liquid state. To obtain reference data for normal conditions, however, it may be necessary to first dissolve the pure polymers in their common solvent. A solid polymer mixture can then be cast from a mixture of the solutions by evaporating the common solvent.

Phase separation studies of our mixture models for non-additive hard spheres was only limited to mixtures of symmetric molecules. This study should be extended to asymmetric fluids and also supercritical solutions. The later may be useful in the development of solid state batteries from superionic conductors.

During the course of this work, the residual Helmholtz free energies of hard-sphere chains equation of state of Chiew (1990) and of Malakhov and Brun (1992) based

on Percus-Yevick thermodynamic perturbation theory (TPT) were found to be inconsistent with the average intermolecular correlation functions. Further studies on this could lead to useful consistent equations of state for polymers.

In their present form, our models were designed to reproduce the second virial coefficient and the repulsive part of the third virial coefficient correctly. This is the main source of the improvements of our models over the van der Waals and the MDA theories. Further improvements could be made if similar derivations are made using a fluid potential such as the square well model that has both the hard core and attractive terms. Of course, the expected improvement in accuracy is to the compromise of simplicity. Molecular parameters other than size and energy could also be incorporated according to Equation 2.47 to extend the mixing rules to more complex polar and associating solutions.

NOMENCLATURE

A	Helmholtz free energy
A_0, A_1, A_2	Specific constants for pure polymer in Tait equation
B	Second virial coefficient
B_0, B_1	Specific constants for pure polymer in Tait equation
C	Third virial coefficient
$c_{ij}(r)$	direct correlation function
D	Fourth virial coefficient
E	Excess property
G	Gibbs free energy; also as model parameter function
g_{ij}	Radial distribution function
h	Planck's constant
i, j, k	Component specie
k	Boltzmann constant
k_{ij}	Unlike pair interaction parameter
m	mass of molecule
n_i	Number of systems of an ensemble being in state i
n	Number of molecules (part of the total N)
N	Total number of molecules in a system
P	Absolute pressure
p_i	Probobility of an ensemble being in quantum state i

$P^{(N)}$ Probability that uniquely defines a molecule in a system

Q Canonical ensemble partition function

$q^{(1)}, q^{(2)}$ Energy parameters in Tait equation for mixtures

r Chain length (number of repreat units)

$\mathbf{r}$ Radial position vector (r radial distance)

R Collision radius of molecules

s Surface area of molecules

S Entropy

T Absolute temperature

T_c Critical temperature

T_s Dimensionless temperature (T/T_B)

T_B Boyle's temperature

T_r Reduced temperature

U Internal energy

v Volume of molecules

V System volume

V_c Critical volume

x Mole fraction of component

Y Isothermal-isobaric ensemble partition function

Z Compressibility factor

Z_N Configurational integral $Z(T, V, N)$

Greek Symbols

Ω	Microcanonical ensemble partition function
Ξ	Grand canonical ensemble partition function
μ	Chemical potential
β	Boltzmann factor ($1/kT$)
ε	Energy parameter (potential well depth for L-J fluids)
Λ	de Broglie wave length ($\Lambda^2 = \beta h^2/2\pi m_i$)
ϕ	Intermolecular potential energy function
λ	Reduced potential well width in square well potential fluid
σ	Collision diameter of molecules
ρ	Number density (N/V)
δ	Cronecker delta
γ	Activity coefficient
α	Contribution of repulsive forces to the second virial coefficient
ξ	Packing fraction
ω	Accentric factor

Abbreviations

BH	Barker-Henderson
comb	Combinatorial contribution

COR	Chain of rotators
CPU	Central processing unit
CS	Carnahan-Starling
DFT	Dense fluid theory
DVPCF	Approximate distinguishing value of pair correlation function
G1, G2	Model notations
H1, H2	Model notations
HDPE	High density polyethylene
KH	Kihara potential
HS	Hard spheres
LDPE	Low density polyethylene
liq	Liquid
LJ 12,6	Lennard-Jons 12, 6 potential
MC	Monte Carlo
MD	Molecular Dynamics
mix	Mixture
MDA	Mean density approximation theory
MSCL	Mansoori-Carnahan-Starling-Leland
NRTL	Non-random two liquid theory
PCF	Pair correlation function
PHCT	Perturbed hard chain theory
PF	Partition function

PS   Poly(styrene)

PVAc   Poly(vinylacetate

PY   Percus-Yevick

P4Hs   Poly(4-hydroxystyrene)

rdf   Radial distribution function

SC   Self consistent

SS12   Inverse-12 soft-sphere potential

TPT   Thermodynamic pertubation theory

UNIQUAC   Universal quasi-chemical theory

vdW-1f   van der Waals one fluid theory

WCA-LL-GH   Weeks Chandler-Andersen-Lee-Levesque-Grundke-Henderson

LIST OF REFERENCES

Abrams, D. S. and Prausnitz, J. M., "Statistical thermodynamics of liquid mixtures: A new expression for the excess Gibbs energy of partly or completely miscible systems", AIChE J., 21, 116-128 (1975).

Adachi, Y., Fujihara, I., Takamiya, M. and Nakanishi, K., "Generalized equation of state for Lennard-Jones fluids. I. Pure fluids and simple mixtures", Fluid Phase Equilibria, 39, 1 - 38 (1988).

Adams, D.J., "Calculating the low temperature vapor line by Monte Carlo", Molec. Phys., 32, 647 - 657 (1976).

Adams, D.J., "Calculating the high-temperature vapor-line by Monte Carlo", Molec. Phys., 37, 211 - 221 (1979).

Adams, D.J. and McDonald, I.R., "Fluids of hard spheres with non-additive diameters", J. Chem. Phys., 63, 1900 - 1903 (1975).

Alblas, B.P., van der Marel, C., Geerstma, W., Meijer, J.A., van Osten, A.B., Dijkstra, J., Stein, P.C. and van der Lugt, W., J. Non-Cryst. Solids 61/62, 201 (1984).

Alder, B.J., "Studies in molecular dynamics . III. A mixture of hard spheres", J. Chem. Phys., 40, 2724 - 2730 (1964).

Allen. M.P. and Tildesley, D.J., "Computer simulation of liquids", Clarendon Press, Oxford (1987).

Amar, J.G., "Application of the Gibbs ensemble to the study of fluid-fluid phase equilibrium in a binary mixture of symmetric non-additive hard spheres", Molec. Phys., 67, 739-745 (1989).

Aziz, R.A., Meath, W.J. and Allnatt, A.R., J. Chem. Phys., 78, 295 (1983).

Aziz, R.A. and Slaman, M.J., "On the Xe - Xe potential energy curve and related properties", Molec. Phys., 57, 825 - 840 (1986).

Ballone, P., Pastore, G. and Galli, G., "Additive and non-additive hard sphere mixtures. Monte Carlo simulation and integral equation results", Mol. Phys., 59, 275-290 (1986).

Barker, J.A., "Lattice theory of the liquid state", Pergamon, Oxford (1963).

Barreiros, S.F., Calado, J.C.G., Clancy, P., da Ponte, M.N. and Streett, W.B., "Thermodynamic properties of liquid mixtures of argon + krypton", J. Phys. Chem., 86, 1722-1728 (1982).

Beret, S. and Prausnitz, J. M., "Perturbed hard chain theory: An equation of state for fluids containing small or large molecules", AIChE J. 21: 1123-1132 (1975).

Bokis, C. P. and Donohue, M. D., "Shape parameters and the density dependence of hard-chain equations of state", AIChE Journal, 38: 788-792 (1992).

Bokis, C. P. and Donohue, M. D., "Temperature and density dependence of equations of state for chain molecules", Presented at the AIChE J annual meeting, Miami beach, Fl, (1992).

Borgelt, P., Hoheisel, C. and Stell, G. J., "Static and dynamic properties of the Widom-Rowlinson model mixture I", Chem. Phys., 92, 6161-6165 (1990).

Born, M. and Green, H.S., "A general kinetic theory of liquids. I: The molecular distribution functions", Proc. R. Soc. London Ser. A 188, 10 (1946).

Boublik, T. Vega, C. and Diaz-Pena, M., "Equation of state of chain molecules", J. Chem. Phys., 93: 730-736 (1990).

Boublik, T., Nezada, I. and Hlavaty, K. Statistical thermodynamics of simple liquid mixtures. Elsevier, Amsterdam, (1980).

Boublik, T. and Nezada, I. (1986) P-V-T behavior of hard body fluids: Theory and experiment. Collection Czechoslovak Chem. Commun., 51: 2301.

Boublik, T., "Hard sphere equation of state", J. Chem. Phys., 53, 471 (1970).

Carnahan, N. F. and Starling, K. E.,. "Equation of state for nonattracting rigid sphere", J. Chem. Phys., 51, 635 - 638 (1969).

Chang, J. and Sandler, S.I., "An equation of state for the hard sphere chain fluid: Theory and Monte Carlo simulation", Chem. Eng. Sci., 49, 2777 - 2791 (1994).

Chao, K.C. and Greencorn, R.A., "Thermodynamics of fluids. An introduction to equilibrium theory", Mercel Dekker, Inc., New York, 1975.

Chien, C.H., Greenkorn, R.A. and Chao, K.C., "Chain-of-Ratators equation of state", AIChE J, 29, 560-571 (1983).

Chiew, Y. C., "Percus-Yevick integral-equation theory for athermal hard-sphere chains. Part I: Equations of state", Mol. Phys., 70: 129-143. (1990).

Chiew, Y.C., "Percus-Yevick integral equation theory for athermal hard-sphere chains. Part II: Average intermolecular correlation functions", Mol. Phys., 73, 359-373 (1990).

Chueh, P.L. and Prausnitz, J.M., "Vapor-liquid equilibria at high pressures. Vapor-phase

fugacity coefficients in nonpolar and quantum-gas mixtures", Ind. Eng. Chem.

Fundamentals, 6, 492-498 (1967).

Compostizo, A., Cancho, S.M., Crespo, A. and Rubio, R.G., "Polymer solutions with

specific interactions: Equation of state for Poly(4-hydroxystyrene) + Acetone",

Macromolecules, 27, 3478-3482 (1994).

Danner, R.P. and Hidg, M.S., "Handbook of polymer solution thermodynamics", Design

Institute for Physical property Data, AIChE, New York, (1993).

Denlinger, M.A. and Hall, C.K., "Molecular dynamics simulation results for the pressure

of hard chain fluids", Molec. Phys., 71, 541 (1990).

Donohue, M. D. and Prausnitz, J. M., "Perturbed hard chain theory for fluid mixtures:

Thermodynamic properties for mixtures in natural gas and petroleum technology",

AIChE J. 24, 849 - 860 (1978).

Douslin, D.R., Harrison, R.H. and Moore, R.T., "Pressure-Volume-Temperature relations

in the system Methane-Tetrafluoromethane. I. Gas densities and the principle of

corresponding states", J. Phys. Chem., 71, 3477 (1967).

Ehrenberg, V., Schaink, H.M. and Hoheisel, C., "Pressure and coexistence curve of two-

and three- dimensional nonadditive hard core mixtures. Exact computer

calculation results compared with scaled particle theory predictions", Physica A

169, 365 - 374 (1990).

Flory, P.J., "Statistical thermodynamics of liquid mixtures", J. Am. Chem. Soc., 87,

1833 - 1838 (1965).

Fredenslund, A. and Mollerup, J., "Measurment and prediction of equilibrium ratios for the C_2H_6 - CO_2 system", J. Chem. Soc. Faraday Trans. I, 70, 1653 - 1660 (1974).

Fries, P. H. and Hansen, J-P., "A Monte Carlo study of semidilute hard spheres mixture", Mol. Phys., 48, 891 - 901 (1983).

Gaminiti, R., J. Chem. Phys., 77, 5682 (1982).

Gao, J. and Weiner, J.H., J. Chem. Phys., 94, 3168 (1989).

Grundke, E.W. and Henderson, D., "Distribution functions of multicomponent fluid mixtures of hard spheres", Mol. Phys., 24, 269 - 281 (1972).

Gubbins, K. E., "The future of thermodynamics", Chem. Engg. Progr. Sept. Issue (1989).

Guo, M., Li, Y., Li, Z. And Lu, J., "Molecular simulatyion of liquid-liquid equilibria for Lennard-Jones fluids", Fluid Phase Equil. 98, 129 (1994).

Hámad, E. Z., "Statistical mechanical modeling of complex mixtures: Distribution function approach", PhD Thesis, University of Illinois (1988).

Hamad, E. Z. and Mansoori, G. A., "Mixture radial distribution functions: Are they all independent?", Fluid Phase Equil., 51: 13-21 (1989).

Hamad, E. Z. "Exact limits on the excess thermodynamic functions", Submitted (1995).

Hamad, E., "Consistency test for mixture pair correlation function integrals", J. Chem. Phys. 101: 10195-10196 (1994).

Hamad, E. Z., "Exact theoretical limits for mixture properties and mixing rules", Submitted (1995).

Hansen, J.P. and Varlet, L., "Phase transition of theLennard-Jones system", Phys., Rev., 184, 151 (1969).

Harismiadis, V. I., Koutras, N. K. and Tassios, D. P., "How good is conformal solutions theory for phase equilibrium predictions? Gibbs ensemble simulations of binary Lennard-Jones mixtures", Fluid Phase Equilibria, 65: 1 - 18 (1991).

Hill, T. L., "Statistical mechanics", McGraw Hill Inc., New York, (1956).

Hino, T. Song, Y. and Prausnitz, J.M., "Liquid-liquid equilibria for copolymer mixtures from a perturbed hard-sphere-chain equation of state", Macromolecules, 27, (1994).

Hoheisel, C., "Theoretical treatment of liquids and liquid mixtures", Elsvier, Amsterdam, (1993).

Honnell, K.G. and Hall, C.K., "A new equation of state for athermal chains", J. Chem. Phys., 90, 1841 (1989).

Ichigawa, K., Granstaff, S.M. and Thomsom, J.C., J. Chem. Phys. 61, 4059 (1974).

Ihm, G., Song, Y. and Mason, E.A., "Equation of state for mixtures of non-polar molecular fluids", Molec. Phys., 75, 897-915 (1992).

Isecescue, D.A., Ionescu, I.V., Leca, M., Roncea, C., Michaita, D. and Rizescu, E., "Studies in the field of polyethylene: V. Correlation between compressibility, Crystallinity and Molecular weight of high pressure polyethylenes", European J, 7, 913 (1971).

Ihm, G., Song, Y. and Mason, E.A., "A new strong principle of corresponding states for nonpolar fluids", J. Chem. Phys., 94, 3839-3848 (1991).

Johnson, J.K., Zollweg, J.A. and Gubbins, K.E., "The Lennard-Jones equation of state revisited", Molec. Phys., 73, 591 (1993).

Jung, J., Jhon, M. and Ree. R.H., "Homo- and heterocoordination in nonadditive hard-sphere mixtures and a test of the van der Waals one-fluid model", J. Chem. Phys., 100, 528-531 (1994).

Jung, J., Jhon, M. and Ree. R.H., "Fluid-fluid phase separations in nonadditive hard-sphere mixtures", J. Chem. Phys., 102, 1349-1360 (1995).

Jung, J., Jhon, M. and Ree. R.H., "An analytic equation of state and structural properties of nonadditive hard-sphere mixtures", J. Chem. Phys., 102, 1349-1360 (1994).

Kihara, T. and Miyoshi, K., "Geometry of three convex bodies applicable to three molecular clusters in polyatomic gases", J. Stat. Phys. 13, 337 - 345 (1975).

Kirkwood, G. J., "Statistical mechnics of fluid mixtures", J. Chem. Phys. 3, 300-313 (1935).

Kirkwood, J. G. and Buff, F. P., "The statistical mechanics theory of solutions I.", J. Chem. Phys. 19, 774 - 777 (1951).

Kratky, K.W., Fifth to tenth virial coefficients of a hard sphere fluid", Physica, 87A, 584 - 600 (1977).

Lee, L. L. "Molecular thermodynamics of non-ideal fluids", Butterworth Publishers, Stoneham MA (1988).

Lee, L.L. and Levesque, D., "Pertubation theory for mixtures of simple liquids", Mol. Phys., 26, 1351 - 1370 (1973).

Levesque, D. and Verlet, L., "Pertubation theory and equation of state for fluid", Phys. Rev., 182, 307 - 316 (1969).

Lotfi, A., Vrabec, J. And Fischer, J., "Vapor liquid equilibria of the Lennard-Jones fluid from the N p T plus test particle method", Molec. Phys., 76, 1319 - 1333 (1992).

Luengo, G. Rubio, R.G., Sanchez, I.C. and Panayiotou, C.G., The system poly(4-hydroxystyrene)/(poly(vinyl acetate))/acetone: An experimental and theoretical study, Macromol. Chem. Phys., 195, 1043-1062 (1994).

Malakhov, A.O. and Brun, E.B., "Multicomponent hard sphere heterochain fluid: Equation of state in a continuum space", Macromolecules, 25, 6262-6269 (1992).

Mansoori, G.A., Carnahan, N.F., Starling, K.E. and Leland, Jr. T.W., Equilibrium Thermodynamic properties of the mixture of hard spheres. J. Chem. Phys., 54, 1523 (1971).

McElroy, P.J. and Fang, J., "Compression factors and virial coefficients of ethene and ethene + ethane mixtures", J. Chem. Eng. Data, 38, 410-413 (1993).

McElroy, P.J. and Ababio, B.D., "Compression factors and virial equation of state coefficients for the system carbon monoxide + ethane", J. Chem. Eng. Data, 39, 327-329 (1994).

Melnyk, T.W. and Sawford, B.L., Equation of state of a mixture of hard spheres with non-additive diameters. Molec. Phys., 29, 891-902 (1975).

Metropolis, N., Rosenbluth, A.W., Rosenbluth, M.N. and Teller, A.H., Equation of state calculation for fast computing machines., J. Chem. Phys., 21, 1087 (1953).

Miyano, Y., "Equation of state for Lennard-Jones fluid Mixtures", Fluid phase Equilibria, 66, 125 - 141 (1991).

Miyano, Y., "An equation of state foe Lennard-Jones pure fluids applicable over a very wide temperature range", Fluid Phase Equilibria, 85, 71-80 (1993).

Muller, M. and Binder, K., "Computer simulation of asymmetric polymer mixtures", Macromolecules, 28, 1825 (1995).

Nicolas, J.J., Gubbins, K.E., Streett, W.B. and Tildesley, D.J., "Equation of state for the Lennard-Jones fluid", Mol. Phys., 37, 1429 - 1454 (1979).

Nixon, J.H. and Silbert, M., "Percus-Yevick results for a binary mixture of hard spheres with non-additive diameters: I. Negative non-additive parameter", Molec. Phys., 52, 207-224 (1984).

Pade, H., (Thesis), "Sur la representation approchee d'une fonction pour des fractions rationnelles", Ann. de l'Ecole Normale Sup. 3^{ieme} Serie, 9, Suppl., [3] - 93, (1892).

Panagiotopoulos, A.Z., "Direct determination of phase coexistense properties of fluids by Monte Carlo simulation in a new ensemble", 61, 813-826 (1987).

Percus, J. K. and Yevick, G. J., "Analysis of classical statistical mechanics by means of collective coordinates", Phys. Rev. 110: 1-13 (1958).

Phan, S., Kierlik, E. and Rosinberg, M.L., "Equations of state for hard chain molecules", J. Chem., Phys., 5326-5335 (1993).

Pitzer, K.S. and Curl, R.F. Jr., "The volumetric and thermodynamic properyies of fluids. III. Empirical equation for the second virial coefficient", J. Am. Chem. Soc., 79, 2369 - 2370 (1957).

Pitzer, K.S., de Lima, M.C.P. and Schreiber, D.R., J, Phys. Chem., 89, 1854 (1985).

Prausnitz, J. M., Lichtenthaler, R. N. and de Azevedo, E. G., "Molecular thermodynamics of fluid-phase equilibria", New Jersey. Preentice-Hall Inc, (1986).

Prausnitz, J. M., and Gunn, R.D., "Volumetric properties of nonpolar gaseous mixtures", AIChE J. 4, 430-435 (1958).

Prigogine, I. "The Molecular Theory of Solutions", North-Holland: Amsterdam, (1957).

Prigogine, I., Trappeniers, N. and Mathot, V., Discussion Faraday Soc., 15, 93 (1953).

Reamer, H.H., Olds, R.H., Sage, B.H. and Lacey, W.N., "Phase Equilibria in Hydrocarbon Systems. Volumetric Behavior of Ethane-Carbon Dioxide System", Ind. Eng. Chem., 37, 688-691 (1945).

Reed, T. M. and Gubbins, K. E., "Applied statistical mechanics", New York McGraw Hill Book Company Inc., (1973).

Rigby, M. and Smith, E. B., J. Chem. Soc., Faraday Trans., 2,59: 2469. (1963).

Rodgers, P. A., "Pressure-Volume-Temperature Relationships for polymeric liquids: A review of equations of state and their characteristic parameters for 56 polymers", J. Appl. Polym. Sci., 48, 1061-1080 (1993).

Saager, B. and Fischer, J., Fluid Phase Equil., 57, 35 (1990).

Santos, A., de Haro, M.L. and Yuste, S.B., "An accurate and single equation of state for hard disks", J. Chem. Phys., 103, 4622-4625 (1995).

Sanchez, I.C., "Virial coefficients and close-packing of hard spheres and disks", J. Chem. Phys., 101, 7003-7006 (1994).

Schweizer, K.S. and Curro, J.G., "Equation of state of polymer melts: General

formulation of a microscopic integral equation theory", J. Chem. Phys., 89, 3342

(1988).

Schweizer, K.S. and Curro, J.G., "Equation of state of polymer melts: Numerical results

for athermal freely jointed chain fluids", J. Chem. Phys., 85, 3350-3362 (1988a).

Schouten, J.A., van den Bergh, L.C. and Trappeniers, N.J., Chem. Phys. Lett., 114, 40

(1985).

Shukla, K. P., Luckas, M., Marquardt, H. and Lucas, K., "Conformal solutions: Which

model for which application?", Fluid Phase Equilibria, 26: 129 - 147 (1986).

Song, Y., Lambert, S.M. and Prausnitz, J.M., Equation of State for Mixtures of Hard-

Sphere Chains Including Copolymers. Macromolecules, 27, 441-448 (1994).

Song, Y., Lambert, S. M. and Prausnitz, J. M. A Perturbed Hard-Sphere-Chain Equation

of State for Normal Fluids and Polymers. Ind. Eng. Chem. Res., 33: 1047-1057

(1994a).

Song, Y. and Mason, E.A., Statistical mechanical theory of a new analytical equation of

state, J. Chem. Phys., 91, 7840-7853 (1989)

Song, Y. and Mason, E.A., "A new strong principle of corresponding states for non-polar

fluids", J. Chem. Phys., 94, 3839-3848 (1991)

Song, Y. and Mason, E.A., "Analytical equation of state for molecular fluids: Kihara

model for rod like molecules", Phys. Rev. A, 42, 4743 - 4748 (1990).

Song, Y. and Mason, E.A., "Analytical equation of state for molecular fluids:

Comparison with experimental data", Phys. Rev. A, 42, 4749 - 4755 (1990).

Song, Y. and Mason, E.A., "Statistical mechanical basis for accurate analytical equation of state for fluids", Fluid Phase Equil., 75, 105-115 (1992).

Ihm, G., Song, Y. and Mason, E.A., "Strong principles of corresponding states: Reduction of p-v-T surface to a line", Fluid Phase Equil., 75, 117 - 125 (1992a).

Streett, W.B., "Liquid-vapor phase behavior and liquid phase density in the system Neon-Argon at high pressures", J. Chem. Phys., 49, 3282-3286 (1967).

Tait, P.G., "Physics and chemistry of the voyage of H.M.S. Challenger, II, part IV, S.P. LXI, H.M.S.O, London, (1888).

Tao, F-M. and Mason, E.A., Statistical mechanical equation of state for nonpolar fluids: Prediction of phase boundaries, J. Chem. Phys., 100, 9075-9087(1994).

Thomas, A. and Donohue, M.D., "Equation of state for chain molecules using a site interaction model: Theory, simulation and correlation of experimental data", Ind. Eng. Chem. Res., 32, 2093-2104 (1993).

Tsonopoulos, C., "An empirical correlation of second virial coefficients", AIChE J. 20, 263-272 (1974).

Tsonopoulos, C., "Second virial coefficients of polar haloalkanes", AIChE J. 21, 827-829 (1975).

Tsonopoulos, C., "Second virial coefficients of water pollutants", AIChE J. 24, 1112-1115 (1978).

Verlet, L., "Computer experiments on classical fluids. I. Thermodynamical properties of Lennard-Jones molecules", Phys. Rev., 159, 98 - 103 (1967).

Vimalchand, P. and Donohue, M. D. Comparison of equations of state for chain molecules. J. Phys. Chem., 93: 4355 - 4360 (1989).

Watts, R. O. and Henderson, D., Mol. Phys. 16: 217 (1969).

Wallis, K.P., Clancy, P. Zollweg, A. and Streett, W.B., Excess thermodynamic properties for {xCO_2 + (1-x)C_2H_6} I: experiment and theory. J. Chem. Thermodynamics, 16, 811-823(1984).

Weeks, J. D., Chandler, D. and Andesen, H. C., "Role of repulsive forces in determining the equilibrium structure of simple liquids", J. Chem. Phys., 54: 5237 - 5247 (1971).

Whalen, J.W., Molecular Thermodynamics: A Statistical Approach, John Wiley & Sons, Inc., New York (1991).

Wood, W.W. and Parker, F.R., "Monte Carlo equation of state of molecules interacting with the Lennard-Jones potential. I. A supercritical isotherm at about twice the critical temperature", J. Chem. Phys., 27, 720 - 733 (1957).

Yethiraj, A. and Hall, C. K., "RESEARCH NOTE On equations of state for hard chain fluids", Molec. Phys., 80, 469 - 477 (1993).

Yvon, J., Actualities Scientifiques et Industriel, Herman et cie, Paris (1935).

Zeck, S. and Wolf, D., "Requirements of thermodynamic data in the chemical industry", Fluid Phase Equil., 82: 27-38 (1993).

APPENDICES

APPENDIX A

DEVELOPMENT OF MIXTURE MODEL FROM HS PCF

(MATHEMATICA® CODING)

```
Off [General::spell]     ;     Off [General::spell1];

s[n_]:=x1 d1^n + x2 d2^n;

y      = ro s[3];

a      =s[1] s[2] / s[3];

zhs    = (1 + y (3a - 2) + y^2 (3gm - 3a + 1)
           - gm y^3) / (1 - y)^3;

g11    = 1 / (1 - y) + 3 / 2 d1 ro s[2] / (1 - y)^2
           + f (d1  ro  s[2])^2 / (1 - y)^3;

g12    = 1 / (1 - y) + 3 / 2 (d1 d2 / d12) ro s[2] / (1 - y)^2
           + f (d1 d2 / d12  ro  s[2])^2 / (1 - y)^3;

d      = D[g11 , ro];     ro   = .;

d0     =Simplify[ d  2/5];

dx11 =     Coefficient[d0, x2];     ro   = .;

d      = Simplify[D[g12 , ro]];

dx12 =     Coefficient[ % , x1];

dx21 =     Coefficient[ d , x2];
```

APPENDIX B

COMPLEX MIXTURE MODEL FROM THIRD AND FOURTH VIRIAL COEFFICINTS

$$fdx11 = 1/10\left(\sigma_{11}^3 + 6\sigma_{11}^2\sigma_{22} + 15\sigma_{11}\sigma_{22}^2 - 20\sigma_{12}^3 + 8\sigma_{22}^3\right)$$
$$+ \frac{1}{3\sigma_{22}^3}\left[\sigma_{11}^6\sigma_{12}^3/5\left(-13\sigma_{11}^3 + 180\sigma_{12}^3 - 63\sigma_{11}^2\sigma_{22} - 105\sigma_{11}\sigma_{22}^2 + \sigma_{22}^3\right)\right]^{\frac{1}{2}} \quad \text{(B.1)}$$

$$fdx22 = 1/10\left(8\sigma_{11}^3 + 15\sigma_{11}^2\sigma_{22} + 6\sigma_{11}\sigma_{22}^2 - 20\sigma_{12}^3 + \sigma_{22}^3\right)$$
$$+ \frac{1}{3\sigma_{22}^3}\left[\sigma_{22}^6\sigma_{12}^3/5\left(\sigma_{11}^3 + 180\sigma_{12}^3 - 105\sigma_{11}^2\sigma_{22} - 63\sigma_{11}\sigma_{22}^2 - 13\sigma_{22}^3\right)\right]^{\frac{1}{2}} \quad \text{(B.2)}$$

$$fdx12 = \sigma_{11}^3 - \frac{1}{6\sigma_{12}^3}\left[\sigma_{11}^6\sigma_{12}^3/5\left(-13\sigma_{11}^3 + 180\sigma_{12}^3 - 63\sigma_{11}^2\sigma_{22} - 105\sigma_{11}\sigma_{22}^2 + \sigma_{22}^3\right)\right]^{\frac{1}{2}} \quad \text{(B.3)}$$

$$fdx21 = \sigma_{22}^3 - \frac{1}{6\sigma_{12}^3}\left[\sigma_{22}^6\sigma_{12}^3/5\left(\sigma_{11}^3 + 180\sigma_{12}^3 - 105\sigma_{11}^2\sigma_{22} - 63\sigma_{11}\sigma_{22}^2 - 13\sigma_{22}^3\right)\right]^{\frac{1}{2}} \quad \text{(B.4)}$$

The model parameters are given as follows:

$$f_{11} = x_1\sigma_{11}^3 + x_2 fdx11 \quad \text{(B.5)}$$

$$f_{12} = x_1 dx12 + x_2 fdx21 \quad \text{(B.6)}$$

$$f_{22} = x_2\sigma_{22}^3 + x_1 fdx22 \quad \text{(B.7)}$$

APPENDIX C

DERIVATION OF MIXTURE MODEL FOR CHAIN MOLECULES

$g11 = 1 + a\, ro\, (c111\, x1 + c112\, x2);$

$g12 = 1 + a\, ro\, (c121\, x1 + c122\, x2);$

$g22 = 1 + a\, ro\, (c221\, x1 + c222\, x2);$

$z = 1 + b\, ro\, (x1^2\, d1^3\, g11 +$

$\quad 2\, x1\, x2\, d12^3\, g12 + x2^2\, d2^3\, g22);$

$cc = 1/2\, D[z,ro,ro];$

$a = 5\, pi/12; b = 4\, pi/6;$

$ro = 0; c = Expand[cc];$

$C111 = Coefficient[c,x1^3];$

$C112 = Coefficient[c,x1^2\, x2];$

$C122 = Coefficient[c,x1\, x2^2];$

$C222 = Coefficient[c,x2^3];$

$c112 = d1^3\, f112[d2/d1]; d2c112 = D[c112,d2];$

$c121 = d1^3\, f121[d2/d1]; d2c121 = D[c121,d2];$

$c122 = d1^3\, f122[d2/d1]; d2c122 = D[c122,d2];$

$c221 = d1^3\, f221[d2/d1];$

$d1c221 = D[c221,d1];$

$d1c121 = D[c121,d1];$

$d1c122 = D[c122,d1];$

```
c112 = d1^3 f112[x];

c121 = d1^3 f121[x];

c122 = d1^3 f122[x];

c221 = d1^3 f221[x];

cc112 = 2/3 (pi/6 N)^2 d1^3 \

    (d1^3-18 d1 d12^2 + 32 d12^3);

(d2^3-18 d2 d12^2 + 32 d12^3);

eq1 = 5pi^2/18 (d1^3 c112 +

    2 d12^3 c121) = = 3 cc112;

eq2 = 5pi^2/18 (d2^3 c221 +

    2 d12^3 c122) = = 3 cc122;

Solve[eq1,f112[x]];

Solve[eq2,f221[x]];

f112[x] = -(-(d1^3*N^2) + 18*d1*d12^2*N^2 -

    32*d12^3*N^2 + 10*d12^3*f121[x])/(5*d1^3);

f221[x] = -(-32*d12^3*d2^3*N^2 +

    18*d12^2*d2^4*N^2 - d2^6*N^2 +

    10*d1^3*d12^3*f122[x])/(5*d1^3*d2^3);

d2 = x d1;d12 = d1 (x+1)/2;

eq3 = d1^2 D[f112[x],x] + d12^2 (d1^2 f121'[x] - \

    (3d1^2 f121[x]-d1 d2 f121'[x])) = = 0;

eq4 = d2^2 (3d2^2 f221[x]-d1 d2 D[f221[x],x]) + \
```

```
        d12^2 ((3d1^2 f122[x]-d1 d2 f122'[x])-

        d1^2 f122'[x]) = = 0;

DSolve[eq3,f121[x],x];

DSolve[eq4,f122[x],x];
```

!

APPENDIX D

EVALUATION OF MIXTURE PROPERTIES USING FROM TAO AND MASON, (1994) PURE EQUATION OF STATE

Off[General::spell];Off[General::spell1];

.....................data for carbon dioxide and ethane.........................

tc1=304.2;tc2=305.4;pc1=73.8;pc2=48.8;tb1=720.4;tb2=770.8;

a1=-0.0648;a2=1.8067;c1=2.6038;c2=0.9726;kij=0.08;

aa1=0.143;aa2=1.66;k=1.093;x1=.;x2=.;t=.;241.15;r=83.14;

w1=0.225;w2=0.098;vc1=94.0;vc2=148;vb1=63.9;vb2=90.6;

...........................data for argon and krypton.................................

tc1=150.8;tc2=209.4;pc1=48.7;pc2=55;tb1=401.4;tb2=556.9;

a1=-0.0648;a2=1.8067;c1=2.6038;c2=0.9726;vb1=42.5;vb2=52.3;

aa1=0.143;aa2=1.66;k=1.093;x1=0.485;x2=0.515;r=83.14; kij=.;

....

tc12=Sqrt[tc1 tc2] (1-kij);

pc12=4tc12 (pc1 vc1/tc1 + pc2 vc2/tc2)/

    (vc1^(1/3)+vc2^(1/3))^3;

lm1 =0.4324-0.3331w1;lm2=0.4324-0.3331w2;

lm12=0.4324-0.3331w12;tb12=Sqrt[tb1 tb2];

vb12=1/8 (vb1^(1/3)+vb2^(1/3))^3;w12=0.5(w1+w2);

ts1=t/tb1;ts2=t/tb2;ts12=t/tb12;

```
tr1=t/tc1;tr2=t/tc2;tr12=t/tc12;

zxc1=pc1/r/tc1;zxc12=pc12/r/tc12;

zxc2=pc2/r/tc2;kr1=k tc1/t;kr2=k tc2/t;kr12=k tc12/t;

bb[u_,w_,zxc_]:=1/zxc (0.1445-0.33/u-0.1385/u^2-
          0.0121/u^3-0.000607/u^8
          + w (0.0637+0.331/u^2-0.423/u^3-0.008/u^8));

ro=1/v;
```

```
f1[x_]:=a1 Exp[-c1 x] + a2 (1-Exp[-c2/x^0.25]);

f2[x_]:=a1(1-c1 x) Exp[-c1 x] +
       a2(1-(1+c2/4/x^0.25) Exp[-c2/x^0.25]);
```

=================model fij=================

```
c111=vb1;

c112=1/5 (2 vb12^(1/3)-vb1^(1/3))^2 (vb1^(1/3)+
       4 vb12^(1/3));

c122=1/5 (vb2^2/vb12)^(1/3) (vb12^(1/3) (3 vb12^(1/3)+
       2 vb2^(1/3)) - 3(vb12^(1/3)-vb2^(1/3))^2);

c222=vb2;

f1m =x1 c111 + x2 c112;f2m=x1 c122 + x2 c222;

f12m=x1 c112 + x2 c122;

vr1=ro f1m;vr2=ro f2m;vr12=ro f12m;
```

```
c111=b[ts1,vb1];

c112=1/5 (2 (b[ts12,vb12])^(1/3)-(b[ts1,vb1])^(1/3))^2

        ((b[ts1,vb1])^(1/3)+ 4 (b[ts12,vb12])^(1/3));

c122=1/5 ((b[ts2,vb2])^2/(b[ts12,vb12]))^(1/3)

        ((b[ts12,vb12])^(1/3) (3 (b[ts12,vb12])^(1/3) + 2

        (b[ts2,vb2])^(1/3))

        - 3(b[ts12,vb12]^(1/3)-b[ts2,vb2]^(1/3))^2);

c222=b[ts2,vb2];

f1m=x1 c111+ x2 c112;f2m=x1 c122 + x2 c222;f12m=x1 c112 +

        x2 c122;

vr1=ro f1m;vr2=ro f2m;vr12=ro f12m;
```

```
c111=(b[ts1,vb1]+vb1)/2;

c112=1/5 (2 (b[ts12,vb12]/2+vb12/2)^(1/3)-

(b[ts1,vb1]/2+vb1/2)^(1/3))^2

        ((b[ts1,vb1]/2+vb1/2)^(1/3) +

        4 (b[ts12,vb12]/2+vb12/2)^(1/3));

c122=1/5 ((b[ts2,vb2]/2+vb2/2)^2/(b[ts12,vb12]/2+vb12/2))^(1/3)

        ((b[ts12,vb12]/2+vb12/2)^(1/3) (3

        (b[ts12,vb12]/2+vb12/2)^(1/3)+2 (b[ts2,vb2]/2+vb2/2)^(1/3))

        - 3((b[ts12,vb12]/2+vb12/2)^(1/3)-(b[ts2,vb2]/2+vb2/2)^(1/3))^2);

c222=(b[ts2,vb2]+vb2)/2;
```

f1m=x1 c111+ x2 c112;f2m=x1 c122 + x2 c222;f12m=x1 c112 + x2 c122;

vr1=ro f1m;vr2=ro f2m;vr12=ro f12m;

==

zpure1=-p/ro/r/t + 1 +(bb[tr1,w1,zxc1]-vb1 f1[ts1]) ro +

vb1 ro f1[ts1]/(1-lm1 vb1 ro f2[ts1]) +

aa1 (vb1 f1[ts1]-bb[tr1,w1,zxc1]) f2[ts1] vb1 ro^2

(Exp[kr1]-aa2)/(1+1.8 f2[ts1]^4 (vb1 ro)^4)==0;

zpure2=-p/ro/r/t + 1 +(bb[tr2,w2,zxc2]-vb2 f1[ts2]) ro +

vb2 ro f1[ts2]/(1-lm2 vb2 ro f2[ts2]) +

aa1 (vb2 f1[ts2]-bb[tr2,w2,zxc2]) f2[ts2] vb2 ro^2

(Exp[kr2]-aa2)/(1+1.8 f2[ts2]^4 (vb2 ro)^4)==0;

----

ab1 =f1[ts1]/bb[tr1,w1,zxc1];

ab2 =f1[ts2]/bb[tr2,w2,zxc2];

ab12=f1[ts12]/bb[tr12,w12,zxc12];

f[vb_,ab_,ft_,kr_,lm_]:=1-vb ab + vb ab/(1-lm ft vb ro) +\

ft21=f2[ts1];ft22=f2[ts2];ft212=f2[ts12];

eq1=-p/ro/r/t + 1 + x1^2 bb[tr1,w1,zxc1] ro
f[vb1,ab1,ft21,kr1,lm1]+

2x1 x2 bb[tr12,w12,zxc12] ro f[vb12,ab12,ft212,kr12,lm12]+

x2^2 bb[tr2,w2,zxc2] ro f[vb2,ab2,ft22,kr2,lm2]==0;

---

t=310.939;x1=0.8223;x2=1-x1;

TableForm[Table[{t,x1,p,FindRoot[eq1,{v,70}]},{p,75,700,25}]];

t=310.939;x1=0.6687;x2=1-x1;

TableForm[Table[{t,x1,p,FindRoot[eq1,{v,60}]},{p,75,700,25}]];

t=310.939;x1=0.4868;x2=1-x1;

TableForm[Table[{t,x1,p,FindRoot[eq1,{v,60}]},{p,75,700,25}]];

t=310.939;x1=0.3237;x2=1-x1;

TableForm[Table[{t,x1,p,FindRoot[eq1,{v,60}]},{p,75,700,25}]];

t=310.939;x1=0.1720;x2=1-x1;

TableForm[Table[{t,x1,p,FindRoot[eq1,{v,60}]},{p,75,700,25}]];

FindRoot[zpure2,{v,35.17}];